

TECHNISCHE UNIVERSITÄT MÜNCHEN

Lehrstuhl für Chemisch-Technische Analyse und

Chemische Lebensmitteltechnologie

Enrichment Behavior of Immunoglobulin by Foam Fractionation Using Response Surface Methodology

Yen-Chih Chen

Vollständiger Abdruck der von der Fakultät Wissenschaftszentrum Weihenstephan für Ernährung, Landnutzung und Umwelt der Technische Universität München zur Erlangung des akademischen Grades eines

Doktor der Naturwissenschaften (Dr. rer.nat.)

genehmigten Dissertation

Vorsitzender: Univ.-Prof. Dr.-Ing. Thomas Becker

Prüfer der Dissertation: 1. Univ.-Prof. Dr. rer. nat. Dr. agr. habil. Dr. h.c. Harun Parlar

2. Univ.-Prof. Dr.-Ing. Roland Meyer-Pittroff (i.R.)

Die Dissertation wurde am 29.11.2011 bei der Technischen Universität München eingereicht und durch die Fakultät Wissenschaftszentrum Weinstephan für Ernährung, Landnutzung und Umwelt am 05.04.2012 angenommen.

Acknowledgements

The research work presented in this PhD thesis was realized at the Chair for Chemical and Technical Analysis and Chemical Food Technology of the Technical University of Munich, in Freising, Weihenstephan. I would like to express my sincere gratitude to:

Prof. Dr. Dr. h.c. Harun Parlar, the Head of the Chair and my supervisor, for his invaluable guidance, inspiration, and encouragement, as well as for providing me with the interesting topic of “foam fractionation” for the thesis, along with the freedom to implement my ideas through this study;

Mr. Albrecht Friess, for the kind, untiring and timely help in the improvement of this thesis, as well as for helping me during the study;

Prof. Thomas Becker and Prof. Roland Meyer-Pittroff for serving on my doctoral committee and providing useful suggestions to my research;

Prof. Elvira Schecklies, for the kind supply of the rabbit immunoglobulin G as a standard in the early stage of this work;

Dr. Reil for the help with ordering chemicals, and Iwona and Lorenz for the good atmosphere in the laboratory and companionship;

Mr. Jim Goodpaster, an English tutor and friend, for improving my English writing and speaking skills, and for his encouragement;

And last, but not least, I want to express my deepest gratitude to my wonderful family to whom I owe so much:

My father Dr. Yau-Ming Chen, my mother Mrs. Ling-Chang Du and my grandparents, for their endless support, encouragement, care and love, and for being a source of strength during the difficult moments.

TABLE OF CONTENTS

TABLE OF CONTENTS	ii
LIST OF FIGURES	vi
LIST OF TABLES	viii
LIST OF ABBREVIATIONS	x
1. Introduction	1
1.1 Objectives	4
2. Theoretical Background	5
2.1 Immunoglobulin	5
2.1.1 Properties of Immunoglobulin	5
2.1.2 Applications of Immunoglobulin	7
2.1.3 Traditional Methods for Immunoglobulin Enrichment	8
2.2 Foam Fractionation	11
2.2.1 Adsorptive Bubble Separation	11
2.2.2 Principles of Foam Fractionation	12
2.2.3 Adsorption in Foam Fractionation	13
2.2.4 Diffusion Mechanisms of Adsorption	15
2.2.5 Thermodynamics of Adsorption	16
2.2.6 Properties of Foam	20
2.2.7 Types of Foam	21
2.2.8 Stability of Foam	22
2.2.9 Parameters of Foam Fractionation	25
2.2.10 Problems Occurring in Foam Fractionation	27

2.3 Milk	28
2.3.1 Basic Components and Properties of Milk	28
2.3.2 Milk as a Source for Immunoglobulin Production	31
2.4 Response Surface Methodology	33
2.4.1 Approximating Response Functions	34
2.4.2 The Sequential Nature of RSM	37
2.4.3 Objectives and Applications of RSM	38
2.4.4 Useful References on RSM	39
2.4.5 Desirable Properties of Response Surface Designs	40
2.4.6 Central Composite Design	41
3. Materials and Methods	43
3.1 Materials	43
3.1.1 Chemicals	43
3.1.2 Equipment	43
3.2 Methods	44
3.2.1 Methods for Model system	44
3.2.1.1 Preparation of the Start Solution	44
3.2.1.2 Foam Fractionation Apparatus, Parameters and Procedures	44
3.2.1.3 Quantification of Immunoglobulin Concentration	46
3.2.1.4 Evaluation of Foam Fractionation Efficiency	47
3.2.1.5 Separating of IgG and IgM	49
3.2.1.6 Testing of Different Multi-Component Mixtures	49
3.2.2 Methods for Milk system	49
3.2.2.1 Pretreatment before Foam Fractionation	49
3.2.2.2 Preparation of the Start Solution	50

3.2.2.3	Foam Fractionation Apparatus, Parameters and Procedures	50
3.2.2.4	Quantification of Immunoglobulin Concentration	51
3.2.2.5	Evaluation of Foam Fractionation Efficiency	52
3.2.2.6	Total Protein Assay	52
3.2.3	Methods for RSM in a Model system.....	53
3.2.3.1	Preparation of the Start Solution for the Model System	53
3.2.3.2	Foam Fractionation Apparatus, Parameters and Procedures	54
3.2.3.3	Quantification of Immunoglobulin Concentration	55
3.2.3.4	Evaluation of Foam Fractionation Efficiency	55
3.2.3.5	Process for Response Surface Methodology.....	56
3.2.4	Methods for RSM in a Milk system	61
3.2.4.1	Preparation of the Start Solution for the Milk System	61
3.2.4.2	Foam Fractionation Apparatus, Parameters and Procedures	61
3.2.4.3	Quantification of Immunoglobulin Concentration	62
3.2.4.4	Evaluation of Foam Fractionation Efficiency	63
3.2.4.5	Total Protein Assay	64
3.2.4.6	Process for Response Surface Methodology.....	64
4.	Results and Discussion.....	68
4.1	Enrichment of Immunoglobulin in a Model System.....	68
4.1.1	Influence of Initial pH value	68
4.1.2	Influence of Initial Immunoglobulin Concentration	70
4.1.3	Influence of Nitrogen Flow Rate	71
4.1.4	Influence of Initial Albumin Concentration	73
4.1.5	Influence of Column Height.....	74
4.1.6	Influence of Foaming Time	76

4.1.7 Separating of IgG and IgM	79
4.1.8 Testing of Different Multi-Component Mixtures	80
4.2 Enrichment of Immunoglobulin in a Milk System	81
4.2.1 Influence of Initial pH value	81
4.2.2 Influence of Initial Immunoglobulin Concentration	83
4.2.3 Influence of Column Height	85
4.2.4 Influence of Nitrogen Flow Rate	87
4.2.5 Influence of Foaming Time	89
4.3 Using RSM in a Model System	93
4.3.1 Experimental Design of Variables and Results for IgG	93
4.3.2 Enrichment Ratio of IgG Using Foam Fractionation	94
4.3.3 Recovery of IgG Using Foam Fractionation	103
4.3.4 Optimization of the Operating Variables for IgG Foam Fractionation	112
4.3.5 Optimization of the Operating Variables for IgM Foam Fractionation	113
4.4 Using RSM in a Milk System	116
4.4.1 Experimental Design of Variables and Results for IgG	116
4.4.2 Enrichment Ratio of IgG Using Foam Fractionation	117
4.4.3 Recovery of IgG Using Foam Fractionation	126
4.4.4 Optimization of the Operating Variables for IgG Foam Fractionation	135
4.4.5 Optimization of the Operating Variables for IgM Foam Fractionation	136
5. Summary and Conclusions	139
6. Literature	146

List of Figures

Figure 2.1 Simplified representation of a basic immunoglobulin unit.....	6
Figure 2.2 Horizontal representation of adsorptive bubble separation.....	12
Figure 2.3 A photo representation of foam	22
Figure 2.4 A cross section of films with the Plateau borders between them	23
Figure 2.5 Central composite designs for a two variables example	42
Figure 3.1 Basic components and flow of the foam fractionation equipment.....	45
Figure 3.2 Standard curve of different concentrations of rabbit IgG.....	48
Figure 3.3 Standard curve of different concentrations of human IgM	48
Figure 3.4 Flowchart of RSM process.....	57
Figure 3.5 Central composite design for a three-variable example	59
Figure 4.1 Enrichment of rabbit IgG and human IgM in response to the initial pH value	69
Figure 4.2 Enrichment of rabbit IgG and human IgM in response to the initial immunoglobulin concentration.....	71
Figure 4.3 Enrichment of rabbit IgG and human IgM in response to nitrogen flow rate	72
Figure 4.4 Enrichment of rabbit IgG and human IgM in response to the initial albumin concentration	74
Figure 4.5 Enrichment of rabbit IgG and human IgM in response to the column height	76
Figure 4.6 Enrichment of rabbit IgG and human IgM in response to the foaming time	77
Figure 4.7 Recovery of rabbit IgG and human IgM in response to the foaming time	78
Figure 4.8 Enrichment ratio of rabbit IgG and human IgM in response to the initial pH value in a mix solution containing both IgG and IgM.....	79
Figure 4.9 Enrichment ratio of rabbit IgG from serum and milk in response to the initial pH value	80
Figure 4.10 Enrichment of rabbit IgG from milk in response to the initial pH value	82

Figure 4.11 Enrichment of human IgM from milk in response to the initial pH value	83
Figure 4.12 Enrichment ratio of rabbit IgG in response to the initial immunoglobulin concentration	84
Figure 4.13 Enrichment ratio of human IgM in response to the initial immunoglobulin concentration	85
Figure 4.14 Enrichment ratio of rabbit IgG in response to the column height.....	86
Figure 4.15 Enrichment ratio of human IgM in response to the column height.....	87
Figure 4.16 Enrichment ratio of rabbit IgG in response to the nitrogen flow rate	88
Figure 4.17 Enrichment ratio of human IgM in response to the nitrogen flow rate ...	89
Figure 4.18 Enrichment ratio of rabbit IgG in response to the foaming time	90
Figure 4.19 Enrichment ratio of human IgM in response to the foaming time	91
Figure 4.20 Recovery of rabbit IgG in response to the foaming time	92
Figure 4.21 Recovery of human IgM in response to the foaming time	92
Figure 4.22 Perturbation plot for the enrichment ratio of IgG in a model system ...	101
Figure 4.23 Two-dimensional isoresponse curve for the enrichment ratio of IgG...	102
Figure 4.24 Three-dimensional surface for the enrichment ratio of IgG.....	103
Figure 4.25 Perturbation plot for the recovery of IgG in a model system.....	110
Figure 4.26 Two-dimensional isoresponse curve for the recovery of IgG	111
Figure 4.27 Three-dimensional surface for the recovery of IgG in a model system	112
Figure 4.28 Perturbation plot for the enrichment ratio of IgG in a real system	124
Figure 4.29 Two-dimensional isoresponse curve for the enrichment ratio of IgG...	125
Figure 4.30 Three-dimensional surface for the enrichment ratio of IgG.....	126
Figure 4.31 Perturbation plot for the recovery of IgG in a real system.....	133
Figure 4.32 Two-dimensional isoresponse curve for the recovery of IgG	134
Figure 4.33 Three-dimensional surface for the recovery of IgG in a real system....	135

List of Tables

Table 2.1	Approximate concentration of major components in milk	29
Table 2.2	Bovine milk proteins and some of their properties.....	31
Table 3.1	Experimental codes, ranges and levels of the three selected independent process variables.....	59
Table 3.2	Experimental design of process variables for IgG in a model system.....	60
Table 3.3	Experimental design of process variables for IgG in a real system.....	67
Table 4.1	Experimental design of process variables and results for IgG in a model system showing values for the response variables calculated from measurements ...	93
Table 4.2	The sequential model sum of squares for the IgG enrichment ratio	94
Table 4.3	The lack of fit tests for the IgG enrichment ratio in a model system.....	95
Table 4.4	The model summary statistics for the IgG enrichment ratio.....	96
Table 4.5	The analysis of variance table for the IgG enrichment ratio	99
Table 4.6	The sequential model sum of squares for the IgG recovery.....	104
Table 4.7	The lack of fit tests for the IgG recovery in a model system	105
Table 4.8	The model summary statistics for the IgG recovery in a model system ...	106
Table 4.9	The analysis of variance table for the IgG recovery in a model system ...	108
Table 4.10	Predicted solutions for both the enrichment ratio and recovery of IgG from foam fractionation in a model system.....	113
Table 4.11	Predicted solutions for both the enrichment ratio and recovery of IgM from foam fractionation in a model system.....	115
Table 4.12	Experimental design of process variables and results for IgG in a real system showing values for the response variables calculated from measurements ..	116
Table 4.13	The sequential model sum of squares for the IgG enrichment ratio	117
Table 4.14	The lack of fit tests for the IgG enrichment ratio in a real system.....	118
Table 4.15	The model summary statistics for the IgG enrichment ratio.....	119
Table 4.16	The analysis of variance table for the IgG enrichment ratio	122
Table 4.17	The sequential model sum of squares for the IgG recovery.....	127
Table 4.18	The lack of fit tests for the IgG recovery in a real system	128
Table 4.19	The model summary statistics for the IgG recovery in a real system	129
Table 4.20	The analysis of variance table for the IgG recovery in a real system	131

Table 4.21 Predicted solutions for both the enrichment ratio and recovery of IgG from foam fractionation in a real system.....	136
Table 4.22 Predicted solutions for both the enrichment ratio and recovery of IgM from foam fractionation in a real system.....	138

List of Abbreviations

ABS	Adsorptive Bubble Separation
ATPS	Aqueous Two-Phase System
BCA	Bicinchoninic Acid
BSA	Bovine Serum Albumin
CCD	Central Composite Design
c.m.c.	critical micelle concentration
DOE	Design of Experiments
ER	Enrichment Ratio
HIC	Hydrophobic Interaction Chromatography
IEC	Ion Exchange Chromatography
IgG	Immunoglobulin G
IgM	Immunoglobulin M
IMAC	Immobilized Metal Affinity Chromatography
PB	Plateau Borders
PEG	Polyethylene Glycol
pI	Isoelectric Point
R	Recovery
RSM	Response Surface Methodology
SPC	Statistical Process Control

1. Introduction

The demand for purified biochemicals, such as proteins has markedly increased in the last few decades. As such, there is an interest in cost-effective methods that can isolate and enrich biochemicals. Immunoglobulins represent an important kind of protein in the biological sciences, with numerous pharmaceutical or biotechnological applications.

Immunoglobulins, also known as antibodies, are gamma globulin proteins produced in the blood and other body fluids of humans and other vertebrate species. They are one of the defense mechanisms for defending organisms against invasion by irritants known as antigens, such as bacteria, viruses, or other foreign matter. Each animal can produce millions of different kinds of immunoglobulins, each immunoglobulin being able to bind to a particular antigen [GALFRE and SECHER 1990].

Immunoglobulins act as the first line of defense against many infections and diseases [BUTLER 1983, EL-LOLY 2007, HEREMANS 1974a, HEREMANS 1974b, KORHONEN 1998, KORHONEN, *et al.* 2000, TOMASI and BIENENSTOCK 1968]. And, due to their inherent ability to prevent infections and control diseases, immunoglobulins have been used in many forms, such as colostrums, milk-derived products and concentrated immunoglobulins [EL-LOLY 2007, KELLY 2003, KORHONEN, *et al.* 2000]. Immunoglobulins are used in a wide variety of applications, such as disease treatment [HILPERT, *et al.* 1987, ZEITLIN, *et al.* 2000], infection control [LILIUS and MARNILA 2001], prenatal therapy [KELLY 2003, STEPHAN, *et al.* 1990], functional foods [DONOVAN and ODLE 1994, KORHONEN 1998] and various research applications. Bovine colostrums and milk derived products are good sources for a large number of naturally-contained antimicrobial substances [REITER and ORAM 1967], growth factors [DONOVAN and ODLE 1994, PAKKANEN and AALTO 1997] and nutrients [BUTLER 1983, PAKKANEN and AALTO 1997, REITER and ORAM 1967]. Enriched bovine colostrums, produced from hyper-immunized cows, are also a very good source of immunoglobulins, and

have been used as raw material to provide passive immunity to neonates to protect them from a variety of pathogens during early development of their own immune systems [LILIUS and MARNILA 2001, WEINER, *et al.* 1999, ZEITLIN, *et al.* 2000]. They are also used for patients who suffer from gastrointestinal-tract-related infections [HILPERT, *et al.* 1987, STEPHAN, *et al.* 1990].

Isolated and purified immunoglobulins are also used in many research applications, including the use of immunoglobulins to identify and locate intracellular and extracellular proteins, as well as in immuno-precipitation, electrophoresis, immuno-fluorescence and immunoassays [BUTLER 1969, BUTLER 1983]. Immunoglobulins with specific activities can be produced through hyper-immunization protocols, using vaccines containing inactivated pathogenic microbial material against which immunoglobulin activities are desired [HUSU, *et al.* 1993, KUROIWA, *et al.* 2009]. Immunoglobulins can be enriched further by applying various processing technologies. Production of immunoglobulin-enriched products, which contain crude or purified immunoglobulins, has beneficial applications in both human and animal healthcare [KELLY 2003].

The enrichment of immunoglobulin is rather complex due to the fact that the current production techniques result in complex mixtures with a large number of contaminants present [CALMETTES, *et al.* 1991, GALFRE and SECHER 1990, LIU, *et al.* 2002, VANCAN, *et al.* 2002]. Most of the immunoglobulin-enrichment methods developed so far involve multiple steps, thus are time-consuming and complex. The traditional methods also cost a lot and involve the use of solvents or reagents that are often undesirable for the environment. As stated above, traditional immunoglobulin enrichment methods, based mostly on chromatographic processes, generally involve costly purification and lead to expensive final products. As such, there is a definite need to develop techniques capable of increasing capacity and decreasing total costs. Foam fractionation represents a promising method for separation and concentration of biochemicals. It is simple, easily scalable, inexpensive and environmentally

friendly. Foam fractionation thus represents an alternative to the traditional methods used for immunoglobulin enrichment. However, little, if any, literature exists documenting the utilization of foam fractionation in the enrichment of immunoglobulins.

Foam fractionation is based on the tendency of certain molecules (or colloids) present in highly dilute aqueous solutions to preferentially adsorb at the large gas-liquid interface of foams generated by injecting gas into a solution via a frit to increase bubble formation, such bubbles subsequently rising upwards.

The application of foam fractionation to biological products is not commonly used for two main reasons. The first is the lack of a sufficient understanding of the complex principles governing the process, both for the gas-liquid dispersion hydrodynamics and for the protein adsorption mechanisms (which makes prediction of the performance difficult). The second is the presumed denaturation of the biological molecules during the process. Malysa and Warszynski studied the dynamic effects (motion) associated with foam-layer formation and stability, wherein they observed that the competition between the rate of equilibrium coverage reestablishment (disequilibrium induced by motion) by surface diffusion (increasing the stability of film) and the rate of film drainage (decreasing the stability of film) determines the volume and stability of the foam layer [MALYSA and WARSZYNSKI 1995]. Also, Bhakta and Ruckenstein have reviewed the theoretical work on static foam decay and compared various models in terms of their ability to describe drainage, coalescence, and collapse of foam [BHAKTA and RUCKENSTEIN 1995].

Still, in spite of this extensive body of work in the literature, a detailed mathematical description of the complex mass transfer process, which depends on the operational modes (continuous, semi-batch, or static foam) and the physicochemical properties of the solution and surfactants, is very complex and has not been done to date in a relatively simple model. However, protein denaturation (the loss of biological activity owing to the change, usually unfolding, of the molecular tertiary structure) occurring when biological

molecules are exposed to a gas-liquid surface can be minimized by choosing suitable operating conditions. A number of researches have noted that foam separation can be used successfully for the purification of proteins and enzymes without necessarily adversely affecting the protein structure. As such, it appears that there are no significant obstacles blocking use of foam fractionation processing of protein molecules.

1.1 Objectives

The overall aim of this research is to develop an enrichment process for immunoglobulin using foam fractionation that reduces costs and lowers the risk of damage to the environment. Various processes have been used to enrich immunoglobulins, but this appears to be the first time that foam fractionation has been applied to immunoglobulin enrichment. To accomplish the overall aim of this work, the research was divided into three distinct phases or steps, each with its own associated sub-objective. In that there are several different parameters affecting the efficiency of foam fractionation, a model system was first utilized to help select the test ranges for different parameters. The first objective is to study the different factors affecting the enrichment of immunoglobulin using foam fractionation. The separation of IgG and IgM by foam fractionation was also investigated. Next, serum and milk were utilized as an immunoglobulin source to serve as examples of a real system. The second objective is to develop a foam fractionation process for selective enrichment of immunoglobulin from a multi-component mixture. Lastly, the statistical method known as response surface methodology (RSM) was applied in this work to help analyze the interaction and relative importance of different starting conditions (factors). RSM can also be used to predict results from various starting conditions and to provide starting conditions for obtaining optimal results. The third objective is to enhance the effectiveness and convenience of enriching immunoglobulin by foam fractionation using RSM.

2. Theoretical Background

2.1 Immunoglobulin

2.1.1 Properties of Immunoglobulin

Immunoglobulins, also known as antibodies, are gamma globulin proteins produced in the blood and other body fluids of humans and other vertebrate species. They are one of the defense mechanisms for defending organisms against invasion by irritants known as antigens, such as bacteria, viruses, or other foreign matter. Each animal can produce millions of different kinds of immunoglobulins, each immunoglobulin being able to bind to a particular antigen [GALFRE and SECHER 1990].

Structurally, all immunoglobulin molecules are comprised of at least one Y-shaped unit based on four polypeptide chains, wherein a pair of identical heavy chains is attached to another pair of identical light chains (Figure 2.1). The heavy chains constitute a so-called constant region that is responsible for the characteristics of immunoglobulin molecules in the immune system, whereas the light chains are responsible for defining the antigen-binding specificity. The terms heavy and light used here correspond to the relative molecular weights of the chains, wherein a heavy chain is approximately double the weight of a light chain.

There are five main classes of immunoglobulins that exist in mammals: IgG, IgM, IgA, IgD and IgE. Each class is classified based on the characteristics of that class's heavy chains. Some of the five main classes are further divided into subclasses, such as IgG1 and IgG2 in the IgG class. Additionally, various subclasses show slight variations in the heavy chain structure within a given class. IgG and IgM were both taken as target immunoglobulins in this research. IgG is the main immunoglobulin class in normal serum and is the critical immunoglobulin for secondary immune responses. IgM only accounts for approximately 10% of the immunoglobulin pool, but it is the critical

immunoglobulin of the primary immune response. The IgM molecule consists of five Y-shaped subunits and corresponds roughly to a pentameric form of the basic IgG molecule, the five Y-shaped subunits being linked together in a circular form by disulfide bond and the so-called J-chain. In this work, the relative importance of IgG and IgM is the main reason why they were selected as targets.

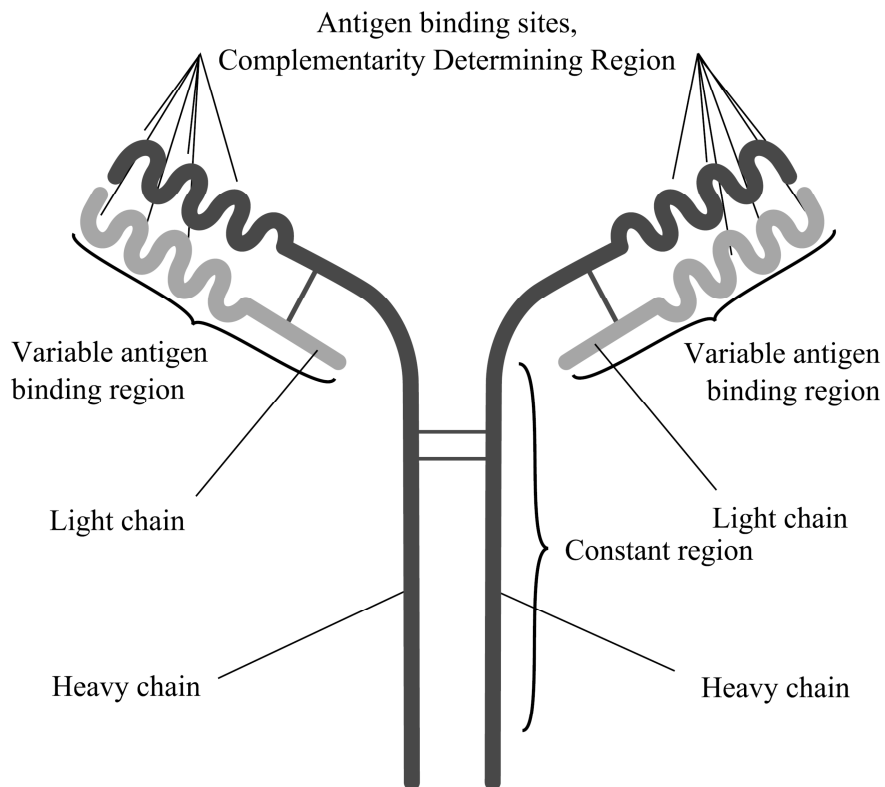


Figure 2.1: Simplified representation of a basic immunoglobulin unit [MRC 2005]

By way of background, it should be held in mind that immunoglobulins are fragile compounds. As such, the risk of denaturation of these proteins needs to be taken into consideration during the enrichment process. Denaturation refers to structural changes of the proteins, which, in the case of immunoglobulin, compromise/defeat their efficacy. Various factors can induce denaturation, such as extreme temperature and pH, such factors being extensively described in the literature [GRAY 1993]. Due to the fragility of immunoglobulins, the design of any immunoglobulin-enrichment process must carefully avoid factors that can cause denaturation.

2.1.2 Applications of Immunoglobulin

Immunoglobulins act as the first line of defense against many infections and diseases [BUTLER 1983, EL-LOLY 2007, HEREMANS 1974a, HEREMANS 1974b, KORHONEN 1998, KORHONEN, *et al.* 2000, TOMASI and BIENENSTOCK 1968]. Due to their inherent ability to prevent infections and control diseases, immunoglobulins have been used in many forms, such as colostrums, milk derived products and concentrated immunoglobulins [EL-LOLY 2007, KELLY 2003, KORHONEN, *et al.* 2000]. Immunoglobulins are used in a wide variety of applications, such as disease treatment [HILPERT, *et al.* 1987, ZEITLIN, *et al.* 2000], infection control [LILIUS and MARNILA 2001], prenatal therapy [KELLY 2003, STEPHAN, *et al.* 1990], functional foods [DONOVAN and ODLE 1994, KORHONEN 1998] and various research applications. Bovine colostrums and milk derived products are good sources for a large number of naturally-contained antimicrobial substances [REITER and ORAM 1967], growth factors [DONOVAN and ODLE 1994, PAKKANEN and AALTO 1997] and nutrients [BUTLER 1983, PAKKANEN and AALTO 1997, REITER and ORAM 1967]. Enriched bovine colostrums, produced from hyper-immunized cows, are also a very good source of immunoglobulins, and have been used as a raw material to provide passive immunity to neonates to protect them from a variety of pathogens during early development of their own immune systems [LILIUS and MARNILA 2001, WEINER, *et al.* 1999, ZEITLIN, *et al.* 2000]. They are also used for patients who suffer from gastrointestinal-tract-related infections [HILPERT, *et al.* 1987, STEPHAN, *et al.* 1990].

Isolated and purified immunoglobulins are also used in many research applications, including using immunoglobulins to identify and locate intracellular and extracellular proteins, as well as in immuno-precipitation, electrophoresis, immuno-fluorescence and immunoassays [BUTLER 1969, BUTLER 1983]. Immunoglobulins with specific activities can be produced through hyper-immunization protocols, using vaccines containing inactivated pathogenic microbial material against which immunoglobulin activities are desired [HUSU,

et al. 1993, KUROIWA, *et al.* 2009]. Immunoglobulins can be enriched further by applying various processing technologies. Production of immunoglobulin-enriched products, which contain crude or purified immunoglobulins, has beneficial applications in both human and animal healthcare [KELLY 2003].

2.1.3 Traditional Methods for Immunoglobulin Enrichment

The enrichment of immunoglobulin is rather complex due to the fact that the current production techniques result in complex mixtures with a large number of contaminants present [CALMETTES, *et al.* 1991, GALFRE and SECHER 1990, LIU, *et al.* 2002, VANCAN, *et al.* 2002]. This section describes the traditional methods available for the enrichment of immunoglobulin. Of these methods, chromatography is predominately used, wherein protein A affinity purification is usually used in combination with at least one ion exchange step [BIRCH and RACHER 2006]. In addition, other refining steps, such as ion exchange, hydrophobic interaction and size exclusion chromatography, can be used [HOLSCHUH and SCHWAMMLE 2005]. A concise overview of the traditional enrichment methods available is provided below.

Protein A has been extensively used as an affinity support for the isolation of certain immunoglobulins, among them immunoglobulin G (IgG). Protein A is a cell wall associated protein domain exposed on the surface of the Gram-positive bacterium *Staphylococcus aureus*. Protein A affinitively interacts with some groups of immunoglobulins, which is the reason for its broad application in immunoglobulin separation. The separation mechanism is quite simple: selective binding of the immunoglobulin and subsequent recovery by elution. The simplicity of this process is a clear advantage, but the cost of the columns is much higher than that of conventional ion exchange columns. Additionally, the price of protein A media is several times the cost of non-affinity supports, thus raising the cost per unit of target product.

Ion exchange chromatography (IEC) was first successfully applied to fractionation of plasma proteins in the mid-1950s. By the 1970s it was firmly established as a standard method for purification of immunoglobulins. Ion exchange chromatography separates immunoglobulins based on the pH value, which affects the polarity of the immunoglobulins. If the pH is acidic, the immunoglobulins are present in cation form. Conversely, if the pH is basic, the immunoglobulins are present in anion form. The net charge of the immunoglobulin interacts with a charged column. This means that the optimum state in which to operate is far from the isoelectric point (pI), in which the immunoglobulins have a neutral net charge [LIU, *et al.* 2003]. However, one of the most important difficulties with IEC is the potential of losing glycosylation isoforms of immunoglobulin. So, the use of IEC in immunoglobulin production has its limitations.

Another strategy involves purifying immunoglobulins with immuno-affinity columns, which can lead to very high selectivity. Immuno-affinity chromatography usually consists of silica gel columns with ligands that have a highly specific interaction with the desired immunoglobulins to be captured. This technique is not only used for the purification of immunoglobulins but is also widely applied in the manufacture and detection of pesticides, drugs, and hormones. However, despite the obvious advantages, immuno-affinity chromatography has some unfortunate disadvantages, like degradation or leaching of ligands, which consequently raise costs [FASSINA, *et al.* 2001, JOHNSON 1986, STEVENSON 2000, SUBRAMANIAN 2002].

Recently, hydrophobic interaction chromatography (HIC) has been utilized to separate immunoglobulins. Immunoglobulins can interact with the stationary phase through hydrophobic residues on the surface of proteins, such as leucine. Hydrophobic interaction chromatography leads to high selectivity and capacity, which both lead to favorable industrial applications. Also, under favorable conditions of ionic strength and pH, immunoglobulins can be adsorbed, which increases industrial applicability [BOSCHETTI and GUERRIER 2001]. However, the risk of immunoglobulin denaturation due to excessively

hydrophobic support material is the greatest concern with HIC. Unfortunately, many HIC ligands provide more than sufficient energy to cause denaturation, and numerous studies have confirmed on-column protein-conformational changes.

Immobilized metal affinity chromatography (IMAC) is a chromatographic method that can be used to purify immunoglobulins. The origins of IMAC date to the early 1960s, but it didn't emerge as practical tool for protein purification until 1975. IMAC is based on specific coordinate covalent binding between amino acids and various immobilized metal ions, such as copper, nickel, zinc and cobalt. Its strengths are that it gives good capacities and selectivities for immunoglobulin enrichment [VANCAN, *et al.* 2002]. However, some metals, such as nickel, are toxic in biological systems and will precipitate many immunoglobulins.

In the literature, the application of reverse micellar extraction or aqueous two-phase system (ATPS) extraction for the specific case of immunoglobulin separation is reported less than other methods. However, reverse micellar extraction of proteins using anionic surfactant and isooctane as a solvent has received some attention [CABRAL and AIRES-BARROS 1993, HONG, *et al.* 2000, NISHIKI, *et al.* 1998, VASUDEVAN, *et al.* 1995, WOLL, *et al.* 1989]. Reverse micelles have the ability to solubilize proteins or other bio-compounds in an organic phase, allowing recovery and concentration from diluted aqueous solutions. Although an immunoglobulin molecule is bigger in size than an average protein, its behavior is similar to other proteins and thus can be separated by reverse micellar extraction [GERHARDT and DUNGAN 2002]. Some immunoglobulins can also be separated using their antigen-immunoglobulin ligands in reverse micelles and non-ionic surfactants. However, due to insufficient interaction of the protein with the surfactant, a specific anionic surfactant needs to be introduced into the system. Unfortunately, the anionic surfactant may cause strong denaturation [ADACHI, *et al.* 2000]. In the case of ATPS extraction, its successful incorporation for use in purification processes is still far from optimum and there is still room for further optimization [LOW, *et al.* 2007]. Still, some literature does exist regarding the specific application of ATPS for purification of IgG. Using ATPS extraction with polyethylene glycol (PEG),

IgG can be extracted in polymer-polymer or polymer-salt ATPS [AZEVEDO, *et al.* 2007a, AZEVEDO, *et al.* 2007b, ROSA, *et al.* 2007]. Nevertheless, difficulties remain regarding the use of the ATPS methods as a platform step due to complex interactions of the multiple components involved.

As stated above, traditional immunoglobulin enrichment methods, based mostly on chromatographic processes, generally involve costly purification and lead to expensive final products. As such, there is a definite need to develop techniques capable of increasing capacity and decreasing total costs. Foam fractionation, which uses no organic solvents, is a candidate for the enrichment of biochemicals, and, on a larger scale, could be a method to substitute for or complement the currently available separation techniques. Therefore, foam fractionation processes have much potential due to their simplicity and scalability. However, little, if any, literature exists documenting the utilization of foam fractionation in the enrichment of immunoglobulin.

2.2 Foam Fractionation

2.2.1 Adsorptive Bubble Separation

Adsorptive bubble separation (ABS) comprises various methods of separating dissolved or suspended materials by means of adsorption or attachment at the surface of bubbles rising through a liquid [LEMLICH 1972a]. A horizontal representation for ABS is presented in Figure 2.2

The first level, generic adsorptive bubble separation (ABS) may be subdivided into two major categories: foam separation and non-foaming ABS. These categories, in turn, have their corresponding subdivisions. A comprehensive description of the main categories and corresponding subdivisions is given in the works from various groups of scientists [KARGER, *et al.* 1967, LEMMICH 1972b, MAHNE 1971]. The main distinction between foam separation and non-foaming ABS is that foam separation requires generation of foam or froth to carry off the materials while the non-foaming ABS does not.

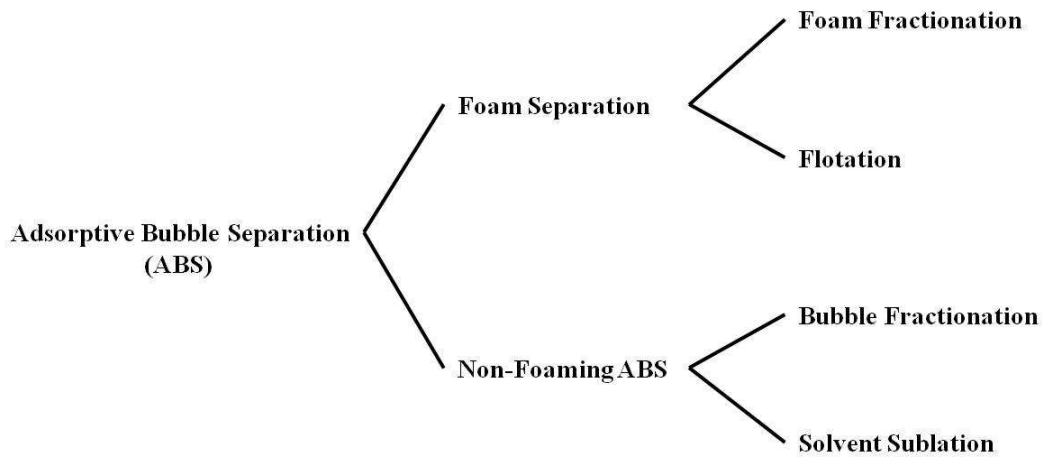


Figure 2.2 Horizontal representation of adsorptive bubble separation

Non-foaming ABS includes two subdivisions: bubble fractionation and solvent sublation. Bubble fractionation is the adsorption of molecular or particulate materials at the surface of rising bubbles followed by re-deposition at *or just under the surface of the liquid pool*. Solvent sublation is the adsorption of molecular or particulate materials at the surface of rising bubbles, followed by re-deposition at *either the interface of an immiscible liquid or atop the main liquid*.

Foam separation includes two subdivisions: flotation and foam fractionation. Flotation is the removal of particulate materials by foaming. Foam fractionation, the other subdivision of foam separation, is dealt with in detail in the main section that follows since it is the method utilized for the immunoglobulin enrichment in the current work.

2.2.2 Principles of Foam Fractionation

Foam fractionation is based on the tendency of certain molecules (or colloids) present in highly dilute aqueous solutions to preferentially adsorb at the large gas-liquid interface of foams generated by injecting gas into a solution, via a frit to increase bubble formation, such bubbles subsequently rising upwards.

The principles of how foam fractionation works are summarized in the classic book “Progress in Separation and Purification” by Lemlich [LEMLICH 1968]. A survey of the recent literature indicates a renewed interest in using foam fractionation to separate proteins and enzymes. The current interest seems to indicate a desire for a low-cost, highly effective purification method for biological products, particularly in the first concentration step that is used to remove about 90% of the water from dilute solutions. Several papers further support these studies by providing a theoretical understanding and empirical observations of protein foam fractionation [HALLER, *et al.* 2010, LINKE, *et al.* 2007, LOCKWOOD, *et al.* 2000, URAIZEE and NARSIMHAN 1990a, URAIZEE and NARSIMHAN 1990b].

The primary mechanisms underlying foam fractionation are as follows: First, surface-active substances such as proteins preferentially adsorb on bubble surfaces (generated by bubbling gas through a solution). Second, the surface-active substances are carried upwards by the bubbles as they rise, the bubbles then accumulating at and above the surface of the solution. Finally, as these bubbles (the foam phase) collapse, a concentrated protein solution (foamate) remains and is recovered from the low liquid content foam phase.

2.2.3 Adsorption in Foam Fractionation

The ability of molecules to adsorb at a gas-liquid interface is defined by the physicochemical properties of the molecules. The properties of both dilute aqueous solutions and the gas-liquid interface created by such solutions are well understood these days. Like pure water, dilute aqueous solutions have a polar nature and the gas-liquid interface formed between such solutions and gases is of a non-polar nature. The ability of dissolved molecules to transfer from the bulk of a polar liquid to a non-polar interface depends either on the possession by these molecules of an hydrophobic and an hydrophilic part or on them being hydrophobic [ADAMSON 1960, KISHIMOTO 1962, LEMLICH 1972b, LEMLICH 1972c, MAAS 1974, PARTHASARATHY, *et al.* 1988, TOWNSEND and NAKAI 1983, URAIZEE and NARSIMHAN 1996]. This

transfer process is also known as a partition process and is directly connected to the physicochemical properties of the molecules [LEMLICH 1972a, NOBLE, *et al.* 1998, NORD 2000].

A large gas-liquid interface provides a large surface for adsorption, which is an important requirement for mass transfer to take place. In foam fractionation, the large surface for adsorption is created with the generation of foam by bubbling a gas through an aqueous dilute solution. The foaming of various solutions depends on the presence in solution of surface-active solutes that lower the surface tension [MAAS 1974]. Foam is a disperse system that contains a high surface area formed by bubbles that possess a certain life-time [KITCHENER and COOPER 1959]. Adsorption is a time-dependent process; consequently, the average life-time of the bubbles is an important factor for adsorption.

Adsorption is the phenomenon governing enrichment by foam fractionation. A large variety of factors have an influence on adsorption, and, as a result, on the effectiveness of the enrichment. Foam fractionation is possible due to the material (or a complex of it with other materials) to be separated selectively adsorbing at the gas-liquid interface. The principles of adsorption of materials at the gas-liquid interface are important to understanding the theory and mechanisms by which the various materials interact in a dilute solution leading to separation.

Adsorption of materials at the gas-liquid interface occurs when the interaction among solvent water molecules is greater than among the solute molecules, hence the existence of solute molecules interferes with the water molecules and conditions for their existence are more desirable at the gas-liquid interface than in the bulk of the liquid [CHARM 1972, SOMASUNDARAN 1972]. As the size of a hydrophobic molecule increases, or the size of hydrophobic part for surface active molecules with a hydrophilic and a hydrophobic part increases, the molecules interfere with the water molecules to a greater extent, making it even less desirable for them to stay in the bulk [SOMASUNDARAN 1972]. Therefore, an increase in overall-size causes an increase in adsorption.

For organic molecules, the increase of hydrocarbon chain length and the presence of halogens in the molecules increases hydrophobicity, while the presence of polar groups, hetero-atoms (such as oxygen and nitrogen), ramifications, double bonds and triple bonds decreases the hydrophobicity [DAVIES and RIEDEL 1963]. Molecules that only possess a hydrophobic part are non-surface active, and their separation by foam requires the careful addition of surface active materials; however, the presence of such surface active materials in the solution represents competition for adsorption sites for the hydrophobic molecules [KELLER, *et al.* 1997, SOMASUNDARAN 1972]. Another factor that is also detrimental to the adsorption of the desired molecule is the presence of other hydrophobic molecules in solution.

The adsorption of a non-ionic surfactant molecule onto a gas-liquid interface is generally considered to be governed by two processes: (1) the diffusion of the surfactant molecule to the sub-surface from the bulk solution, and (2) the adsorption of the molecule from the sub-surface onto the interface. Diffusion-controlled models assume a local equilibrium between the sub-surface and the interface. Thus the rate of adsorption is determined by the mass transfer from the bulk solution to the sub-surface, which is described by the Ward-Tordai equation.

2.2.4 Diffusion Mechanisms of Adsorption

The most theoretical work regarding surfactant adsorption onto the gas-liquid interface was published by Ward and Tordai in 1946 [WARD and TORDAI 1946]. The Ward and Tordai theory accounts for the diffusion of monomers from the bulk to the interface, and also the back diffusion into the bulk as the interface becomes more crowded. At the start of the process, monomers from the subsurface adsorb directly, the assumption being that every molecule arriving at the interface is likely to arrive at an empty site, a reasonable assumption for the start of adsorption. However, as the surface becomes more crowded, there is an increased probability that a monomer will arrive at an already occupied site, at

which point back diffusion from the subsurface to the bulk must then also be considered.

The rate at which certain non-ionic molecules can adsorb to a bubble surface can be estimated by solving the following the Ward-Tordai equation.

$$\Gamma(t) = 2 \sqrt{\frac{D}{\pi}} \left\{ C_b \sqrt{t} - \int_0^{\sqrt{t}} C(\tau) d(\sqrt{t-\tau}) \right\} \quad (2.1)$$

where:

$\Gamma(t)$ is the dynamic surface excess

D is the coefficient of molecular diffusion

C_b is the bulk concentration

$C(\tau)$ is the sub-surface concentration

t is time since the formation of the fresh surface

τ is a dummy variable with the units of time

The equation of Ward and Tordai was an important contribution to the theory of diffusion-controlled adsorption. However, it is not convenient to directly use the equation to explain experimental data since neither the surface excess nor the sub-surface concentration can be easily measured. Thus, theoretical models are needed to describe the adsorption of materials at the gas-liquid interface, such as the famous Gibbs isotherm. Eastoe and Dalton also summarize five different equilibrium relationships to relate the surface excess to the sub-surface concentration, the so-called adsorption isotherms. These include the Henry isotherm, Langmuir isotherm, Frumkin isotherm, Freundlich isotherm and Volmer isotherm [EASTOE and DALTON 2000].

2.2.5 Thermodynamics of Adsorption

Several theoretical models are available for describing the adsorption of materials at the gas-liquid interface. The most popular, developed by Lemlich, is

based on the Gibbs adsorption theorem [GIBBS 1928, LEMLICH 1968, LEMLICH 1972b]. The equilibrium adsorption of a dissolved material at the gas-liquid interface is given by Gibbs as:

$$d(\gamma) = - RT \sum \Gamma d(\ln a) \tag{2.2}$$

where:

γ is the surface tension

R is the gas constant

T is the absolute temperature

Γ is the surface excess of the component

a is the activity of the component

The adsorption of dissolved materials at the interface reduces the surface tension (γ) of the solution. In practice, there are difficulties in accurately measuring small changes in the surface tension (γ), and doing so requires knowledge of the activity coefficients in order to obtain the activities (a), which severely limit the utility of the above equation. As a result, its application is practical only in special cases. The most important among these is the case of a single non-ionic surface active solute dissolved in pure water at a sufficient low concentration such that the activity coefficient is constant. For this case, the above equation simplifies to the following equation:

$$\Gamma = - \frac{1}{RT} \frac{d(\gamma)}{d(\ln C)} \tag{2.3}$$

where:

Γ is the equilibrium surface excess of component

R is the gas constant

T is the absolute temperature

γ is the surface tension

C is the concentration of component in the bulk

The adsorption isotherm (Gibbs isotherm), which is the equilibrium surface excess (Γ) versus concentration (C), can therefore be obtained by measuring the surface tension (γ) at various bulk surfactant concentrations. In accordance with the above equation at concentrations below the critical micelle concentration (c.m.c.), an equilibrium surface excess (Γ) that is constant means that the surface reached saturation. Methods like foam fractionation operate best at low solute concentrations in solutions [KARGER and DEVIVO 1968]. At high concentrations, aggregates or micelles are formed, which may interfere with adsorption [MAAS 1974]. The specific concentration level at which the micelles start to form is the critical micelle concentration (c.m.c.). At concentrations above the critical micelle concentration, the above equation does not apply, as micelles constitute another species.

The main problem for interpreting dynamic surface tension (γ) is the proper selection of an appropriate isotherm. The purpose of an adsorption isotherm is to relate the surfactant concentration in the bulk and the adsorbed amount at the interface. It is assumed that adsorption is monomolecular. In addition to the Gibbs isotherm, a number of other equations are used. These include the Henry, Langmuir, Frumkin, Freundlich, and Volmer isotherms mentioned earlier. The foregoing is a list of traditional isotherms used in solution chemistry, although there have also been recent advancements to account for other physical properties of surfactants. Being the most fundamental isotherms, the Henry isotherm and the Langmuir isotherm are described in further detail below.

The Henry isotherm is the simplest isotherm. In accordance with simple adsorption theory, the effect of solute concentration in solution (C) on the solute concentration at the surface (Γ) for the adsorption process is linear and can be expressed by the following equation:

$$\Gamma = K_H C \tag{2.4}$$

where:

Γ is the equilibrium surface excess of surfactant

K_H is the equilibrium adsorption constant (an empirical measure of the surface activity of the surfactant)

C is the concentration of surfactant in the bulk

The Langmuir isotherm is the most commonly used non-linear isotherm. It is based on the assumption of equivalent and independent adsorption sites at the surface. The rate of change of surface coverage due to *adsorption* is proportional to both the amount of surfactant in solution and the number of vacant sites available. The rate of change of the equilibrium surface excess (Γ) due to *desorption* is proportional to the number of adsorbed species. At equilibrium, these two rates are equal, and introducing the Langmuir equilibrium adsorption constant K ($K = K_{\text{ads}} / K_{\text{des}}$) results in the Langmuir isotherm equation:

$$\Gamma = \Gamma_{\infty} \left(\frac{KC}{1+KC} \right) \quad (2.5)$$

where:

Γ is the equilibrium surface excess of surfactant

Γ_{∞} is the surface excess at saturation

K is the Langmuir equilibrium adsorption constant

C is the concentration of surfactant in the bulk

Deviations from the Langmuir isotherm may be attributed to the failure of the assumption of equivalent and independent sites. For example, intermolecular deviations from the Langmuir isotherm may be attributed to the failure of this assumption. Such intermolecular forces act between the molecules at the interface, and these can be the relatively small van der Waals or London dispersion forces, or larger forces due to electrostatic effects or hydrogen bonding. The enthalpy of adsorption often becomes less negative as the equilibrium surface excess (Γ) increases, suggesting that the most energetically favorable sites are occupied first.

2.2.6 Properties of Foam

In foam fractionation, gas is forced through a frit to produce bubbles that rise upwards in a liquid column to subsequently collect as foam. As the bubbles travel through the continuous phase (the liquid), surfactants adsorb at the gas-liquid interface. When the gas bubbles emerge from the liquid, they form bubble cells with a honeycomb-like structure. These cells accumulate above the bulk liquid surface to form a foam phase with a small amount of liquid entrained loosely trapped in the spaces between the bubbles.

Foams are highly concentrated dispersions of gas (dispersed phase) in a liquid (continuous phase) containing surface-active macromolecules, such as surfactants. These preferentially adsorb at the gas-liquid interface and are responsible for both the tendency of the liquid to foam and the stability of the resulting foam. Foams can persist for a few minutes or several days depending on the conditions.

Liquid-based foams exhibit interesting mechanical properties. If pushed gently, they resist deformation elastically like solids. And if pushed hard, they can flow and deform arbitrarily like liquids. Thus, they are neither solid, liquid nor vapor, yet they exhibit the features of all three of these basic states of matter. Such behavior characterizes soft matter.

In foam fractionation, foam provides the necessary large gas-liquid interface for adsorption. As such, this characteristic of foam is critical for the foam fractionation process. As mentioned, foaming of solutions is dependent on the presence of dissolved surface active solutes. Dynamic foams are complex systems with a large surface area, and, as a consequence, foams tend to collapse spontaneously. The average shape, stability and size of the bubbles comprising foams are important factors contributing to the quality of the foams.

2.2.7 Types of Foam

Depending on the surface activity of surfactants, there are two types of foams: unstable (wet, large bubbles) foam and meta-stable (dry, small bubbles) foam. In unstable foams, the bubbles are not drained and have a spherical form that is only slightly distorted by their neighbors. Unstable foams are constantly collapsing as the liquid drains from between the bubbles and the life-time is short. In meta-stable foams, the foams persist long enough for drainage to proceed extensively such that the bubbles press against each other and will distort in shape rather than coalesce. The region of contact will then flatten out into a film with a thickness determined by the combination of applied van der Waals force (an attractive force originating from the dielectric mismatch between gas and liquid) and the electric double-layer force (a repulsive force originating from the adsorbed surfactant). Meta-stable foams do not collapse immediately since the mean life-time of a bubble is longer [KITCHENER and COOPER 1959]. In unstable foams, the bubbles are not drained and have a spherical form that is only slightly distorted by their neighbors, whereas, in meta-stable foams, the bubbles persist long enough for drainage to proceed extensively so that the bubbles press against each other and the films of liquid between them become planar or slightly planar formations called lamellae of almost uniform thickness. The typical ideal bubble is considered to have 12 pentagonal faces. In reality, a typical bubble deviates from this ideal, so this assumed shape is a kind of an average of the shapes. A photo of foam is presented in Figure 2.3.

The physical properties of bulk foam ultimately arise from the physical chemistry at the bubble interface and the collective structure formed by the random packing of gas bubbles. In summary, foams consist of polyhedral bubbles filled with gas separated by liquid films. In reality, as mentioned, the bubbles differ markedly in their shape and size. And, even among bubbles having the same volume, there is variation in the number of faces and the number of edges per face. But the bubbles (and structures they form) can be approximated with ideal bubbles (having 12 pentagonal faces) to simplify analysis.

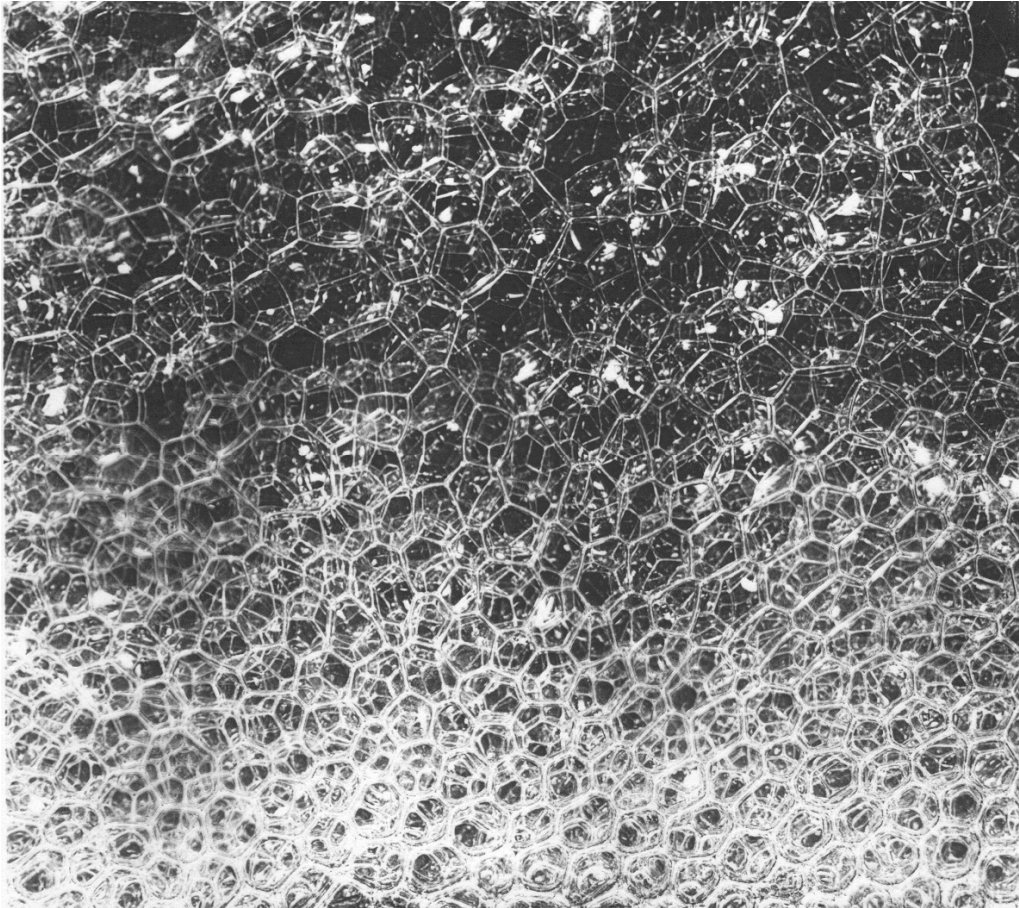


Figure 2.3 A photo representation of foam [CILLIERS]

2.2.8 Stability of Foam

The development and stability of foam is governed by three main processes: drainage, film rupturing and foam coarsening. The complex hydrodynamic conditions of the rising foam are further described by Stevenson Jameson [STEVENSON and JAMESON 2007], but the basic principles are discussed below.

The films between bubbles are almost planar and intersect three at a time to form channels or capillaries that are usually called Plateau borders (PB), named after the Belgian physicist Plateau. The Plateau borders are essentially randomly oriented and have a curved triangular cross section [LEMLICH 1968]. A representation of the cross section of intersecting films with the Plateau borders between them is presented in Figure 2.4.

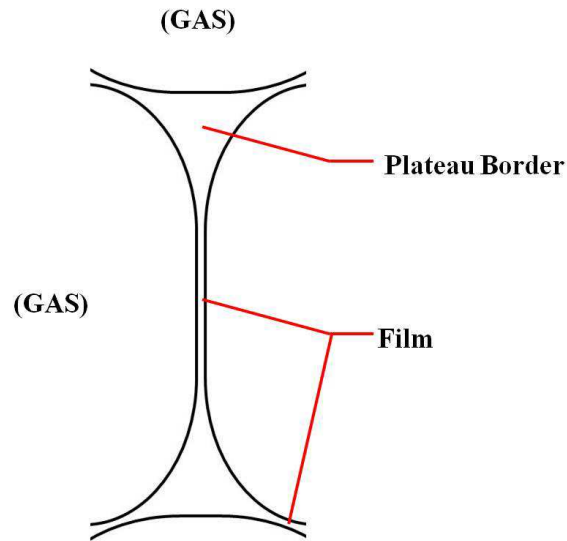


Figure 2.4 A cross section of films with the Plateau borders between them

Plateau border channels form a complex interconnected network through which liquid flows out of the foam under the force of gravity. At the same time, the liquid in the films is sucked in to the Plateau border channels due to the capillary action.

As mentioned, drainage of interstitial liquid in foams with larger bubbles occurs more rapidly than in foams with smaller bubbles. This is the case (at least in part) due to the larger cross-sectional area of the Plateau borders in foams with larger bubbles.

During drainage, unadsorbed surfactant and/or less surface-active molecules will flow downwards back to the bulk solution. In the process of draining downwards, some of the molecules will be further adsorbed onto lower-level bubbles if there are free attachment sites available. The remaining portion will return to the bulk solution continuously modifying its concentration.

The drainage through foam of low liquid content occurs simultaneously with the flow of the interstitial liquid through the Plateau borders. In foam fractionation,

foam drainage is an important process as it ultimately provides for a foam overflow at the foam column outlet with low liquid content that is rich in the target product. As stated, foam drainage occurs primarily through the interconnecting network of capillaries. The flow is caused by a pressure forcing the liquid from between the bubbles. The flow or drainage of interstitial liquid then progressively results in a thinning of the liquid membrane, which structurally weakens the bubbles. The persistence of foams results from the persistence of the membranes separating the bubbles. Solutions with good foam stability are able to resist excessive localized thinning, while a controlled general thinning inevitably proceeds. On the whole, a portion of the bubbles collapse due to this thinning and never makes it completely through the column.

The drainage of interstitial liquid results in the thinning of the films by suction. When the films get too thin (which is especially characteristic for larger bubbles), they weaken and rupture, leading to the direct coalescence of neighboring bubbles, and, eventually, collapse of some of the foam. Coalescence results in a decrease in the number of bubbles and in an increase in the mean bubble volume as bubbles fuse together (though some bubbles just collapse).

Film rupturing is promoted by, among other factors, the presence of a weakly surface-active compound, which determines the prevalence of the attractive van der Waals forces over the repulsive electric double-layer forces. Also, a low viscosity solution will lead to a rapid drainage of interstitial liquid from the lamellae.

When two bubbles coalesce into a single larger bubble, the total gas-liquid interface is reduced (larger volumes require less surface area). With a loss of surface area, a greater amount of surface-active molecules will be forced into the interstitial liquid, which ultimately will influence the drainage.

In foam fractionation, the average size of the bubbles can be an important factor for separation. An increase of bubble size results from coalescence of the bubbles that arise from two sources: fusing and rupturing. The fusion of gas from smaller

bubbles to larger bubbles is a result of surface tension that makes the pressure in smaller bubbles greater than the pressure in larger bubbles. With time, this results in the formation of larger bubbles and a decrease in the number of smaller bubbles. The other source is the rupturing of the walls separating the individual bubbles [LEMLICH 1968]. Both of these sources, fusing and rupturing, are at work to some extent regardless of the kind of foam.

As a result of smaller bubbles fusing into larger bubbles due to surface tension that makes the pressure in smaller bubbles greater than the pressure in larger ones, some bubbles grow while others disappear. The net result of this process is that the average bubble size grows with time. This process is known as foam coarsening.

Foam coalescence and coarsening both lead to uneven bubble size distribution in the foam. The bubbles are larger in the region where these two phenomena occur more. A direct visual measurement of bubble diameters in a foam column indicates that the average bubble size grows as foam is pushed up the column.

2.2.9 Parameters of Foam Fractionation

The parameters that influence foam fractionation include several basic variables, such as pH of the solution, concentrations of solute and surfactant, gas flow rate, height of liquid pool and foaming tower.

pH of solution

In general, the pH value of a solution will determine the sign and magnitude of the charge of a variety of molecules. Therefore, adsorption of those molecules at the gas-liquid interface of dilute aqueous solutions and the extent of their removal by foam fractionation can be positively influenced by the solution's pH value. For some types of molecules, a remarkable degree of separation can be achieved by choosing appropriate pH conditions. This effect is due to the different functional groups that some types of molecules possess. For such a

molecule, there will be a pH value, known as the isoelectric point (pI), where the net charge of the molecule is zero. At this point, the solubility of such a molecule is at a minimum. As one might expect, the pI is different for different molecules. Ahmad as well as Uraizee and Narsimhan proved in their work with proteins, that the enrichment is greater at the pH corresponding to the pI [AHMAD 1975, URAIZEE and NARSIMHAN 1996].

Concentration of solute and surfactant

In foam fractionation, enrichment is largely dependent on the concentration of materials to be separated that are present in the bulk of a dilute solution. Robert and Vermeulen demonstrated in their foam fractionation study of rare-earth elements that a low concentration of the materials in the bulk is a desired property for extraction [ROBERTSON and VERMEULEN 1969]. Ahmad as well as Uraizee and Narsimhan showed in their work with proteins that low concentrations of materials present in the bulk is the key for an effective separation [AHMAD 1975, URAIZEE and NARSIMHAN 1996]. They pointed out that there is an optimal concentration range, which is more suitable to achieve a more effective separation. Karger and DeVivo in their work on the fundamentals of foam fractionation postulated that conventional foam fractionation operates best with concentrations between 10^{-3} to 10^{-7} molar solutions [KARGER and DEVIVO 1968]. Maas found that, at higher concentrations, micelles are formed, which has a negative effect on enrichment [MASS 1974].

Gas flow rate

The gas flow rate has a marked effect on the enrichment ratio attained in foam fractionation. A low gas flow rate is, in general, beneficial for enrichment, even though the rate of separation will be lower at lower flow rates. During the process of foam fractionation at low flow rates, provisions must be taken to ensure that there is a sufficient gas flow to maintain the foam height that is essential for good separation – the optimum flow rate being determined by the concentration of the surfactant and the stability of the foam. Various authors, including Grieves and Bhattacharyya, Kishimoto, and Schnepf and Gaden, have

found that, for different substances, high enrichment and low foam density are obtained at low flow rates [GRIEVES and BHATTACHARYYA 1970, KISHIMOTO 1962, SCHNEPF and GADEN 1959].

Height of liquid pool and foam height

In foam fractionation, the height of liquid pool above the frit can affect the enrichment ratio. Variation of the height of the liquid pool implies a change of contact time between the solution and the rising bubbles before they reach the top of the liquid pool. This change may affect the mass transfer of the desired materials that occurs between the solution and surface of the rising bubbles. To a certain extent, an increase in pool height results in an increase of the bubbles residence time in the pool, and thus more time for the bubbles to approach adsorption equilibrium, hence improving the enrichment ratio. In their work with proteins and microbial cells, Parthasarathy *et al.* ascertained the influence of the pool height above the frit on enrichment [PARTHASARATHY, *et al.*1988]. Additionally, different foam heights exhibit a significant effect on separation. An increase in foam height up to a certain extent brings about a drastic change in the mass transfer process due to the increase in the interfacial transfer area and an overall increase in drainage. Therefore, a proper foam height is essential to obtain a good enrichment. Ahmad and Uraizee and Narsimhan investigated the influence of foam height on enrichment in their work with proteins [AHMAD 1975, URAIZEE and NARSIMHAN 1996].

2.2.10 Problems Occurring in Foam Fractionation

The application of foam fractionation to biological products is not commonly used for two main reasons. The first is the lack of a sufficient understanding of the complex principles governing the process, both for the gas-liquid dispersion hydrodynamics and for the protein adsorption mechanisms (which makes prediction of the performance difficult). The second is the presumed denaturation of the biological molecules during the progress. Malysa and Warszynski studied the dynamic effects (motion) associated with foam-layer formation and stability,

and they observed that the competition between the rate of equilibrium coverage reestablishment (disequilibrium induced by motion) by surface diffusion (increasing the stability of film) and the rate of film drainage (decreasing the stability of film) determines the volume and stability of the foam layer [MALYSA and WARSZYNSKI 1995]. Also, Bhakta and Ruckenstein have reviewed the theoretical work on static foam decay and compared various models in terms of their ability to describe drainage, coalescence, and collapse of foam [BHAKTA and RUCKENSTEIN 1995]. In spite of this extensive body of work in the literature, a detailed mathematical description of the complex mass transfer process, which depends on the operational modes (continuous, semi-batch, or static foam) and the physicochemical properties of the solution and surfactants, is very complex and has not been done to date in a relatively simple model. However, protein denaturation (the loss of biological activity owing to the change, usually unfolding, of the molecular tertiary structure) occurring when biological molecules are exposed to a gas-liquid surface can be minimized by choosing suitable operating conditions. A number of researches have noted that foam separation can be used successfully for the purification of proteins and enzymes without necessarily adversely affecting the protein structure. As such, it appears that there are no significant obstacles blocking use of foam fractionation processing of protein molecules.

2.3 Milk

2.3.1 Basic Components and Properties of Milk

Milk is the primary source of nutrition for neonates before they start digesting solid foods. Early lactation milk is known as colostrums, which carries the primary defensive immunoglobulins from the mother to the baby until the baby's immune system develops sufficiently to lower the risk of many diseases [KELLY 2003, KORHONEN, *et al.* 2000]. Generally, during the early stage of growth, neonates consume milk from their mothers' breasts for a certain period, but, in other cases, they consume milk from several alternative sources such as milk

from domesticated animals, milk powders and artificial milk supplements [PLAYNE, *et al.* 2003]. Table 2.1 provides the approximate concentration of the major milk components for different animal species. Among all the domesticated animals, cow's milk has been the most widely consumed by humans since ancient times, as remains the case today; hence it was selected as a test solution for this work.

Table 2.1 Approximate concentration of major components in milk of different species (condensed from [PLAYNE, *et al.* 2003])

Components (g/L)	Species				
	Human	Cow	Buffalo	Goat	Sheep
Total solids	129	125	171	130	163
Lactose	71	48	49	45	53
Fat	38	31	75	45	74
Proteins	10	34	38	29	55
◆ Caseins	4	28	32	23	46
◆ Whey proteins	5.5	6	6	6	9
Oligosaccharides	3.8	0.045	-	41	46
Ash	2	7	8	8	9
◆ Calcium	0.34	1.14	1.85	1.3	1.93
◆ Phosphorous	0.14	0.93	1.25	1.06	0.99

Although milk from various species, such as cattle, buffalo, sheep, goats and camels, has been studied scientifically for several decades, cow's milk has been proven to have a lot of benefits for human health and nutrition because of its similarity to the composition of human milk [AGOSTONI, *et al.* 2000, LONNERDAL and STKINSON 1995, STEIJNS 2001].

Bovine milk is a complex heterogeneous fluid, which consists of distinct essential nutrients, such as fat, proteins, minerals and several other minor components [FARRELL, *et al.* 2004]. Typical milk composition includes approximately 87% water and 13% milk solids, wherein milk solids are further classified into fat solids (3.7% of total) and non-fat solids (8.9% of total). Non-fat solids are a mixture of proteins (3.4% of total), caseins and whey; lactose (4.8% of total); and other minerals and minor components (0.7% of total) [EIGEL, *et al.* 1984].

Milk has a wide range of bioactive components, including oligosaccharides, glycolipids, growth factors, hormones, vitamins, proteins and peptides [SHAH 2000, STEIJNS 2001]. Among these components, milk proteins have a huge impact on human health [MEISEL 1997]. Milk proteins have been studied extensively and are well characterized in terms of their structural, chemical and functional properties (Table 2.2) [ROSE, *et al.* 1970]. As can be seen from the table, milk proteins are broadly divided into two categories: caseins and whey proteins. Caseins constitute about 80% of the total milk proteins and exist as colloidal suspensions of micelles (clusters of casein molecules associated with calcium and inorganic phosphate in this case). Incidentally, micelles give the white appearance to milk as they are large enough (20–200 nm) to scatter light. Whey proteins account for the approximately remaining 20% of total proteins and are comprised of lactalbumin, lactoglobulin, bovine serum albumin (BSA), immunoglobulins and other minor proteins. All of these milk proteins are well characterized and reported. Most of them are unique in their basic properties, functional properties and applications [MEISEL 1997, WONG, *et al.* 1996].

Table 2.2 Bovine milk proteins and some of their properties(condensed from [EIGEL, *et al.* 1984] and [FARRELL, *et al.* 2004])

	Concentration (g / Kg of solids)	Percentage of total protein	Mw (kDa)	pI
Total proteins	32.7	100		
Total casein	26	79.5		
α -s ₁ -casein	12.0-15.0	30.6	23.6	4.9-5.3
α -s ₂ casein	3.0-4.0	8	25.3	4.9-5.3
β -casein	9.0-11.0	30.8	24	5.2
κ -casein	2.0-4.0	10.1	19	5.8
Total whey proteins	6.3	19.3		
α -Lac	0.6-1.7	3.7	14	4.4
β -Lac	2.0-4.0	9.8	18.3	5.4
BSA	0.4	1.2	67	5.1
LF	0.02-0.1	0.3	77	7.9
LP	0.03	0.1	78	9.6
Ig	0.7	2.1	150-1000	5.0-8.0
IgG1	0.3-0.6	1.2	161	5.5-6.8
IgG2	0.05	0.15	150	7.5-8.3
IgM	0.09	0.3	1000	5.0-8.0
IgA	0.01	0.03	385-417	4.5-6.5
Membrane proteins	0.4	1.2		7.48

2.3.2 Milk as a Source for Immunoglobulin Production

Proteins and other bioactive compounds extracted from various sources including plants and animals have been utilized in many therapeutic applications [HUANG, *et al.* 2002, POLLOCK, *et al.* 1999]. Soon after the invention of recombinant technology, recombinant techniques were popularly applied to produce desired bioactive proteins or peptides in suitable host organisms, such as bacteria, yeast and fungi. This has allowed the traditional pharmaceutical industry to produce

drugs in bulk amounts at low costs. However, bacterial or microbial production is severely limited in synthesizing certain bioactive components, especially those that have complex structures and post-translational modifications, such as glycosylation (attachment of specific carbohydrate units, such as in the addition of glycan chains to proteins). Advances in biotechnology provided a new path for producing recombinant bioactive compounds in large amounts with minimal risks and lower production costs using transgenic plants and animals. Presently, milk is a promising system for the production of recombinant proteins from transgenic animals because it has several advantages over other recombinant production methods [HOUDEBINE 2002a, HOUDEBINE 2002b]. For example, milk is considered a safe source of proteins and it has been well-characterized. Transgenic animals produce desired proteins in their milk after injection of foreign genes. Consequently, milk is a great source for therapeutic protein production. Recombinant proteins produced from milk of transgenic dairy animals could be an abundant and pathogenic-free source for immunoglobulin production. Transgenic animals have great capacity to produce large amounts of recombinant proteins at approximately 40 g/L of bulk solution [BOSZE, *et al.* 2008, ECHELARD, *et al.* 2006, ECHELARD, *et al.* 2008, POLLOCK, *et al.* 1999]. This concentration is 50 to 100 times higher than that of conventional bioreactor production methods (0.5–0.8 g/L).

Hyperimmunization is another kind of technology for large-scale production of specific immunoglobulins in animals for pharmaceutical applications [HUSU, *et al.* 1993]. This is the most rapid and efficient method for developing quick vaccines in sufficient quantities, such as for clinical trials against infections and inflammations [MCVEY and LOAN 1989, MEHRA, *et al.* 2006, ORMROD and MILLER 1993]. Hyperimmunization technology is preferred for specific immunoglobulin production to eliminate poorly characterized mixtures of target antigens. This novel technology has been successfully employed for the production of milk polyclonal immunoglobulins from pregnant cows [BRUSSOW, *et al.* 1978]. These immunoglobulin concentrates have been used to provide passive immunity against rotavirus gastroenteritis. Similarly, the hyperimmunization technology has been used for large-scale production of

specific immunoglobulins in the colostrum of cattle [HUSU, *et al.* 1993, MCVEY and LOAN 1989]. More recently, the production of human immunoglobulins from hyperimmunized cows and their potential application in treating many human diseases have been described [KUROIWA, *et al.* 2009].

However, the major challenge for production of proteins, such as immunoglobulins in bulk amounts, requires economical, efficient and effective protein purification technologies from raw milk to minimize losses that usually happen during multi-step processing. Foam fractionation, being a relatively simple process, could be a good candidate for enrichment and was selected as a method to investigate the enrichment of immunoglobulins from milk in this work.

2.4 Response Surface Methodology

Response surface methodology (RSM) is a collection of statistical and mathematical techniques useful for developing, improving, and optimizing processes [MYERS and MONTGOMERY 1995]. It also has important applications in the design, development, and formulation of new products, as well as in the improvement of existing product designs.

The most extensive applications of RSM are in the industrial realm, particularly in situations where several input variables potentially influence a certain performance measure or quality characteristic of a product or process. Such a performance measure or quality characteristic is called the *response*. Many real-world applications of RSM will involve more than one response. The input variables are sometimes called *independent variables*, as they are subject to the control of the engineer or scientist, at least for purposes of a test or an experiment. And the response is a dependent variable, dependent on, usually, multiple input variables.

The graphical representation of the problem environment has led to the term *response surface methodology*. It is also convenient to view the response surface in the two-dimensional plane. In this presentation, the plane is viewed from above, and all points being a constant response are connected to produce contour lines. As such, this type of representation is called a *contour plot*.

2.4.1 Approximating Response Functions

To approximate a response function, suppose that the scientist or engineer (also referred to as the experimenter) is concerned with a product, process, or system involving a response (y) that depends on controllable input variables ($\varepsilon_1, \varepsilon_2, \dots, \varepsilon_k$). The relationship is:

$$y = f(\varepsilon_1, \varepsilon_2, \dots, \varepsilon_k) + z \tag{2.6}$$

where the exact nature of the true response function (f) is unknown and perhaps very complicated, and z is a term that represents other sources of variability not accounted for in the true response function (f). For example, z includes measurement error for the response, other sources of variation that are inherent in the process or system (background noise or so-called common cause variation in the language of statistical process control), the effect of other variables, and so on. The term z is treated as a statistical error, wherein it is often assumed to have a normal distribution with a mean of zero. If the mean of z is zero, then the equation relationship simplifies to:

$$y = f(\varepsilon_1, \varepsilon_2, \dots, \varepsilon_k) \tag{2.7}$$

The variables ($\varepsilon_1, \varepsilon_2, \dots, \varepsilon_k$) are typically called the *natural variables* because they are expressed in natural units of measurement, such as mg/mL for concentration or mL/min for a flow rate. However, in much RSM work, it is useful to transform the natural variables to *coded variables* (x_1, x_2, \dots, x_k), which are usually defined to be dimensionless with a mean of zero and the same spread

or standard deviation. In terms of the coded variables, the true response function is now written as:

$$y = f(x_1, x_2, \dots, x_k) \tag{2.8}$$

As mentioned, the actual form of the true response function (f) is not known, and, because it is unknown, it must be approximated. In fact, successful use of RSM is critically dependent upon the experimenter's ability to develop a suitable approximation for the true response function (f). Fortunately, a low-order polynomial in a relatively small region of the independent variable space is usually appropriate. In many cases, a *first-order* or a *second-order* model may be used. For the case of two independent variables, the first-order model in terms of the coded variables is expressed as:

$$y = \beta_0 + \beta_1 x_1 + \beta_2 x_2 \tag{2.9}$$

The first-order model is likely to be applicable when the experimenter is interested in approximating the true response surface over a relatively small region of the independent variable space in a location where there is little curvature in the true response function (f). The above form of the first-order model is sometimes called a *main effects model*, because it includes only the main effects of the two independent variables x_1 and x_2 . Moreover, if there is *interaction* between the independent variables, such can be added to the model easily by adding a term as follows:

$$y = \beta_0 + \beta_1 x_1 + \beta_2 x_2 + \beta_{12} x_1 x_2 \tag{2.10}$$

This, then, is the first-order model with interaction. It is the addition of the interaction term $\beta_{12} x_1 x_2$ that introduces curvature into the response function.

However, it is often the case that the curvature in the true response surface is so significant that a first-order model, even with the interaction term included, is

inadequate. Thus, a second-order model will likely be required in these situations. For the case of two variables, the second-order model is expressed as:

$$y = \beta_0 + \beta_1 x_1 + \beta_2 x_2 + \beta_{11} x_1^2 + \beta_{22} x_2^2 + \beta_{12} x_1 x_2 \quad (2.11)$$

This model would likely be useful as an approximation to the true response surface, again in a relatively small region, but where there is substantial curvature in the true response function (f).

The second-order model is widely used in response surface methodology for several reasons. Among them are the following:

- ◆ The second-order model is very flexible, as it can take on a wide variety of functional forms, such that it will often work well as an approximation to the true response surface.
- ◆ It is relatively easy to estimate the parameters in the second-order model.
- ◆ There is considerable practical experience indicating that second-order models work well in solving real response surface problems.

In general, the first-order model is expressed as:

$$y = \beta_0 + \beta_1 x_1 + \beta_2 x_2 + \dots + \beta_k x_k \quad (2.12)$$

and the second-order model is expressed as:

$$y = \beta_0 + \sum_{j=1}^k \beta_j x_j + \sum_{j=1}^k \beta_{jj} x_j^2 + \sum \sum_{i < j=2}^k \beta_{ij} x_{ij} \quad (2.13)$$

Finally, it is useful to note that there is a close connection between RSM and linear regression analysis. For example, consider the above first-order model; the β 's (coefficients) are a set of unknown parameters. To estimate the values of these parameters, data associated with the system being studied must be generated and collected. Regression analysis is a branch of statistical model

building that uses such data to estimate the β 's. Because, in general, polynomial models are linear functions of the unknown β 's, the technique is referred to as *linear regression analysis*. However, it is very important to carefully plan the data collection phase of a response surface study. To accomplish this, special types of experimental designs, called *response surface designs*, are valuable.

2.4.2 The Sequential Nature of RSM

Applying RSM generally involves several sequential steps. For convenience of understanding, these sequential steps may be separated into three phases (Phase Zero, Phase One and Phase Two).

Most applications of RSM are *sequential* in nature. That is, at first some ideas are generated concerning which factors or variables are likely to be important in the response surface study. This usually leads to an experiment designed to investigate these factors with a view towards eliminating the unimportant ones. This type of experiment is usually called a *screening experiment*. At the outset of a response surface study, there is often a rather long list of variables that could be important in explaining the response, but hopefully only a short list of variables that actually are particularly important. The objective of factor screening is to reduce the number of candidate variables to relatively few so that subsequent experiments will be more efficient and require fewer test combinations and runs. Screening experiments are referred to as *phase zero* of a response surface study. A response surface analysis should always be conducted only after a screening experiment has been performed to identify the important factors. Doing so generally drastically simplifies model generation.

Once the important independent variables are identified, *phase one* of the response surface study begins. In this phase, the experimenter's objective is to determine whether the current levels or settings for the independent variables result in a value for the response that is near the optimum (the optimal range being estimated based on pretests and/or analysis), or, whether the process is

operating in some other region that is (possibly) remote from the optimum. If the current settings or levels of the independent variables are not consistent with optimal performance, then the experimenter must determine a set of adjustments to the process variables that will move the process toward the optimum. This phase of response surface methodology makes considerable use of a first-order model and an optimization technique called the *method of steepest ascent*.

Phase two of a response surface study begins when the process is near the optimum. At this point the experimenter usually wants a model that will accurately approximate the true response function within a relatively small region around the optimum. Because the true response surface usually exhibits curvature near the optimum, a second-order model will be used. Once a suitable approximating model has been obtained, this model may be analyzed to determine the optimum conditions for the process.

This sequential nature of response surface methodology allows the experimenter to learn about the process or system under study as the investigation proceeds. This increases the likelihood that the experimenter will learn the answers via RSM to questions such as

- ◆ How much replication is necessary?
- ◆ What is the location of the region of the optimum?
- ◆ What the type of approximating function is required?
- ◆ What is the proper choice of experimental design?
- ◆ What transformations on the responses or process variables are required?

2.4.3 Objectives and Applications of RSM

Response surface methodology is useful in the solution of many types of industrial problems. Generally, these problems fall into three categories:

- ◆ Mapping a response surface over a particular region of interest
- ◆ Optimization of the response
- ◆ Selection of operating conditions to achieve specifications or customer requirements

During the last 25 years, industrial organizations, particularly in Europe, the United States and Japan, have become keenly interested in quality improvement. Statistical methods, including statistical process control (SPC) and design of experiments (DOE) play a key role in this activity. Naturally, quality improvement is most effective when it occurs early in the product and process development cycle. Semiconductors and electronics, automotive and aerospace, biotechnology and pharmaceuticals, and chemical production and materials processing are all industries where experimental design methodology has resulted in products that are easier to manufacture, have higher reliability, have enhanced field performance, and meet or exceed customer requirements.

RSM is an important branch of experimental design in this regard. RSM is a critical technology in developing new processes, optimizing their performance, and improving the design and/or formulation of new products. It is often an important *concurrent engineering tool* because product design, process development; quality control, manufacturing and operations personnel often work together in a team environment to apply RSM. In particular, the objectives of quality improvement, including reduction of variability and improved product and process performance, can often be accomplished directly using RSM. The latter, enhancing process performance, is the goal of the research at hand involving the enrichment of immunoglobulin via foam fractionation.

2.4.4 Useful References on RSM

The origins of RSM are described in the seminal paper by Box and Wilson [BOX and WILSON 1951]. They also describe the application of RSM to chemical processes. This paper had a profound impact on industrial applications of experimental design and was the motivation of much of the research in the field.

There are also some notable review papers published on the topic of RSM [HILL and HUNTER 1996, MEAD and PIKE 1975, MYERS, *et al.* 1989]. Also, a paper by Myers described the recent status and future directions of RSM [MYERS

1999]. A monograph by Myers was the first book devoted exclusively to RSM [MYERS 1976]. There are also at least two full-length books on the subject [BOX and DRAPER 1987, KHURI and CORNELL 1996].

2.4.5 Desirable Properties of Response Surface Designs

There are many classes of experimental designs in the literature, and there are many criteria on which experimental designs are based. Also, there are many computer packages that suggest optimal designs based on special criteria and input from the user. However, before using such designs or software, it is important for the user to first understand a set of properties that should be taken into account when the choice of a response surface design is being made. Among other factors, a good design should:

- ◆ result in a good fit of the model to the data
- ◆ give sufficient information to allow a test for lack of fit
- ◆ allow models of increasing order to be constructed sequentially
- ◆ allow for experiments to be done in blocks
- ◆ provide an estimate of “pure” experimental error
- ◆ provide a check on the homogeneous variance assumption
- ◆ be insensitive (robust) to the presence of outliers in the data
- ◆ be robust to detect errors in control of design levels
- ◆ be cost-effective for the application

As one can readily guess, not all of the above properties are required in every RSM applications. However, most of them must be given at least some serious consideration each time one designs an experiment.

The above list of characteristics shows that designing an experiment is not easy. Although only a few of the characteristics may be important, the user may not be aware of the magnitude of their importance. Also, some of the important characteristics may conflict with each other. Consequently, there are tradeoffs

that almost always must be made when one chooses a design. Box and Draper provide an excellent discourse on the many factors that must be considered in choosing a response surface design [BOX and DRAPER 1975].

2.4.6 Central Composite Design

Many applications of response surface methodology involve fitting and checking the adequacy of a second-order model. A central composite design (CCD) is widely used for fitting a second-order response surface. The CCD is without a doubt the most popular class of second-order designs. It was first introduced by Box and Wilson [BOX and WILSON 1951].

Much of the motivation for CCD stems from its use in *sequential experimentation*. It involves the use of a *two-level factorial* combined with *axial points* (also called star points). That is, the design involves factorial points, axial points, and center points. With this format, the sequential nature of the design becomes very obvious. The factorial points represent a variance-optimal design for a first-order model or first-order + two-factor interaction model. Center points provide information about any existence of curvature in the system. If curvature is found in the system, the addition of axial points allows for efficient estimation of the pure quadratic terms of the model to be generated.

Although CCD requires sequential experimentation, it is a very efficient design in situations that call for non-sequential batch response surface experiments. In effect, the foregoing three components of the design play important and somewhat different roles, as summarized in the following:

- ◆ The factorial points are the only points that contribute to the estimation of the interaction terms.
- ◆ The axial points contribute in a large way to the estimation of the quadratic terms, and without the axial points, only the sum of the quadratic terms can be estimated. However, the axial points do not contribute to the estimation of the interaction terms.
- ◆ The center points provide an internal estimate of error (pure error) and contribute toward the estimation of the quadratic terms.

The areas of flexibility in the use of the central composite design lay in [1] the selection of the axial distance and [2] the number of center points. It is known that the choice of these two parameters can be very important. The choice of the axial distance depends to a large extent on the so-called region of operability and the region of interest. Moreover, the choice of the number of center points often has an influence on the distribution of the scaled prediction variance in the region of interest.

For a two-variable example, the design has 12 total runs, consisting of four runs at the corners of an imaginary square, four runs at the center point of this square, plus four *axial runs*, as shown in Figure 2.5. In terms of the coded variables, the corners of the square are $(x_1, x_2) = (-1, -1), (1, -1), (-1, 1), (1, 1)$; all four center points are overlapped at $(x_1, x_2) = (0, 0)$; and the axial points are at $(x_1, x_2) = (-\sqrt{2}, 0), (\sqrt{2}, 0), (0, -\sqrt{2}), (0, \sqrt{2})$. The second-order model is then fitted using the coded variables.

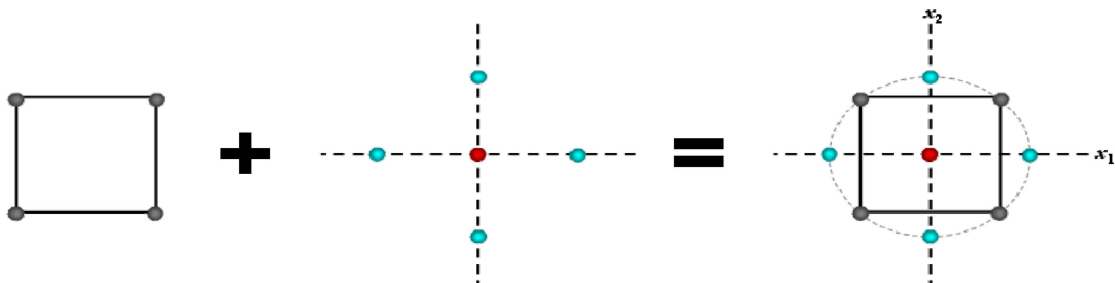


Figure 2.5 Central composite designs for a two variables example

3. Materials and Methods

3.1 Materials

3.1.1 Chemicals

- ◆ Rabbit immunoglobulin G (IgG): Thermo Scientific (Rockford, IL, USA)
- ◆ Human immunoglobulin M (IgM): Thermo Scientific (Rockford, IL, USA)
- ◆ Albumin bovine (fatty acid free): Sigma-Aldrich Co. (Schnelldorf, Germany)
- ◆ Easy-Titer[®] rabbit IgG assay kits: Pierce (Rockford, IL, USA)
(containing goat anti-rabbit IgG sensitized beads, Easy-Titer[®] dilution buffer, and Easy-Titer[®] blocking buffer)
- ◆ Easy-Titer[®] human IgM assay kits: Pierce (Rockford, IL, USA)
(containing goat anti-human IgM sensitized beads, Easy-Titer[®] dilution buffer, and Easy-Titer[®] blocking buffer)
- ◆ Normal goat serum: Pierce (Rockford, IL, USA)
- ◆ Standard homogenized milk: purchased from local store
- ◆ Bicinchoninic Acid (BCA) total protein analysis kit: Pierce (Rockford, IL, USA)
- ◆ Hydrochloric acid (1M and 0.1 M Sol.): p.a., Fluka
- ◆ Sodium hydroxide (1M and 0.1 M Sol.): p.a. Fluka
- ◆ Deionized water: Millipore Milli Q 185 Plus system (Bedford, MA, USA)

3.1.2 Equipment

- ◆ Foam fractionation system: described in detail later in section 3.2.1.2
- ◆ Flow meter: Rate-Master[®] Flowmeter, Model Number: RMA-151-SSV, range 5-50 mL/min gas, Dwyer Instruments, Inc., (Michigan City, Indiana, USA)
- ◆ Gas supply: Bottled pre-purified nitrogen gas
- ◆ Electronic balance: Precisa 40SM-200A, with 0.01 mg precision, Sartorius (Bradford, U.K.)
- ◆ Water deionization: Millipore Milli Q 185 Plus system (Bedford, MA, USA)
- ◆ Ultrasonic bath: Bandelin SONOREX[®] SUPER, with built-in heating ultrasonic bath, RK 100 H, capacity 3L

- ◆ Water bath: Buchi B-480 Waterbath
- ◆ pH meter: pH/mV/Temp. Meter, Model SP-701, pH range from 0 to 14.00 with a resolution of 0.01, Suntex Instruments, Co., LTD.
- ◆ Centrifuge: Beckman Avanti J-20 Series, Beckman Instruments, Inc.
- ◆ Pipette: DragonMed Top Pipette 10-100 μ L, with an accuracy of ± 0.01 μ L
- ◆ ELISA reader: Stat Fax[®] 2100, Awareness Technology Inc.(Palm City, FL, USA)

3.2 Methods

3.2.1 Methods for Model system

3.2.1.1 Preparation of the Start Solution

A solution containing immunoglobulin alone hardly produces foam, but the addition of albumin to the system makes it possible to generate enough foam to rise in a column. Albumin is widely used and well-studied as a foaming agent because of its good foaming ability, stability and low cost [AHMAD 1975, ANAND and DAMODARAN 1995, CLARK, *et al.* 1988, LOCKWOOD, *et al.* 2000, NICOLAI, *et al.* 2008, SCHNEPF and GADEN 1959]. The target immunoglobulin (0.2-1.0 g), either rabbit IgG or human IgM, and albumin bovine (0.125-2.0 g) were added into an empty 1 L volumetric flask and dissolved with deionized water to the 1 L mark. The prepared start solution was stored at 4°C and used within one day. Under constant stirring, the pH of the start solution was adjusted to the desired pH value (from 2 to 11) by adding small amounts of hydrochloric acid solution or sodium hydroxide solution, depending on the required direction of movement.

3.2.1.2 Foam Fractionation Apparatus, Parameters and Procedures

Figure 3.1 depicts the basic equipment used for the enrichment of immunoglobulin in this work. For the foam fractionation procedures, the main

components consisted of three kinds of glassware: five glass columns of different lengths (from 200 to 1000 mm in 200 mm increments with an inside diameter of 15 mm) each having a U-shaped end; a glass two-port container; and a frit assembly consisting of a glass frit holder tube fused with a glass frit (porosity: 16-40 μm). For the foam fractionation procedures, these three pieces of glassware were custom-manufactured because no suitable standard off-the-shelf glassware was readily available for purchase that could suitably conduct the experiments and avoid leakage.

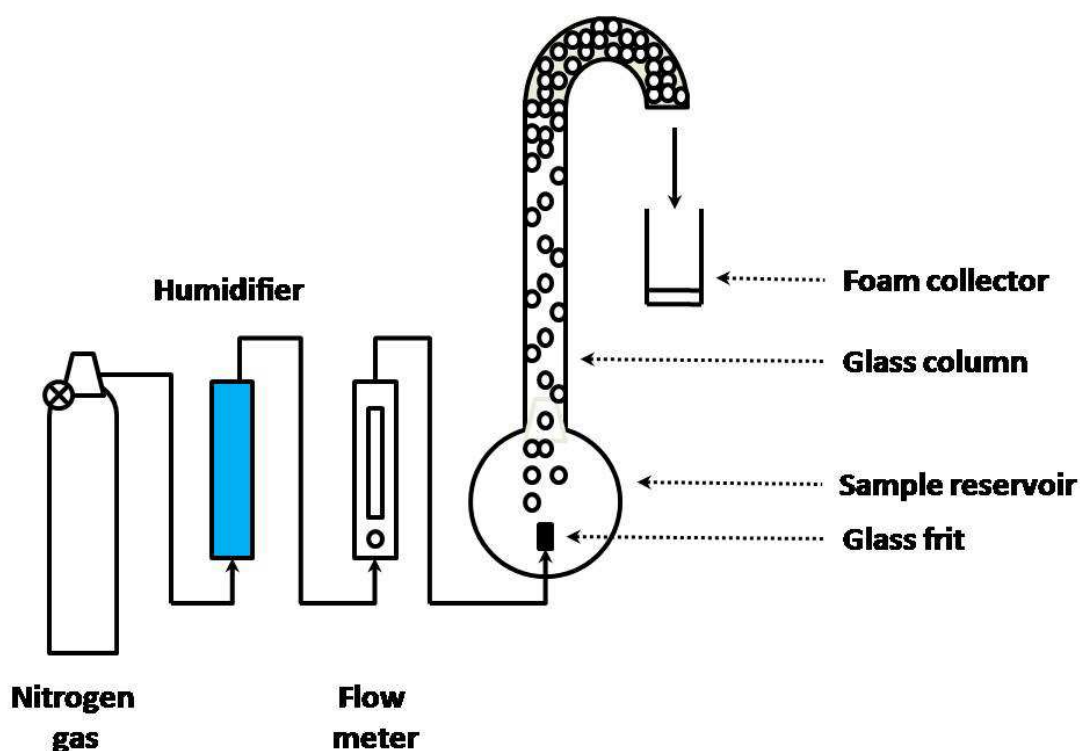


Figure 3.1 Basic components and flow of the foam fractionation equipment

To assemble the equipment, the straight end of one of the glass columns and the frit assembly were tightly inserted into the top port and the side port of the two-port container, respectively, and the externally-protruding end of the frit holder was connected to a nitrogen gas supply line. After assembly, nitrogen gas was continuously supplied at one of five flow rates (from 5 to 25 mL/min in 5 mL/min increments) as measured by a rotameter-type flow meter to generate the foam for a period of five to thirty minutes. Priors to entering the two-port

container, the gas was first passed through water (via a humidifier) to humidify it to thereby minimize loss of water from the solution into the gas in the downstream apparatus. The foam produced by the frit in the two-port container was progressively forced up the vertically-oriented column by newly generated foam until it passed through the U-shaped end of the column. As the foam progressively moved through the column, it drained off excess liquid. Upon emerging from the opening in the U-shaped end, the now mostly collapsed foam, called the foamate, was then collected and analyzed.

The experimental procedure involved foaming with nitrogen at a desired flow rate and collection of the generated foam. To investigate the influence of different parameters on the efficiency of foaming in enrichment, the procedure was varied in terms of six main factors: [A] the initial pH value, [B] the initial immunoglobulin concentration, [C] the nitrogen flow rate, [D] the initial albumin bovine concentration, [E] the column height, and, [F] the foaming time.

3.2.1.3 Quantification of Immunoglobulin Concentration

The quantification of immunoglobulin concentration was determined spectrophotometrically by measuring absorbance at 405 nm. Samples of the start solution and of the foamate were taken to determine the immunoglobulin concentration. For the quantification of rabbit immunoglobulin G in aqueous solutions, the Easy-Titer[®] rabbit IgG assay kit was used, containing goat anti-rabbit IgG sensitized beads, Easy-Titer[®] dilution buffer, and Easy-Titer[®] blocking buffer from Pierce (Rockford, IL, USA). The assay protocols are described in the following steps. First, a 20 μ L volume of the well-mixed sensitized beads was carefully pipetted into each well to be tested of a 96-well microplate. Then, 20 μ L of the properly-diluted sample or standards was added into the appropriate wells containing the beads. After adding the sample or standards, the microplate was mixed for five minutes at room temperature. Then, 100 μ L of the blocking buffer was added to each well and the microplate was mixed again for five minutes. Next, before evaluating the plate, any large bubbles

generated from mixing were burst with a tiny needle. Finally, an ELISA reader was used to measure the absorbance at 405 nm. Thereafter, the immunoglobulin concentration was determined according to a calibration curve. The method used for quantification of human immunoglobulin M was identical to that used for rabbit immunoglobulin G except for using the Easy-Titer[®] human IgM assay kit containing anti-human IgM sensitized beads, again purchased from Pierce.

3.2.1.4 Evaluation of Foam Fractionation Efficiency

In order to evaluate the efficiency of foam fractionation, the enrichment ratio and recovery were determined as follows. First, standard curves were generated for both IgG and IgM, and then the sample concentration was determined from the standard curves (Figure 3.2 provides an example for IgG, as does Figure 3.3 for IgM). Next, adjustment was made for the dilution factor for each sample to determine its starting immunoglobulin concentration. Lastly, after analytical determination of the immunoglobulin concentration, the foam fractionation efficiency was evaluated by calculating the enrichment ratio and the recovery. The equations are as follows:

$$\text{Enrichment Ratio} = \frac{\text{final immunoglobulin concentration (mg/mL)}}{\text{initial immunoglobulin concentration (mg/mL)}} \quad (3.1)$$

$$\text{Recovery (\%)} = \frac{\text{final immunoglobulin content (mg)}}{\text{initial immunoglobulin content (mg)}} \times 100 \quad (3.2)$$

To help average out possible measuring errors, each experimental condition was repeated at least three times.

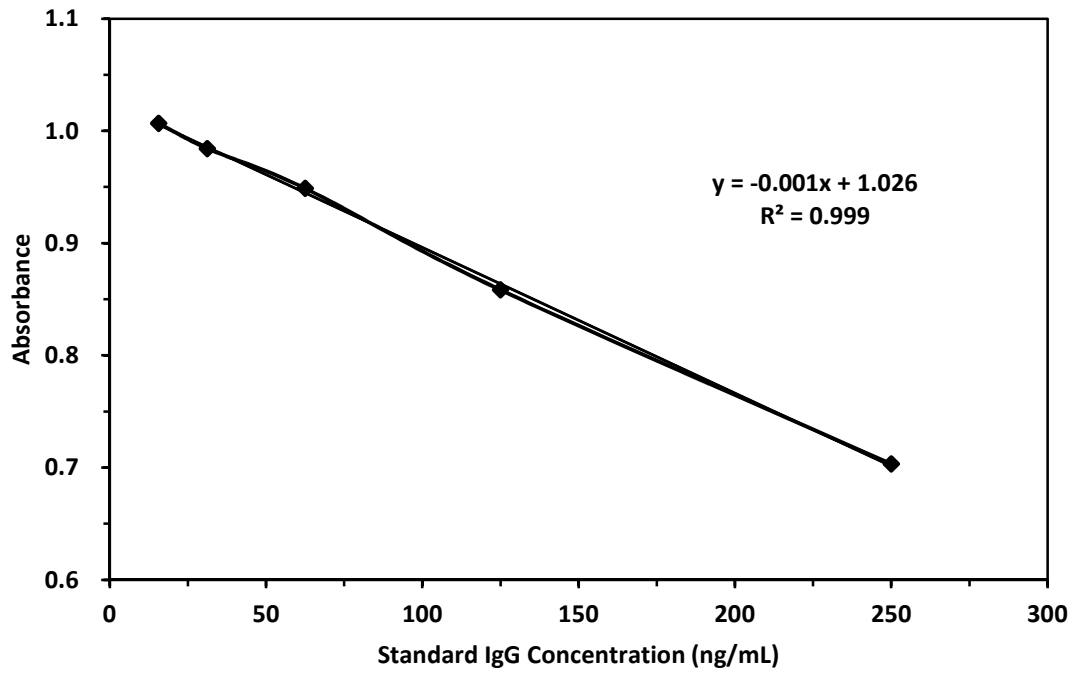


Figure 3.2 Standard curve of different concentrations of rabbit IgG

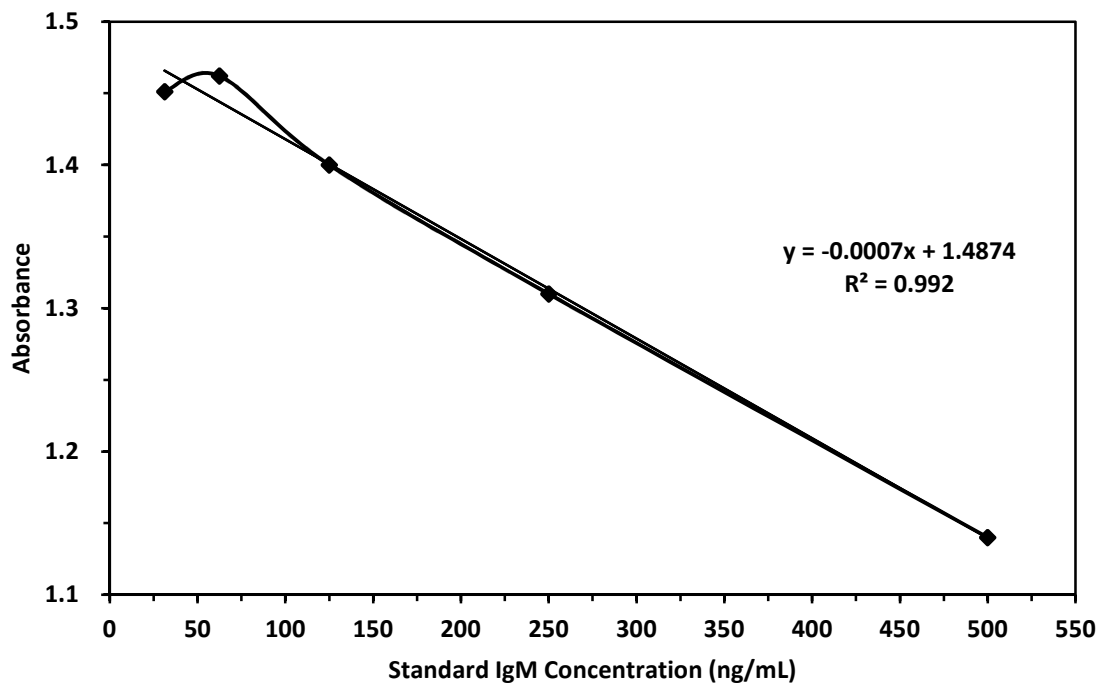


Figure 3.3 Standard curve of different concentrations of human IgM

3.2.1.5 Separation of IgG and IgM

Rabbit IgG (0.1 g) and human IgM (0.1 g), and albumin bovine (1.0 g) were added into an empty 1 L volumetric flask and dissolved with deionized water to the 1 L mark. The prepared start solution was stored at 4°C and used within one day. Under constant stirring, the pH of the start solution was adjusted to the desired pH value (from 2 to 11) by adding small amounts of hydrochloric acid solution or sodium hydroxide solution, depending on the required direction of pH movement.

3.2.1.6 Testing of Different Multi-Component Mixtures

Rabbit IgG (0.2 g) was added into an empty 1 L volumetric flask and dissolved in serum or milk to the 1 L mark. The prepared start solution was stored at 4°C and used within one day. Under constant stirring, the pH of the start solution was adjusted to the desired pH value (from 2 to 11) by adding small amounts of hydrochloric acid solution or sodium hydroxide solution, depending on the required direction of pH movement.

3.2.2 Methods for Milk system

3.2.2.1 Pretreatment before Foam Fractionation

Milk proteins can be classified into two main categories: caseins and whey proteins. Caseins compose about 80% of total milk protein and whey proteins compose the remaining 20%. The main separation method for the two categories is precipitation at pH 4.6. Caseins precipitate at pH 4.6, while the whey proteins remain soluble. In that immunoglobulin belongs to the whey protein portion, the immunoglobulin remains present in the solution after precipitation to be subjected to foam fractionation.

Milk was heated to 45°C in a water bath and the pH adjusted to 4.6 by addition of 1 M HCl with continuous mixing. Precipitated casein proteins were removed by centrifugation at 18,500 x g for 20 minutes and the pH of the resultant whey supernatant was adjusted to 7.0 by the addition of 1 M NaOH, followed by filtration through a 0.22 µm filter. Whey samples were stored at 4°C for short-term analysis and - 18°C for long-term analysis.

3.2.2.2 Preparation of the Start Solution

The target immunoglobulin (0.2-1.0 g), either rabbit IgG or human IgM, was added into an empty 1 L volumetric flask and dissolved in milk (with or without pretreatment) to the 1 L mark. The prepared start solution was stored at 4°C and used within one day. Under constant stirring, the pH of the start solution was adjusted to the desired pH value (from 2 to 11) by adding small amounts of hydrochloric acid solution or sodium hydroxide solution, depending on the required direction of movement.

3.2.2.3 Foam Fractionation Apparatus, Parameters and Procedures

Figure 3.1, shown earlier, depicts the basic equipment used for the enrichment experiments of immunoglobulin in this work. As with the model system, the foam fractionation procedures for the milk system consisted of three kinds of custom-made glassware: five glass columns of different lengths (from 200 to 1000 mm in 200 mm increments with an inside diameter of 15 mm) each having a U-shaped end; a glass two-port container; and a frit assembly consisting of a glass frit holder tube fused with a glass frit (porosity: 16-40 µm). The glassware was custom-manufactured to provide items that tightly assembled to avoid leakage. To assemble the equipment, the straight end of a glass column and the frit assembly were respectively tightly inserted into the top port and the side port of the two-port container, and the externally-protruding end of the frit holder was connected to a nitrogen gas supply line. After assembly, nitrogen gas was

continuously supplied at one of five flow rates (from 5 to 25 mL/min in 5 mL/min increments) as measured by a rotameter-type flow meter to generate the foam for a period of five to thirty minutes. As with the model system experiments, the gas was first passed through water (via a humidifier) to humidify it to thereby minimize loss of water into the gas from solution in the downstream apparatus. Foam produced by the frit in the two-port container was progressively forced up the vertically-oriented column by newly generated foam until it passed through the U-shaped end of the column. With progressive movement up the column, excess liquid drains off the foam. Upon emerging from the opening in the U-shaped end, the now mostly collapsed foam, referred to as foamate, was collected and analyzed.

The experimental procedure involved foaming with nitrogen at a desired flow rate and collection of the generated foam. To investigate the influence of different parameters on the efficiency of foaming in enrichment, the procedure was varied in terms of five main factors: [A] the initial pH value, [B] the initial immunoglobulin concentration, [C] the column height, [D] the nitrogen flow rate and [E] the foaming time.

3.2.2.4 Quantification of Immunoglobulin Concentration

The quantification of immunoglobulin concentration was determined spectrophotometrically by measuring absorbance at 405 nm. Samples of the start solution and of the foamate were taken to determine the immunoglobulin concentration. For the quantification of rabbit immunoglobulin G in aqueous solutions, the Easy-Titer[®] rabbit IgG assay kit was used, containing goat anti-rabbit IgG sensitized beads, Easy-Titer[®] dilution buffer, and Easy-Titer[®] blocking buffer from Pierce (Rockford, IL, USA). The assay protocols are described in the following steps. First, a 20 μ L volume of the well-mixed sensitized beads was carefully pipetted into each well to be tested of a 96-well microplate. Then, 20 μ L of the properly-diluted sample or standards was added into the appropriate wells containing the beads. After adding the sample or

standards, the microplate was mixed for five minutes at room temperature. Then, 100 μL of the blocking buffer was added to each well and the microplate was mixed again for five minutes. Next, before evaluating the plate, any large bubbles generated from mixing were burst with a small needle. Finally, an ELISA reader was used to measure the absorbance at 405 nm. Thereafter, the immunoglobulin concentration was determined according to a calibration curve. The method used for quantification of human immunoglobulin M was identical to that used for rabbit immunoglobulin G except for using the Easy-Titer[®] human IgM assay kit containing anti-human IgM sensitized beads, again obtained from Pierce.

3.2.2.5 Evaluation of Foam Fractionation Efficiency

In order to evaluate the efficiency of foam fractionation, the enrichment ratio and recovery were determined as follows. First, standard curves were generated for both IgG and IgM and then the sample concentration was determined from the standard curves (Figure 3.2 and Figure 3.3, shown earlier, provide an example for IgG and IgM, respectively). Next, adjustment was made for the dilution factor for each sample to determine its starting immunoglobulin concentration. Lastly, after analytical determination of the immunoglobulin concentration, the foam fractionation efficiency was evaluated by calculating the enrichment ratio and the recovery. The equations are the same as defined in equations (3.1) and (3.2). To help average out possible measuring errors, each experimental condition was repeated at least three times.

3.2.2.6 Total Protein Assay

A total protein assay was performed in order to ensure that the total protein content of each batch of milk (purchased from the market) had approximately the same total protein content. The assay was conducted using the bicinchoninic acid (BCA) protein assay, sensitive for protein concentrations in the range between 20 and 1200 $\mu\text{g}/\text{mL}$. The standard curve was generated using 0, 125, 250, 500, 750

and 1000 $\mu\text{g}/\text{mL}$ bovine serum albumin (BSA) calibration standards (prepared from a 1 mg/mL standard solution provided with the commercial BCA assay kit). All samples and calibration standards were diluted to their final concentrations in a 10 mM phosphate buffer in 1.5 mL micro centrifuge tubes. Then, one mL of BCA working reagent was added to 50 μL of the standard or sample, which was then vortexed and incubated at 60°C for 15 minutes, then cooled to room temperature, prior to the absorbance being read immediately at 562 nm. A zero correction was applied to the readings of the samples and standards, and a calibration curve was constructed from the BSA standards. Lastly, absorbance of unknown samples was measured and concentrations calculated from the calibration curve. A total protein concentration of about 32-33 mg/mL was measured for each batch of milk used.

3.2.3 Methods for RSM in a Model system

3.2.3.1 Preparation of the Start Solution for the Model System

A solution containing immunoglobulin alone hardly produces foam, but the addition of albumin to the system makes it possible to generate enough foam to rise in the column. Albumin is widely used as a foaming agent because of its good foaming ability, stability and low cost. The target immunoglobulin (0.2-1.0 g), either rabbit IgG or human IgM, and albumin bovine (0.5 g) were added into an empty 1 L volumetric flask and dissolved with deionized water to the 1 L mark. The prepared start solution was stored at 4°C and used within one day. Under constant stirring, the pH of the start solution was adjusted to the desired pH value (from 2 to 11) by adding small amounts of hydrochloric acid solution or sodium hydroxide solution, depending on the desired direction of movement.

3.2.3.2 Foam Fractionation Apparatus, Parameters and Procedures

Figure 3.1, shown earlier, depicts the basic equipment used for the enrichment of immunoglobulin in this work. For the foam fractionation procedures, the main components consisted of three kinds of glassware: a glass column 1000 mm in length with an inside diameter of 15 mm, the column having a U-shaped end; a glass two-port container; and a frit assembly consisting of a glass frit holder tube fused with a glass frit (porosity: 16-40 μm). For the foam fractionation procedures, these three pieces of glassware were custom-manufactured because no standard off-the-shelf glassware was readily available for purchase that could suitably conduct the experiments and avoid leakage. To assemble the equipment, the straight end of the glass column and the frit assembly were tightly inserted into the top port and the side port of the two-port container, respectively, and the externally-protruding end of the frit holder was connected to a nitrogen gas supply line. After assembly, nitrogen gas was continuously supplied at one of five flow rates (from 5 to 25 mL/min in 5 mL/min increments) as measured by a rotameter-type flow meter to generate the foam for fifteen minutes. Prior to entering the two-port container, the gas was first passed through water (via a humidifier) to humidify it to thereby minimize loss of water from solution into the gas in the downstream apparatus. The foam produced by the frit in the two-port container was progressively forced up the vertically-oriented column by newly generated foam until it passed through the U-shaped end of the column. As the foam progressively moved through the column, excess liquid drained off. Upon emerging from the opening in the U-shaped end, the now mostly collapsed foam, called the foamate, was collected and analyzed.

The experimental procedure involved foaming with nitrogen at a desired flow rate and collection of the generated foam. To investigate the influence of different parameters on the efficiency of foaming in enrichment, the procedure was varied in terms of three main factors: the initial pH value, the initial immunoglobulin concentration, and the nitrogen flow rate.

3.2.3.3 Quantification of Immunoglobulin Concentration

The quantification of immunoglobulin concentration was determined spectrophotometrically by measuring absorbance at 405 nm. Samples of the start solution and of the foamate were taken to determine the immunoglobulin concentration. For the quantification of rabbit immunoglobulin G in aqueous solutions, the Easy-Titer[®] rabbit IgG assay kit was used, containing goat anti-rabbit IgG sensitized beads, Easy-Titer[®] dilution buffer, and Easy-Titer[®] blocking buffer from Pierce (Rockford, IL, USA). The assay protocols are described in the following steps. First, a 20 μ L volume of the well-mixed sensitized beads was carefully pipetted into each well to be tested of a 96-well microplate. Then, 20 μ L of the properly-diluted sample or standards was added into the appropriate wells containing the beads. After adding the sample or standards, the microplate was mixed for five minutes at room temperature. Then, 100 μ L of the blocking buffer was added to each well and the microplate was mixed again for five minutes. Next, before evaluating the plate, any large bubbles generated from mixing were burst with a tiny needle. Finally, an ELISA reader was used to measure the absorbance at 405 nm. Thereafter, the immunoglobulin concentration was determined according to a calibration curve. The method used for quantification of human immunoglobulin M was identical to that used for rabbit immunoglobulin G, except for using the Easy-Titer[®] human IgM assay kit containing anti-human IgM sensitized beads, again obtained from Pierce.

3.2.3.4 Evaluation of Foam Fractionation Efficiency

In order to evaluate the efficiency of foam fractionation, the enrichment ratio and recovery were determined as follows. First, standard curves were generated for both IgG and IgM and then the sample concentration was determined from the standard curves (Figure 3.2 and Figure 3.3, shown earlier, provide an example for IgG and IgM, respectively). Next, adjustment was made for the dilution factor for each sample to determine its starting immunoglobulin concentration. Lastly, after

analytical determination of the immunoglobulin concentration, the foam fractionation efficiency was evaluated by calculating the enrichment ratio and the recovery. The equations are the same as defined in equations (3.1) and (3.2). To help average out possible measuring errors, each experimental condition was repeated at least three times.

3.2.3.5 Process for Response Surface Methodology

Response surface methodology (RSM) is a collection of statistical and mathematical techniques useful for developing, improving and optimizing processes [MYERS and MONTGOMERY 1995]. RSM was used in this work to optimize conditions for immunoglobulin enrichment in both a model system and in milk by foam fractionation. The experimental design and analysis of the data were performed with the help of Design-Expert (version 6.0.5. Stat-Ease, Minneapolis, USA), a statistical analysis software package.

A general flowchart for the RSM process is provided in Figure 3.4. The process sequentially involves: first, (A) selecting both the process variables and response variables; next, (B) using CCD to design the experiment; then, (C) running the experiment and recording the results for response variables; then, (D) using different statistical methods to evaluate the adequacy of different second-order models; followed by (E) using RSM to predict the optimal process variable in order to achieve the desired responses; and, lastly, (F) running experiments to confirm the RSM prediction.

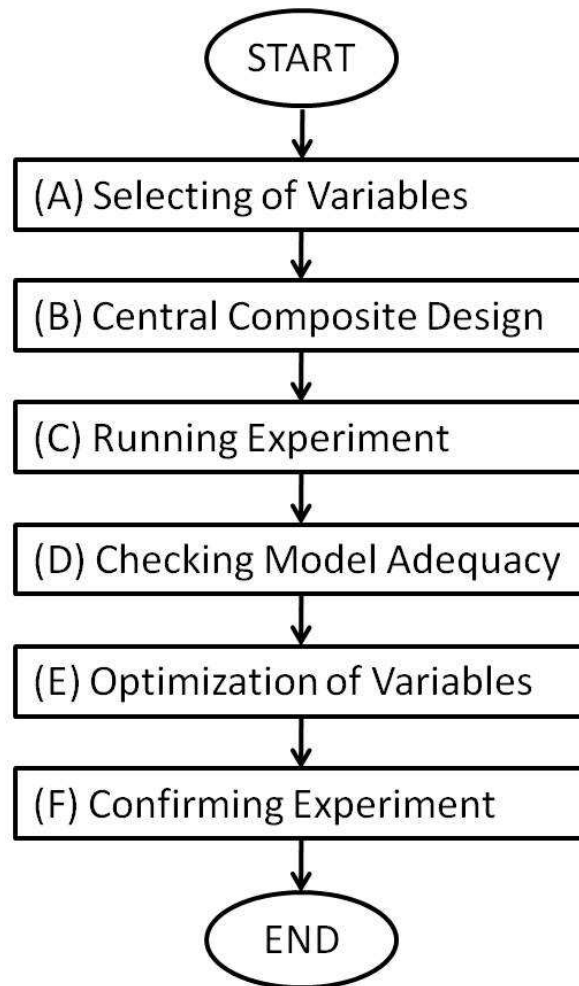


Figure 3.4 Flowchart of RSM process

Selecting of Variables

An understanding of the foam fractionation process and the specific process variables under investigation is useful for achieving a realistic simplified model. Based on the results obtained in the previous experiments, the initial concentration of immunoglobulin, the initial pH value of the start solution and the nitrogen gas flow rate were selected as process variables for foam fractionation. The response variables, analyzed separately, were the enrichment ratio of immunoglobulin and the recovery of immunoglobulin. The three process variables were used to find optimized conditions for enrichment and recovery using RSM.

Second-order Model

The second-order model was used in this part for the three variables. The second-order model contains coefficients for linear, two-factor interaction and quadratic effects. The model equation of response (Y) for an RSM model with three process variables (X_1, X_2, X_3) is expressed as:

$$Y = \beta_0 + \sum_{i=1}^3 \beta_i X_i + \sum_{i=1}^3 \beta_{ii} X_i^2 + \sum_{i=1}^2 \sum_{j=i+1}^3 \beta_{ij} X_i X_j \quad (3.3)$$

where Y is the response variable (either the enrichment ratio or recovery in this case); X_1, X_2 and X_3 are the initial concentration of immunoglobulin, the initial pH value and the nitrogen flow rate, respectively; β_0 is a constant; β_i is the linear coefficient; β_{ii} is the quadratic coefficient and β_{ij} is the two-factor interaction coefficient.

Central Composite Design

One of the most widely used designs for RSM is central composite design (CCD). Nowadays, it is the most popular second-order design. CCD is the standard RSM design and is well suited for fitting a second-order response surface, which often works well for process optimization. Thus, CCD was used in this work and was applied for the three selected process variables, wherein it is recommended by CCD principles to use five equidistant levels for a three-variable model. To accommodate that recommendation, the initial concentrations of immunoglobulin were 0.2, 0.4, 0.6, 0.8 and 1.0 mg/mL; the initial pH values of the start solution were 2, 4.25, 6.5, 8.75, 11; and the constant nitrogen gas flow rates were 5, 10, 15, 20, 25 mL/min. The ranges of independent process variables and their associated codes after scaling are given in Table 3.1. In this case, the central values (zero levels) chosen for experimental design were 0.6 mg/mL for the initial concentration of immunoglobulin, 6.5 for the initial pH value of the start solution, and 15 mL/min for the nitrogen gas flow rate. For example, an initial pH level (value) of 6.5 in the actual range of 2 to 11 would be coded as 0 in the coded range of -2 to +2.

Table 3.1 Experimental codes, ranges and levels of the three selected independent process variables

	Levels				
	(-2)	(-1)	(0)	(+1)	(+2)
Concentration (mg/mL)	0.2	0.4	0.6	0.8	1.0
Initial pH value	2	4.25	6.5	8.75	11
Nitrogen flow rate (mL/min)	5	10	15	20	25

Each central composite design consists of a standard design with orthogonal factorial points and center points, augmented by so-called “axial points”. The orthogonal factorial points contribute in a major way to the estimation of linear terms and two-factor interactions. The orthogonal factorial points are also the only points that contribute to the estimation of the interaction terms. The center points provide an internal estimate of error (pure error) and contribute toward the estimation of quadratic terms. The axial points contribute in a large way to estimation of quadratic terms. In the 20 experiments that were recommended for this work, there are 8 orthogonal factorial points (corner points), 6 center points (overlapped at the center) and 6 axial points (protruding from the face centers), as shown in Figure 3.5, wherein each point is associated with an experimental run. These 20 foam fractionation experiments needed to be conducted in triplicate to average out errors. Then, the average values for both the enrichment ratio and recovery need to be filled in the blanks of the table shown in Table 3.2 with data obtained from running the experiments.

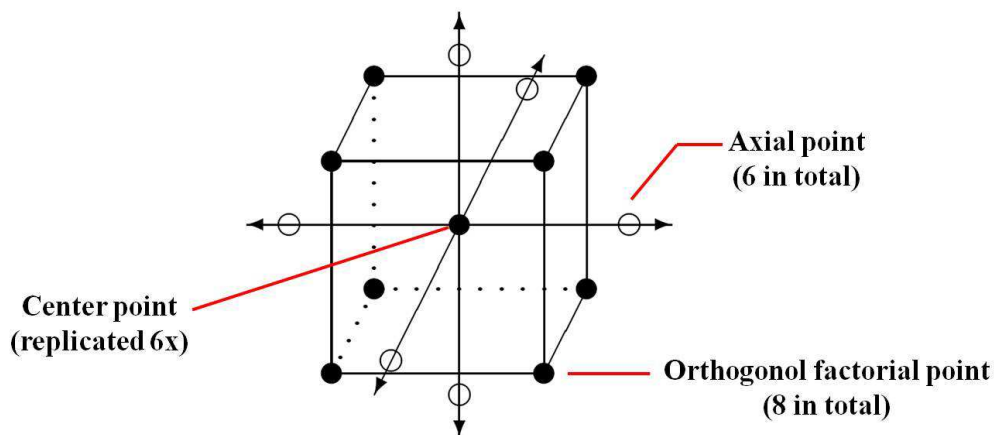


Figure 3.5 Central composite design for a three-variable example

Table 3.2 Experimental design of process variables for IgG in a model system

Run	Type	Factor 1: immunoglobulin concentration (mg/mL)	Factor 2: pH value	Factor 3: nitrogen flow rate (mL/min)	Response 1: enrichment ratio	Response 2: Recovery (%)
1	Center	0.60	6.5	15		
2	Fact	1.00	11.0	5		
3	Fact	0.20	2.0	25		
4	Fact	0.20	2.0	5		
5	Fact	1.00	2.0	25		
6	Center	0.60	6.5	15		
7	Fact	0.20	11.0	25		
8	Fact	1.00	11.0	25		
9	Fact	1.00	2.0	5		
10	Fact	0.20	11.0	5		
11	Center	0.60	6.5	15		
12	Axial	0.60	6.5	5		
13	Axial	0.60	11.0	15		
14	Axial	1.27	6.5	15		
15	Axial	0.60	2.0	15		
16	Axial	0.20	6.5	15		
17	Center	0.60	6.5	15		
18	Center	0.60	6.5	15		
19	Axial	0.60	6.5	30		
20	Center	0.60	6.5	15		

The table shows the software-defined settings to be used for the three process variables for 20 separate experimental runs (one run per line). The settings were defined by the software after first supplying the three working ranges for the three process variables involved, such ranges being determined by preliminary experiments. After running the 20 experiments (in triplicate), the results for the responses are to be filled into the two right (empty) columns. The 20 runs correspond to 8 factorial runs, 6 center runs and 6 axial runs.

3.2.4 Methods for RSM in a Milk system

3.2.4.1 Preparation of the Start Solution for the Milk System

Milk proteins can be classified into two main categories: caseins and whey proteins. Caseins compose about 80% of total milk protein and whey proteins compose the remaining 20%. The main separation method for the two categories is precipitation at pH 4.6. Casein precipitates at pH 4.6, while the whey proteins remain soluble. In that immunoglobulin belongs to the whey protein portion, the immunoglobulin remains present in the solution, such that they are available to be subjected to foam fractionation.

Milk was heated to 45°C in a water bath and the pH adjusted to 4.6 by addition of 1 M HCl with continuous mixing. Precipitated casein proteins were removed by centrifugation at 18,500 x g for 20 minutes and the pH of the resultant whey supernatant was adjusted to 7.0 by the addition of 1 M NaOH, followed by filtration through a 0.22 µm filter. Whey samples were stored at 4°C for short-term analysis and - 18°C for long-term analysis.

The target immunoglobulin (0.2-1.0 g), either rabbit IgG or human IgM, was added into an empty 1 L volumetric flask and dissolved in milk with pretreatment to the 1 L mark. The prepared start solution was stored at 4°C and used within one day. Under constant stirring, the pH of the start solution was adjusted to the desired pH value (from 2 to 11) by adding small amounts of hydrochloric acid solution or sodium hydroxide solution, depending on the required direction of movement.

3.2.4.2 Foam Fractionation Apparatus, Parameters and Procedures

Figure 3.1, shown earlier, depicts the basic equipment used for the enrichment of immunoglobulin in this work. For the foam fractionation procedures, the main components consisted of three kinds of glassware: a glass column 1000 mm in

length with an inside diameter of 15 mm, the column having a U-shaped end; a glass two-port container; and a frit assembly consisting of a glass frit holder tube fused with a glass frit (porosity: 16-40 μm). For the foam fractionation procedures, these three pieces of glassware were custom-manufactured because no suitable standard off-the-shelf glassware was available for purchase that could readily conduct the experiments without leakage. To assemble the equipment, the straight end of the glass column and the frit assembly were tightly inserted into the top port and the side port of the two-port container, respectively, and the externally-protruding end of the frit holder was connected to a nitrogen gas supply line. After assembly, nitrogen gas was continuously supplied at one of five flow rates (from 5 to 25 mL/min in 5 mL/min increments) as measured by a rotameter-type flow meter to generate the foam for fifteen minutes. However, the gas was first passed through water (via a humidifier) to humidify it to thereby minimize loss of water from solution into the gas in the downstream apparatus. The foam produced by the frit in the two-port container was progressively forced up the vertically-oriented column by newly generated foam until it passed through the U-shaped end of the column. As the foam progressively moved through the column, excess liquid drained off. Upon emerging from the opening in the U-shaped end, the now mostly collapsed foam, called the foamate, was then collected and analyzed.

The experimental procedure involved foaming with nitrogen at a desired flow rate and collection of the generated foam. To investigate the influence of different parameters on the efficiency of foaming in enrichment, the procedure was varied in terms of three main factors: the initial pH value, the initial immunoglobulin concentration, and the nitrogen flow rate.

3.2.4.3 Quantification of Immunoglobulin Concentration

The quantification of immunoglobulin concentration was determined spectrophotometrically by measuring absorbance at 405 nm. Samples of the start solution and of the foamate were taken to determine the immunoglobulin

concentration. For the quantification of rabbit immunoglobulin G in aqueous solutions, the Easy-Titer[®] rabbit IgG assay kit was used, containing goat anti-rabbit IgG sensitized beads, Easy-Titer[®] dilution buffer, and Easy-Titer[®] blocking buffer from Pierce (Rockford, IL, USA). The assay protocols are described in the following steps. First, a 20 μ L volume of the well-mixed sensitized beads was carefully pipetted into each well to be tested of a 96-well microplate. Then, 20 μ L of the properly-diluted sample or standards was added into the appropriate wells containing the beads. After adding the sample or standards, the microplate was mixed for five minutes at room temperature. Then, 100 μ L of the blocking buffer was added to each well and the microplate was mixed again for five minutes. Next, before evaluating the plate, any large bubbles generated from mixing were burst with a tiny needle. Finally, an ELISA reader was used to measure the absorbance at 405 nm. Thereafter, the immunoglobulin concentration was determined according to a calibration curve. The method used for quantification of human immunoglobulin M was identical to that used for rabbit immunoglobulin G except for using the Easy-Titer[®] human IgM assay kit containing anti-human IgM sensitized beads, again from Pierce.

3.2.4.4 Evaluation of Foam Fractionation Efficiency

In order to evaluate the efficiency of foam fractionation, the enrichment ratio and recovery were determined as follows. First, standard curves were generated for both IgG and IgM, and then the sample concentration was determined from the standard curves (Figure 3.2 and Figure 3.3, shown earlier, provide an example for IgG and IgM, respectively). Next, adjustment was made for the dilution factor for each sample to determine its starting immunoglobulin concentration. Lastly, after analytical determination of the immunoglobulin concentration, the foam fractionation efficiency was evaluated by calculating the enrichment ratio and the recovery. The equations are the same as defined in equations (3.1) and (3.2). To help average out possible measuring errors, each experimental condition was repeated at least three times.

3.2.4.5 Total Protein Assay

A total protein assay was performed in order to ensure that the total protein content of each batch of milk (purchased from the market) had approximately the same total protein content. The assay was conducted using the BCA protein assay, sensitive for protein concentrations in the range between 20 and 1200 $\mu\text{g/mL}$. The standard curve was generated using 0, 125, 250, 500, 750 and 1000 $\mu\text{g/mL}$ bovine serum albumin (BSA) calibration standards (prepared from a 1 mg/mL standard solution provided with the commercial BCA assay kit). All samples and calibration standards were diluted to their final concentrations in a 10 mM phosphate buffer in 1.5 mL micro centrifuge tubes. Then, one mL of BCA working reagent was added to 50 μL of the standard or sample, which was then vortexed and incubated at 60°C for 15 minutes, then cooled to room temperature, prior to the absorbance being read immediately at 562 nm. A zero correction was applied to the readings for the samples and standards, and a calibration curve was constructed from the BSA standards. Finally, absorbance of unknown samples was measured and concentrations calculated from the calibration curve. A total protein concentration of about 32-33 mg/mL was measured for each batch of milk used.

3.2.4.6 Process for Response Surface Methodology

Response surface methodology (RSM) is a collection of statistical and mathematical techniques useful for developing, improving and optimizing processes [MYERS and MONTGOMERY 1995]. As was done for the model system, RSM was used in this work to optimize conditions for immunoglobulin enrichment in milk by foam fractionation. The experimental design and analysis of the data were performed with the help of Design-Expert (version 6.0.5. Stat-Ease, Minneapolis, USA), a statistical analysis software package.

A general flowchart for the RSM process is provided in Figure 3.4. The process sequentially involves: first, (A) selecting both the process variables and response variables; next, (B) using CCD to design the experiment; then, (C) running the experiment and getting the results for response variables; then, (D) using different statistical methods to evaluate the adequacy of different second-order models; followed by (E) using RSM to predict the optimal process variable in order to achieve the desired responses; and, lastly, (F) running experiments to confirm the RSM prediction.

Selecting of Variables

An understanding of the foam fractionation process and the specific process variables under investigation is useful for achieving a realistic simplified model. Based on the results obtained in the previous experiments, the initial concentration of immunoglobulin, the initial pH value of the start solution and the nitrogen gas flow rate were selected as process variables for foam fractionation. The response variables, analyzed separately, were the enrichment ratio of immunoglobulin and the recovery of immunoglobulin. Hence, these three process variables were used to find the optimized conditions for enrichment and recovery using RSM.

Second-order Model

The second-order model was used in this part for the three variables. The second-order model contains the coefficients corresponding to linear, two-factor interaction and quadratic effects. The model equation of response (Y) for an RSM model with three process variables (X_1, X_2, X_3) is expressed as Eq (3.3).

Central Composite Design

One of the most widely used designs for RSM is central composite design (CCD). These days, it is the most popular second-order design. CCD is the standard RSM design and is well suited for fitting a second-order response surface, which often works well for process optimization. Thus, CCD was used in this part with three selected process variables, wherein it is recommended by CCD principles to use five equidistant levels for a three-variable model. To accommodate that

recommendation, the initial concentrations of immunoglobulin were 0.2, 0.4, 0.6, 0.8 and 1.0 mg/mL; the initial pH values of the start solution were 2, 4.25, 6.5, 8.75, 11; and the constant nitrogen gas flow rates were 5, 10, 15, 20, 25 mL/min. The ranges of the independent process variables and their associated codes after scaling are given in Table 3.1. In this case, the central values (zero levels) chosen for experimental design were 0.6 mg/mL for the initial concentration of immunoglobulin, 6.5 for the initial pH value of the start solution, and 15 mL/min for the nitrogen gas flow rate. For example, an initial pH level (value) of 6.5 in the actual range of 2 to 11 would be coded as 0 in the coded range of -2 to +2.

Each central composite design consists of a standard design with orthogonal factorial points and center points, augmented by the so-called “axial points”. The orthogonal factorial points contribute in a major way to the estimation of linear terms and two-factor interactions. The orthogonal factorial points are also the only points that contribute to the estimation of the interaction terms. The center points provide an internal estimate of error (pure error) and contribute toward the estimation of the quadratic terms. The axial points contribute in a large way to estimation of quadratic terms. In the 20 experiments that were recommended for this work, there are 8 orthogonal factorial points (corner points), 6 center points (overlapped at the center) and 6 axial points (that protrude from the face centers), as shown in Figure 4.3, wherein each point is associated with an experimental run. In all, 20 foam fractionation experiments needed to be conducted in triplicate before the average values for both the enrichment ratio and recovery could be filled in the blanks of the table shown in Table 3.3 with data obtained from running the experiments.

The table shows the software-defined settings to be used for the three process variables for 20 separate experimental runs. The settings were defined by the software after first supplying the three working ranges for the three process variables involved, such ranges being determined by preliminary experiments.

Table 3.3 Experimental design of process variables for IgG in a real system

Run	Type	Factor 1: immunoglobulin concentration (mg/mL)	Factor 2: pH value	Factor 3: nitrogen flow rate (mL/min)	Response 1: enrichment ratio	Response 2: Recovery (%)
1	Fact	1.00	11.0	25		
2	Axial	0.60	11.0	15		
3	Center	0.60	6.5	15		
4	Axial	0.60	6.5	30		
5	Fact	1.00	2.0	5		
6	Center	0.60	6.5	15		
7	Center	0.60	6.5	15		
8	Center	0.60	6.5	15		
9	Axial	1.27	6.5	15		
10	Fact	0.20	11.0	25		
11	Fact	0.20	2.0	25		
12	Fact	0.20	11.0	5		
13	Axial	0.60	6.5	5		
14	Fact	0.20	2.0	5		
15	Center	0.60	6.5	15		
16	Axial	0.60	2.0	15		
17	Fact	1.00	2.0	25		
18	Axial	0.20	6.5	15		
19	Center	0.60	6.5	15		
20	Fact	1.00	11.0	5		

4. Results and Discussion

4.1 Enrichment of Immunoglobulin in a Model System

4.1.1 Influence of Initial pH value

In general, the pH value of a solution will determine the charge sign and magnitude for a large variety of molecules. Therefore, adsorption of these molecules at the gas-liquid interface of dilute aqueous solutions and the extent of their removal by foam fractionation are influenced by the solution's pH value. Therefore, in order to maximize efficiency, it is important to determine how enrichment is affected by the starting pH level.

The dependence of the immunoglobulin enrichment response on the initial pH value was investigated by varying the pH from 2 to 11, all other parameters being kept constant (initial immunoglobulin concentration: 0.2 mg/mL; nitrogen flow rate: 5 mL/min; initial albumin concentration: 1 mg/mL; column height: 600 mm; foaming time: 15 min). Varying the initial pH value was found to influence the enrichment, and a maximum enrichment ratio of immunoglobulin G (IgG) in the collapsed foam was achieved at pH 7 after 15 minutes of foaming, where an enrichment ratio of 5.1 was achieved. The lowest enrichment ratios were obtained at pH 2 and 11, where only 0.3 and 0.1 were achieved, respectively. The results for IgG showed that, under extreme conditions (i.e., too acidic or too basic), the enrichment of IgG was poor. The results for immunoglobulin M (IgM) also tracked similarly. The highest enrichment ratio was reached when the initial pH value was 6 and 7, where enrichment ratios of 4.25 and 4.29, respectively, were achieved. Results for both IgG and IgM are shown in Figure 4.1, wherein it can be seen that the enrichment ratio was generally higher in the middle pH region from about 5.5 to 8.

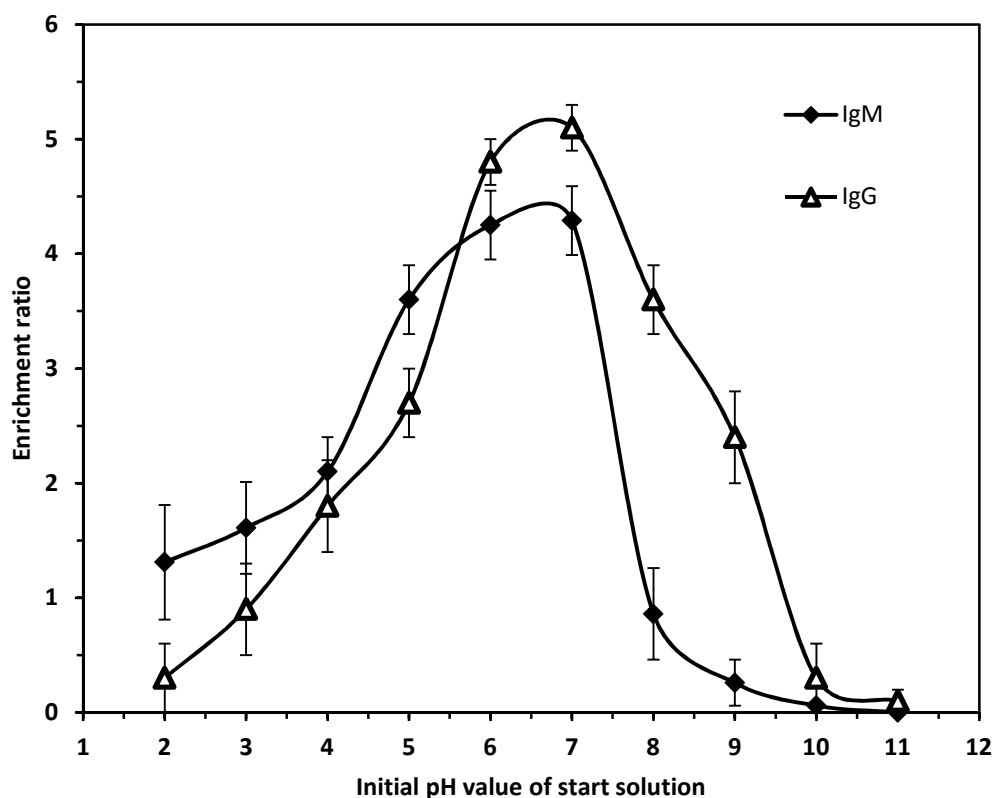


Figure 4.1 Enrichment ratio of rabbit IgG and human IgM in response to the initial pH value (initial immunoglobulin concentration: 0.2 mg/mL; nitrogen flow rate: 5 mL/min; initial albumin concentration: 1 mg/mL; column height: 600 mm; foaming time: 15 min)

It is known that the surface activity of molecules possessing different functional groups is maximal at a pH equal to their isoelectric point (pI), where the net charge of the molecule is zero. This phenomenon is related to the maximal packing of the molecules at the interface as a result of minimized electrostatic repulsion. Thus, a working solution at a pH corresponding to their pI may enhance the performance of foam fractionation. Ahmad (1975) as well as Uraizee and Narsimhan (1996) also proved in their work with proteins that the enrichment is greater at a pH corresponding to the pI [AHMAD 1975, URAIZEE and NARSIMHAN 1996]. The value of the pI for the rabbit IgG is about 6.0-6.5 and the value of the pI for the human IgM is about 5.5-6.5. The optimal pH

values for the enrichment ratio under the set conditions are 7 for IgG and 6-7 for IgM. The experimental results showed a slight shift to smaller pH values from those predicted based on the pI values (0.5-1 less for IgG and 0.5 less for IgM), which may be due to the co-existence with albumin.

4.1.2 Influence of Initial Immunoglobulin Concentration

Next, to investigate the influence of the initial immunoglobulin concentration on the enrichment ratio, the initial immunoglobulin concentration was successively varied, keeping all other parameters constant (initial pH value: 7; nitrogen flow rate: 5 mL/min; initial albumin concentration: 1 mg/mL; column height: 600 mm; foaming time: 15 min). Both the enrichment ratios for IgG and IgM showed that lower initial immunoglobulin concentrations achieved higher enrichment ratios, with initial immunoglobulin concentrations of 0.2 mg/mL appearing optimal in this case (Figure 4.2). As shown in the figure, the obtained enrichment ratios trailed off for both IgG and IgM (more so for IgG) with higher initial immunoglobulin concentrations. This may be due to increased competition for bubbles, providing reduced opportunities for transport.

In foam fractionation, the enrichment is largely dependent on the concentration of materials to be separated that are present in the bulk of the dilute solution. Robertson and Vermeulen (1969) demonstrated in their foam fractionation study of rare earth elements that low concentrations of the materials in the bulk are a desired property for extraction [ROBERTSON and VERMEULEN 1969]. Ahmad (1975) as well as Uraizee and Narsimhan (1996) proved in their work with proteins that a low concentration of materials present in the bulk is the key for effective separation. They demonstrated that there is an optimal concentration range that is more suitable for achieving effective separation [AHMAD 1975, URAIZEE and NARSIMHAN 1996]. Maas (1974) also found that, at higher concentrations, micelles are formed, which has a negative effect on enrichment [MAAS 1974]. As such, the trends and mechanisms discovered in these prior studies seem to be involved in enrichment of immunoglobulins by foam fractionation.

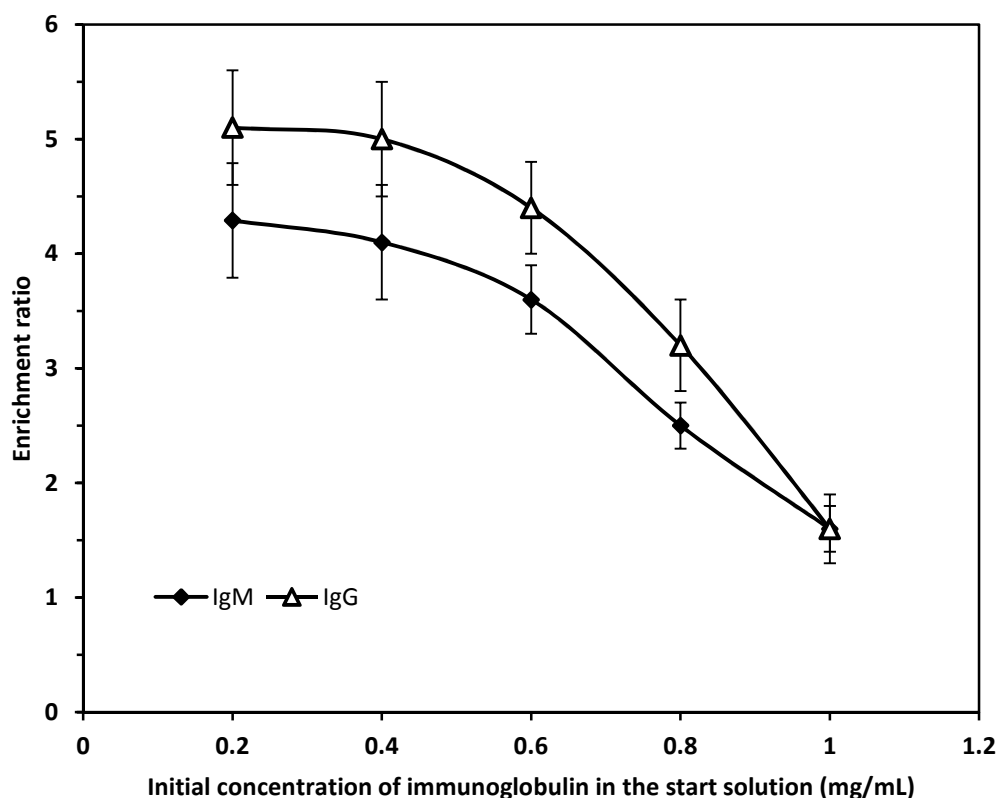


Figure 4.2 Enrichment ratio of rabbit IgG and human IgM in response to the initial immunoglobulin concentration (initial pH value: 7; nitrogen flow rate: 5 mL/min; initial albumin concentration: 1 mg/mL; column height: 600 mm; foaming time: 15 min)

4.1.3 Influence of Nitrogen Flow Rate

As might be expected, the nitrogen flow rate was determined to have a direct influence on the enrichment of immunoglobulin. It determines the speed of formation and movement of gas bubbles in the liquid pool in the foam-generating two-port container, and, in consequence, the time available for surfactant adsorption onto the bubble surfaces. It also determines the speed of foam rising in the column, as well as the maximum potential height of the foam.

The nitrogen flow rate was adjusted stepwise from 5 to 25 mL/min in 5 mL/min increments, all other parameters being kept constant (initial pH value: 7; initial immunoglobulin concentration: 0.2 mg/mL; initial albumin concentration: 1 mg/mL; column height: 600 mm; foaming time: 15 min). A flow rate below 5 mL/min was not sufficient to generate an adequate volume of foam. A flow rate of 15 mL/min or above resulted in foam that was too wet, with a high percentage of entrained solution and a low enrichment ratio. Between these two extremes, a flow rate of 10 mL/min was found to be optimal for the transference of IgG (Figure 4.3).

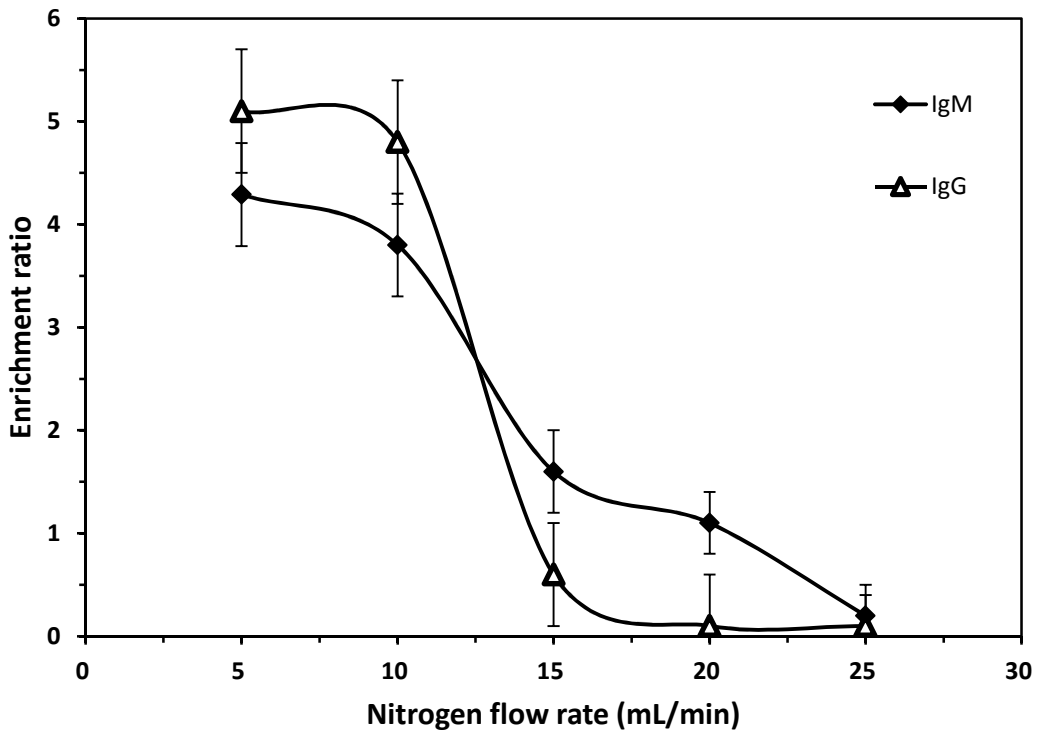


Figure 4.3 Enrichment ratio of rabbit IgG and human IgM in response to the nitrogen flow rate (initial pH value: 7; initial immunoglobulin concentration: 0.2 mg/mL; initial albumin concentration: 1 mg/mL; column height: 600 mm; foaming time: 15 min)

By way of analysis, at low nitrogen flow rates, it takes longer for the foam to reach the top of the column, giving more time for drainage, resulting in less liquid being held up. As a result, the foam becomes less wet and more concentrated. At higher nitrogen flow rates, the liquid being held up is higher, thus the foamate is more dilute, leading to lower enrichment but higher mass recovery for a set time. In addition, the results for IgM also indicated that higher nitrogen flow rates caused a decrease in the enrichment ratio (Figure 4.3). As shown in the figure, the two plotted lines trend downward going to the right with progressively higher nitrogen flow rates. This also matches observations in the literature that, in general, a higher flow rate used in the foam fractionation process usually leads to lower enrichment [LONDON, *et al.* 1954, VARLEY and BALL 1994]. Various authors have also found that, for different substances, high enrichment is obtained at low flow rates [GRIEVES and BHATTACHARYYA 1970, KISHIMOTO 1962, SCHNEPF and GADEN 1959]. Therefore, the nitrogen flow rate must be sufficient to provide stable foam, but not much higher or the enrichment of immunoglobulin will be adversely affected.

4.1.4 Influence of Initial Albumin Concentration

As previously mentioned, a solution containing immunoglobulin alone barely produces foam, but the addition of albumin to the system makes it possible to generate sufficient foam to rise in the column. Albumin is used because of its good foaming ability, stability and low cost [AHMAD 1975, ANAND and DAMODARAN 1995, CLARK, *et al.* 1988, LOCKWOOD, *et al.* 2000, NICOLAI, *et al.* 2008, SCHNEPF and GADEN 1959]. The initial albumin bovine concentration was varied from 0.125 to 2 mg/mL, keeping all other parameters constant (initial pH value: 7; initial immunoglobulin concentration: 0.2 mg/mL; nitrogen flow rate: 10 mL/min; column height: 600 mm; foaming time: 15 min). Initial albumin concentrations higher than 0.5 mg/mL showed only slight differences but were markedly better than concentrations of 0.125 and 0.25 mg/mL. From a cost perspective, 0.5 mg/mL appears adequate for the initial concentration of albumin under the set conditions. Results for IgG and IgM are

both shown in Figure 4.4. Note the relatively level slopes for the curves beyond 0.5 mg/mL concentrations, and particularly beyond 1.0 mg/mL.

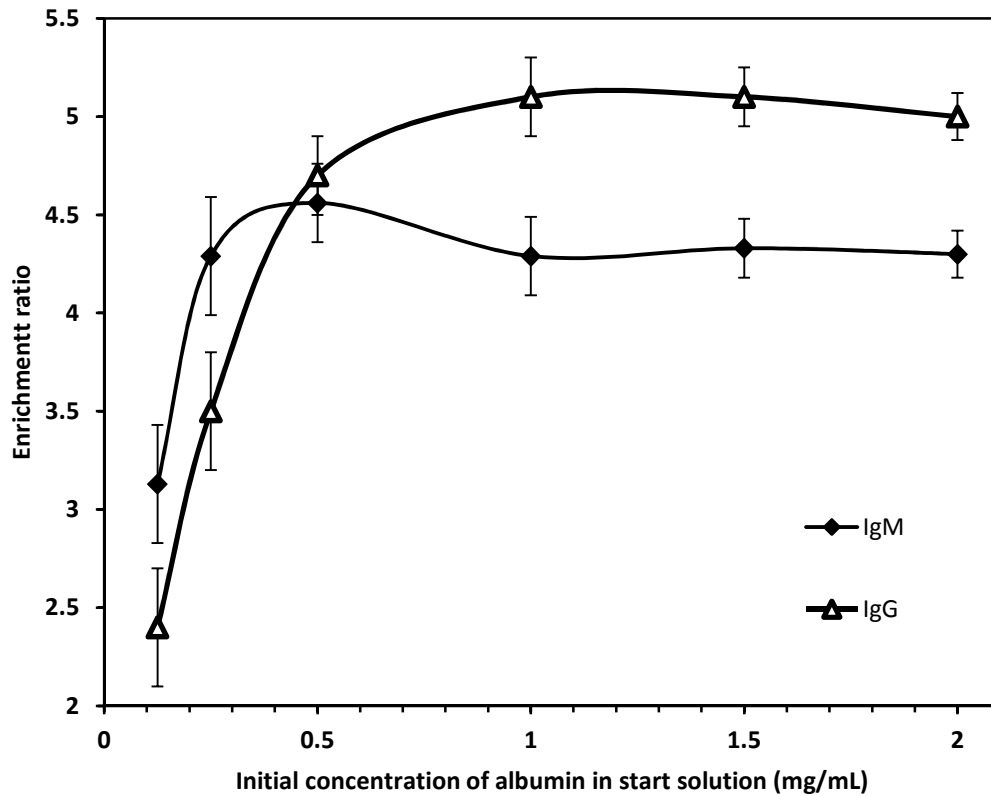


Figure 4.4 Enrichment ratio of rabbit IgG and human IgM in response to the initial albumin concentration (initial pH value: 7; initial immunoglobulin concentration: 0.2 mg/mL; nitrogen flow rate: 10 mL/min; column height: 600 mm; foaming time: 15 min)

4.1.5 Influence of Column Height

The liquid height in the foam-generating vessel is known to influence the protein foam fractionation performance [GRIEVES 1975, URAIZEE and NARSIMHAN 1996], thus the liquid height in the glass two-port container was evaluated before

the column height. The initial volume of the tested solution added to the glass two-port container was varied from 12.5 to 25 to 50 to 100 mL in order to see if resulting changes in the internal liquid height within the glass two-port container would affect the enrichment result. The results revealed that only 12.5 and 25 mL initial volumes resulted in a lower enrichment. Initial volumes of 50 and 100 mL showed higher enrichment ratios. As such, all tests investigating the influences of the column height (as well as subsequent variables) used 100 mL of initial volume of the tested solution.

After the aforementioned pre-test result was obtained, immunoglobulin enrichment in response to the column height was investigated by varying the column height from 200 to 1000 mm in 200 mm increments, all other parameters being kept constant (initial pH value: 7; initial immunoglobulin concentration: 0.2 mg/mL; nitrogen flow rate: 10 mL/min; initial albumin concentration: 0.5 mg/mL; foaming time: 15 min). Varying the column height influenced the enrichment, and a maximum enrichment ratio of immunoglobulin in the collapsed foam was achieved at a column height of 1000 mm (Figure 4.5).

As mentioned, it takes longer for the foam to reach the top of the column with higher column heights, allowing more time for drainage and causing less liquid to be held up. As a result, the foam becomes more concentrated. However, the improvement in the enrichment ratio with column height levels off as the column height approaches 1000 mm. The complete results are plotted in Figure 4.5. As shown, the curves exhibit an approximately linear positive slope up to about 800 mm, before the rates of increase start to drop and then level off around 1000 mm of column height.

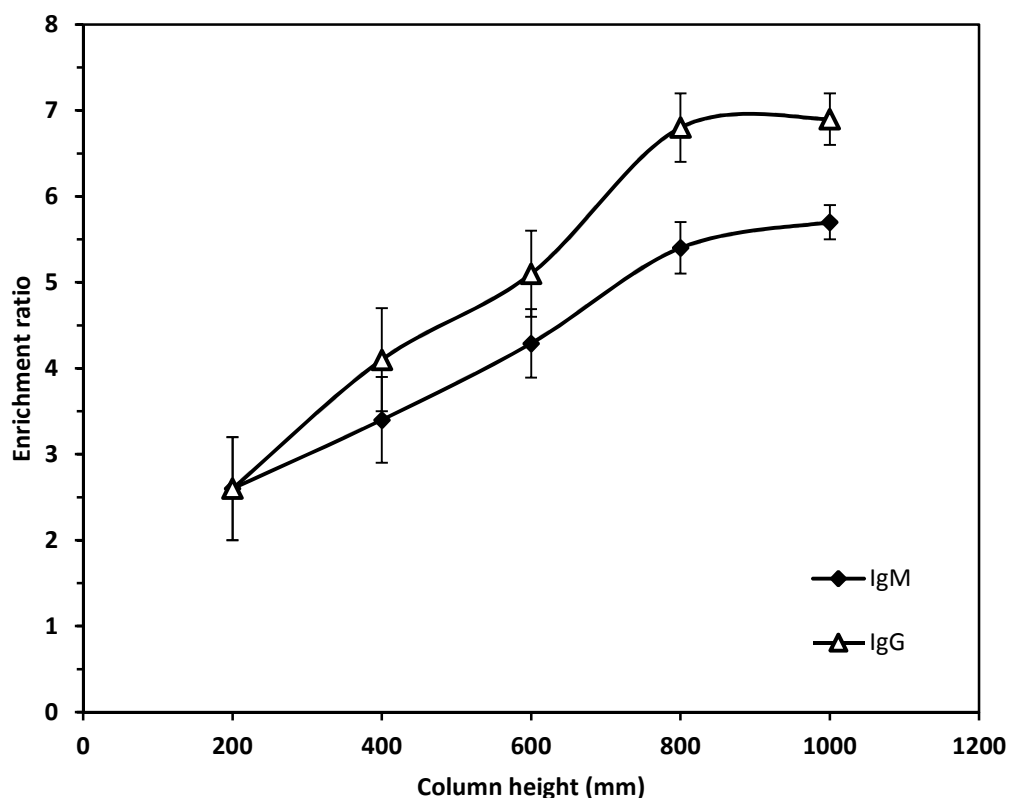


Figure 4.5 Enrichment ratio of rabbit IgG and human IgM in response to the column height (initial pH value: 7; initial immunoglobulin concentration: 0.2 mg/mL; nitrogen flow rate: 10 mL/min; initial albumin concentration: 0.5 mg/mL; foaming time: 15 min)

4.1.6 Influence of Foaming Time

Another parameter that was found to have an optimal range after testing was the foaming time. To test the impact, the foaming time was adjusted from 5 minutes to 30 minutes in 5-minute increments, all other parameters being kept constant (initial pH value: 7; initial immunoglobulin concentration: 0.2 mg/mL; nitrogen flow rate: 10 mL/min; initial albumin concentration: 0.5 mg/mL; column height: 1000 mm). The results showed that 10 minutes of foaming was near-optimal for IgG enrichment under the set conditions. A phenomenon was observed that,

between 10 and 20 minutes, only a small volume of foam was generated and the enrichment ratio thus didn't change much. The enrichment ratio was also optimal during this time range. However, further foaming caused the total volume of the foamate to increase and thus decreased the enrichment ratio due to dilution, so foaming times longer than 20 minutes were counterproductive. The same results were also seen in IgM enrichment, wherein 10 minutes of foaming was suitable to reasonably optimize IgM enrichment under the set conditions. Results for both IgG and IgM are plotted in Figure 4.6. As shown, the optimal time ranges for both IgG and IgM are of about the same duration and commerce and end at about the same time points, although the rise and fall slopes for IgG are steeper.

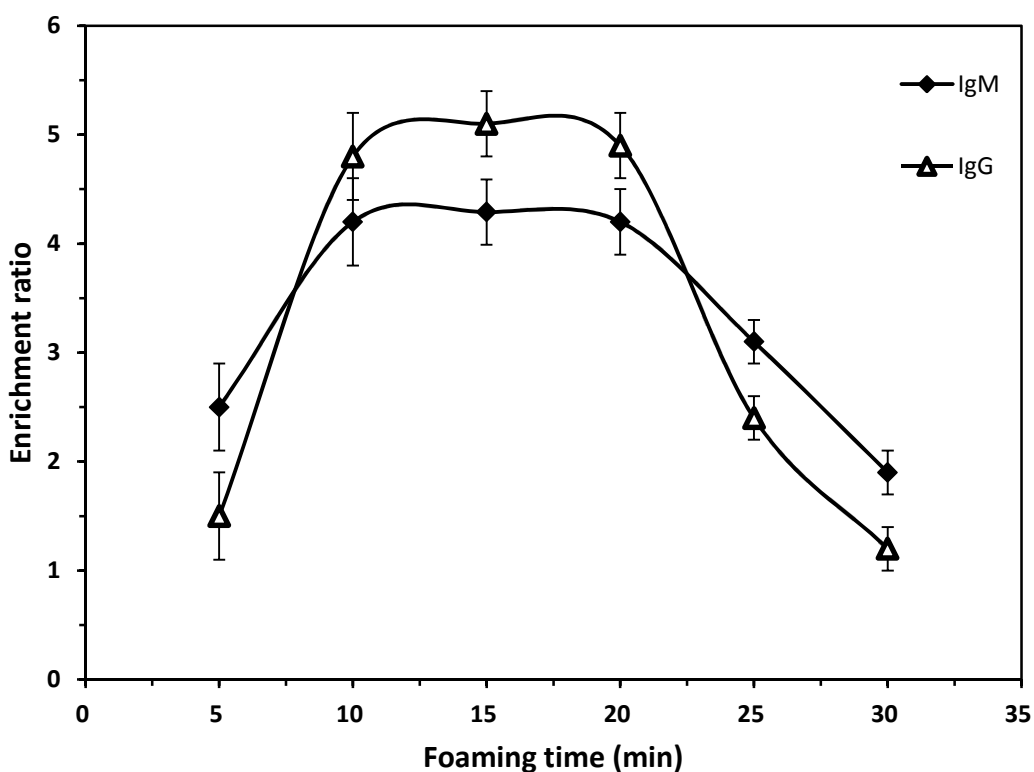


Figure 4.6 Enrichment ratio of rabbit IgG and human IgM in response to the foaming time (initial pH value: 7; initial immunoglobulin concentration: 0.2 mg/mL; nitrogen flow rate: 10 mL/min; initial albumin concentration: 0.5 mg/mL; column height: 1000 mm)

The enrichment ratio is one of the important response factors in purification, but a high enrichment ratio is not always accompanied by a high recovery. Based on these preliminary results, additional experiments were conducted to endeavor to find the optimum conditions for the enrichment of immunoglobulins in view of recovery. For all tests involving foaming time, a foaming time above ten minutes led to IgG recoveries between 95.6% and 97.2%, which illustrates that it is possible to obtain IgG from diluted solutions in the presence of albumin with relatively high enrichment at pH 7 while still at a reasonably high recovery. Similar results with high recovery were also found in the IgM enrichment experiments. Figure 4.7 shows results for the recovery of both IgG and IgM over a range of time periods under conditions of an initial pH of 7, an initial immunoglobulin concentration of 0.2 mg/mL, a nitrogen flow rate of 10 mL/min, an initial albumin concentration of 0.5 mg/mL, and a column height of 1000 mm. As with the results for the enrichment ratio, 10 to 20 minutes of foaming time produced optimal recovery levels (times beyond 20 minutes not being tested since longer foaming times were shown to be counterproductive to the enrichment ratio).

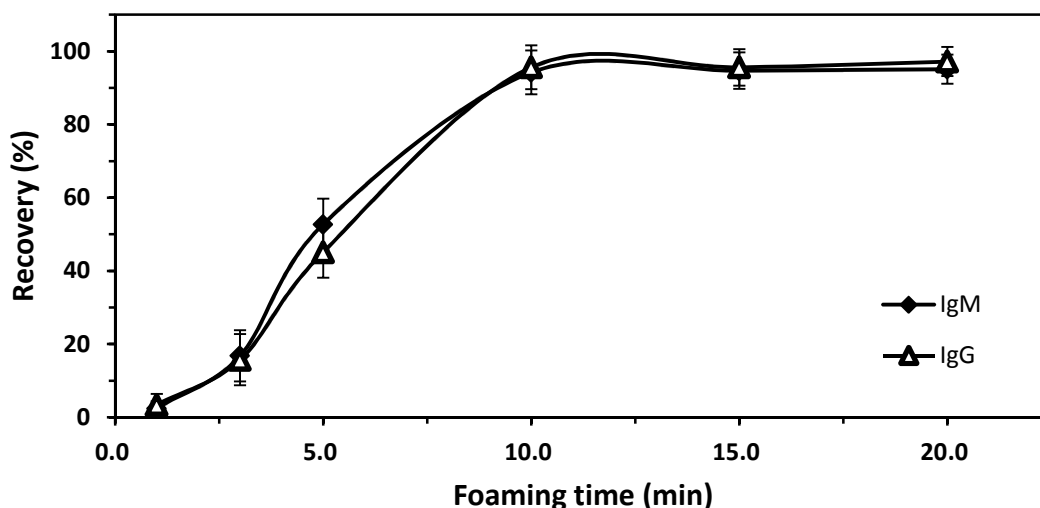


Figure 4.7 Recovery of rabbit IgG and human IgM in response to the foaming time (initial pH value: 7; initial immunoglobulin concentration: 0.2 mg/mL; nitrogen flow rate: 10 mL/min; initial albumin concentration: 0.5 mg/mL; column height: 1000 mm)

4.1.7 Separating of IgG and IgM

Next, the separation of IgG and IgM from each other using foam fractionation was investigated. However, the result was that use of only foam fractionation cannot separate IgG and IgM from each other, and the enrichment of both IgG and IgM decreased (Figure 4.8). This is probably due to the competition of both IgG and IgM onto the gas-liquid interface since the optimal pH value for IgG and IgM are close to each other (pH 7 for IgG and pH 6-7 for IgM).

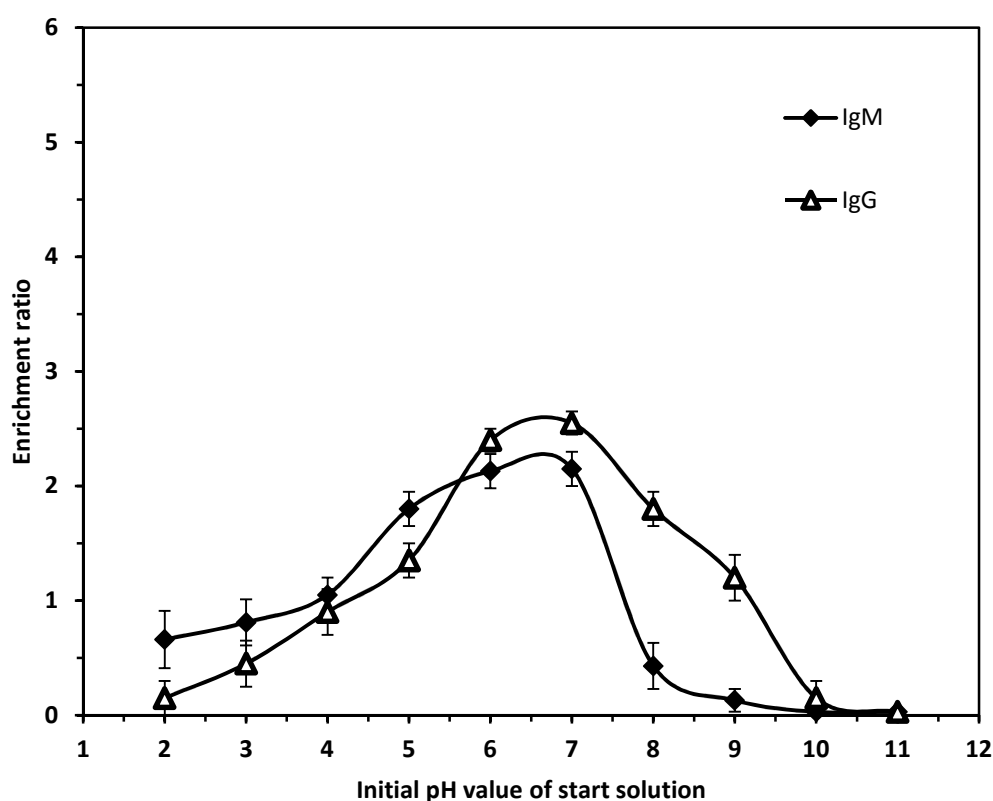


Figure 4.8 Enrichment ratio of rabbit IgG and human IgM in response to the initial pH value in a mix solution containing both IgG and IgM (initial immunoglobulin concentration: 0.1 mg/mL for IgG and 0.1 mg/mL for IgM; nitrogen flow rate: 5 mL/min; initial albumin concentration: 1 mg/mL; column height: 600 mm; foaming time: 15 min)

4.1.8 Testing of Different Multi-Component Mixtures

The results for the model system indicate that foam fractionation has exciting potential for immunoglobulin enrichment. However, immunoglobulin is generally found in mixtures, so it is important to develop an understanding of enrichment of immunoglobulin by foam fractionation from multi-component mixtures. In order to determine suitable candidates for multi-component mixtures, serum and milk were both investigated. The results were that, under the set conditions, an enrichment ratio over 5 could be achieved for the milk system, but an enrichment ratio of only near 2 could be achieved in the serum system (Figure 4.9). Based on these results, milk was selected for further description in the next section. Milk is also a promising alternative to traditional methods, since it has some advantages as a source for immunoglobulin production. Milk is considered a safe and pathogenic-free source of proteins, and it is also already well-characterized and available in abundant amounts for production.

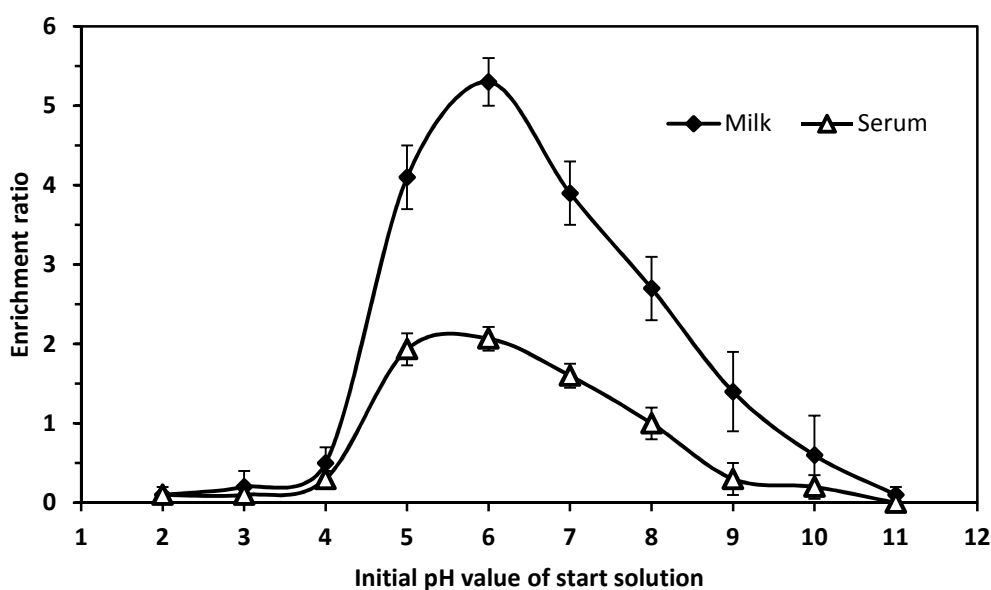


Figure 4.9 Enrichment ratio of rabbit IgG from serum and milk in response to the initial pH value (initial immunoglobulin concentration: 0.2 mg/mL; nitrogen flow rate: 10 mL/min; column height: 600 mm; foaming time: 15 min)

4.2 Enrichment of Immunoglobulin in a Milk System

4.2.1 Influence of Initial pH value

In general, the pH value of a solution will determine the charge sign and magnitude for a large variety of molecules. Therefore, adsorption of these molecules at the gas-liquid interface of the solution and the extent of their take up by foam fractionation are influenced by the solution's pH value, thus it is important to determine how enrichment is affected by the starting pH level, in order to maximize efficiency.

The dependence of the immunoglobulin enrichment response on the initial pH value was investigated by varying the pH from 2 to 11, all other parameters being kept constant (initial immunoglobulin concentration: 0.2 mg/mL; nitrogen flow rate: 10 mL/min; column height: 600 mm; foaming time: 15 min). Varying the initial pH value was found to influence the enrichment, and a maximum enrichment ratio of immunoglobulin G (IgG) in the collapsed foam was achieved at pH 6 after 15 minutes of foaming, where an enrichment ratio of 6.2 was achieved after pretreatment (Figure 4.10). The lowest enrichment ratios were obtained at pH 2 and 11, where only 0.1 or even less was achieved. The results for IgG showed that, under extreme conditions (i.e., too acidic or too basic), the enrichment of IgG was poor. The results for immunoglobulin M (IgM) also tracked similarly. The highest enrichment ratio was reached when the initial pH value was 5 after pretreatment and 7 without pretreatment, where enrichment ratios of 5.1 and 4.3, respectively, were achieved. Results for IgM are shown in Figure 4.11. The graph plots results both with and without pretreatment. The obtained enrichment ratios with pretreatment were generally somewhat higher than those obtained without, particularly in the middle region (away from the extremes). To obtain these results, each of the experiments was performed at least three times, and the plots show the range of readings obtained at each measurement point.

It is known that the surface activity of molecules possessing different functional groups is maximal at a pH equal to their isoelectric point (pI), where the net charge of the molecule is zero. This phenomenon is related to the maximal packing of the molecules at the interface as a result of minimized electrostatic repulsion. Thus, a working solution at a pH corresponding to their pI may enhance the performance of foam fractionation. Ahmad (1975) as well as Uraizee and Narsimhan (1996) also showed in their work with proteins that the enrichment is greater at a pH corresponding to the pI [AHMAD 1975, URAIZEE and NARSIMHAN 1996]. The value of the pI for the rabbit IgG is about 6.0-6.5 and the value of the pI for the human IgM is about 5.5-6.5. The optimal pH values for the enrichment ratio under the set condition are 6 for IgG and 5-7 for IgM. This corresponds with the results reported in other literature that, among some proteins, the optimal pH values for enrichment by foam fractionation is their pI values.

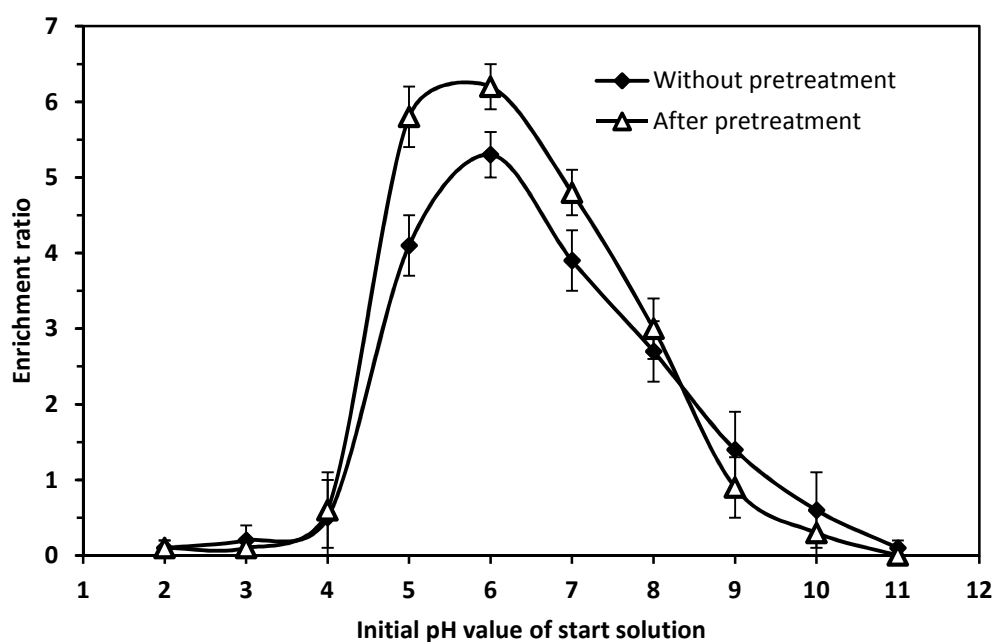


Figure 4.10 Enrichment ratio of rabbit IgG from milk in response to the initial pH value (initial immunoglobulin concentration: 0.2 mg/mL; nitrogen flow rate: 10 mL/min; column height: 600 mm; foaming time: 15 min)

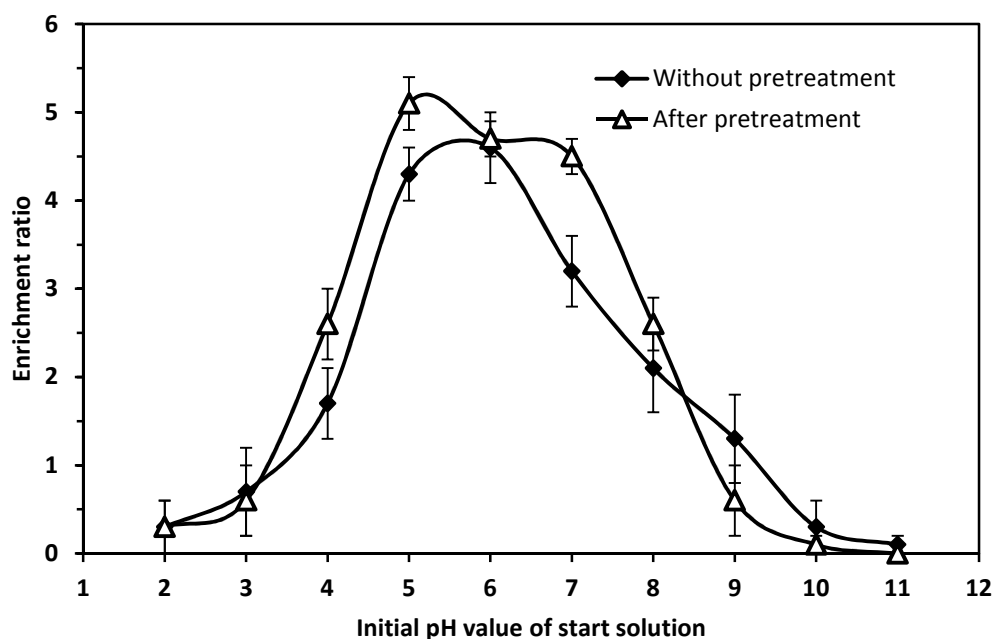


Figure 4.11 Enrichment ratio of human IgM from milk in response to the initial pH value (initial immunoglobulin concentration: 0.2 mg/mL; nitrogen flow rate: 10 mL/min; column height: 600 mm; foaming time: 15 min)

4.2.2 Influence of Initial Immunoglobulin Concentration

A solution containing immunoglobulin alone hardly produces foam, but the combination with milk protein makes it possible to generate enough foam to rise in the column. To investigate the influence of the initial immunoglobulin concentration on enrichment, the initial immunoglobulin concentration was successively varied, keeping all other parameters constant (initial pH value: 6 for IgG and 5 for IgM; nitrogen flow rate: 10 mL/min; column height: 600 mm; foaming time: 15 min). Both the enrichment ratios for IgG and IgM showed that lower initial immunoglobulin concentrations achieved higher enrichment ratios, with initial immunoglobulin concentrations of 0.2 mg/mL appearing optimal in this case (Figure 4.12 and Figure 4.13). This may be due to increased competition for bubbles, providing reduced opportunities for transport. Again,

the graph plots results with and without pretreatment. And, as before, results for the pretreated milk tracked generally higher. In general, pretreatment was associated with a one unit increase in the enrichment ratio, such as from 5 to 6 for the non-treated milk versus the pre-treated.

In foam fractionation, the enrichment is largely dependent on the concentration of materials to be separated that are present in the bulk of the dilute solution. As mentioned for the model system, Robertson and Vermeulen (1969) demonstrated in their foam fractionation study of rare earth elements that low concentrations of the materials in the bulk are a desired property for extraction [ROBERTSON and VERMEULEN 1969]. Ahmad (1975), and Uraizee and Narsimhan (1996) proved in their work with proteins that a low concentration of materials present in the bulk is key for an effective separation. They pointed out that there is an optimal concentration range, which is more suitable for achieving effective separation [AHMAD 1975, URAIZEE and NARSIMHAN 1996]. Maas (1974) also found that, at higher concentrations, micelles are formed, which has a negative effect on enrichment [MAAS 1974].

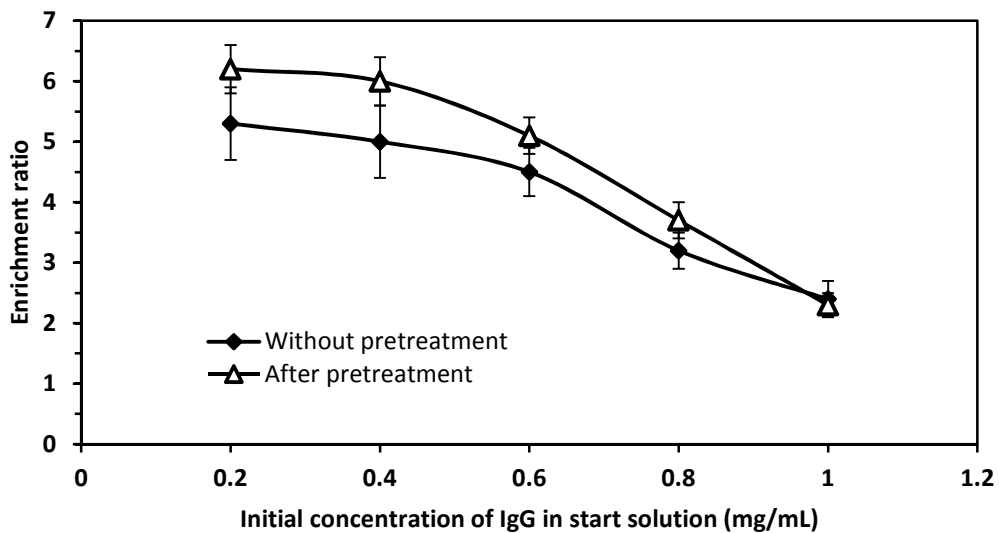


Figure 4.12 Enrichment ratio of rabbit IgG in response to the initial immunoglobulin concentration (initial pH value: 6; nitrogen flow rate: 10 mL/min; column height: 600 mm; foaming time: 15 min)

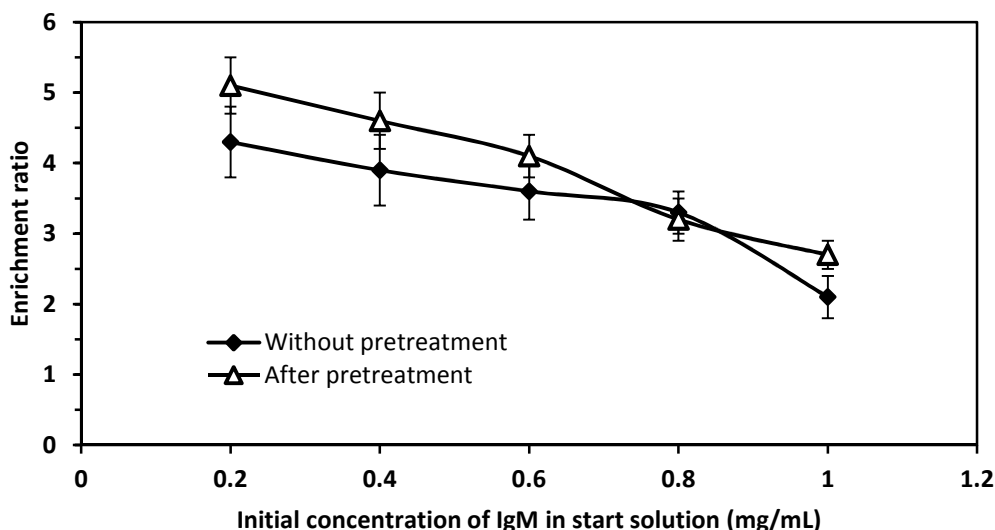


Figure 4.13 Enrichment ratio of human IgM in response to the initial immunoglobulin concentration (initial pH value: 5; nitrogen flow rate: 10 mL/min; column height: 600 mm; foaming time: 15 min)

4.2.3 Influence of Column Height

The liquid height in the foam-generating vessel is known to influence the protein foam fractionation performance [GRIEVES 1975, URAIZEE and NARSIMHAN 1996], thus the liquid height in the glass two-port container was evaluated before the column height. The initial volume of the tested solution added to the glass two-port container was varied from 12.5 to 100 mL in order to see if changes in the internal liquid height within the glass two-port container would affect the enrichment result. The results revealed that 12.5, 25 and 50 mL initial volumes resulted in a lower enrichment, whereas an initial volume of 100 mL showed a higher enrichment ratio. Therefore, as with the model system, all tests investigating the influence of the column height (as well as subsequent variables) used 100 mL of initial volume of the tested solution.

After establishing an appropriate starting volume, immunoglobulin enrichment in response to the column height was investigated by varying the column height from 200 to 1000 mm in 200 mm increments, all other parameters being kept

constant (initial pH value: 6 for IgG and 5 for IgM; initial immunoglobulin concentration: 0.2 mg/mL; nitrogen flow rate: 10 mL/min; foaming time: 15 min). Varying the column height influenced the enrichment, and a maximum enrichment ratio of immunoglobulin in the collapsed foam was achieved at a column height more than 800 mm (Figure 4.14 for IgG and Figure 4.15 for IgM).

Speculating as to the mechanism behind this result, with increasing column height, it takes longer for the foam to reach the top of the column, giving more time for drainage and resulting in less liquid being supported. As a result, the foam becomes more concentrated. However, the improvement in the enrichment ratio with column height levels off as the column height approaches 1000 mm. The complete results are plotted in Figure 4.14 and Figure 4.15. Again, the pretreated milk tracked consistently higher than the non-treated, with the tracks being roughly parallel to each other.

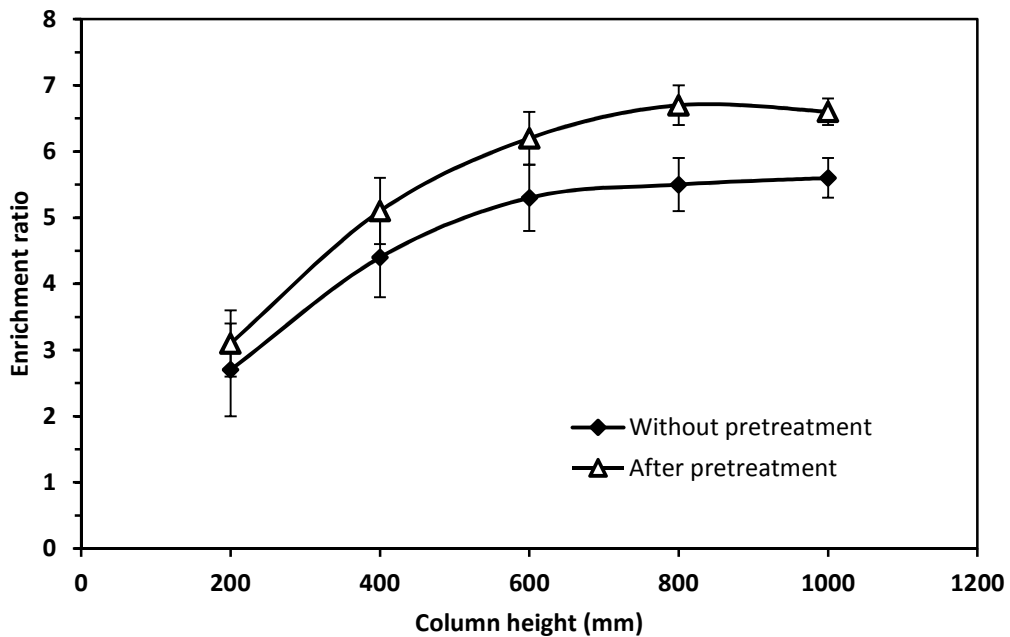


Figure 4.14 Enrichment ratio of rabbit IgG in response to the column height (initial pH value: 6; initial immunoglobulin concentration: 0.2 mg/mL; nitrogen flow rate: 10 mL/min; foaming time: 15 min)

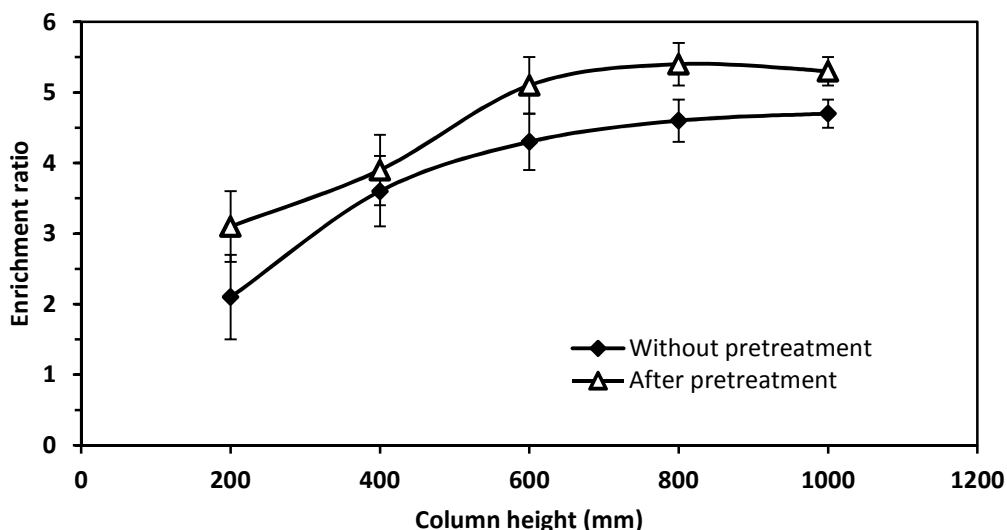


Figure 4.15 Enrichment ratio of human IgM in response to the column height (initial pH value: 5; initial immunoglobulin concentration: 0.2 mg/mL; nitrogen flow rate: 10 mL/min; foaming time: 15 min)

4.2.4 Influence of Nitrogen Flow Rate

As might be expected, the nitrogen flow rate was determined to have a direct influence on the enrichment of immunoglobulin. It determines the speed of formation and movement of gas bubbles in the liquid pool in the foam-generating two-port container, and, in consequence, the time available for surfactant adsorption onto the bubble surfaces. It also determines the speed of foam rising in the column, as well as the maximum potential height of the column. The nitrogen flow rate was adjusted stepwise from 5 to 25 mL/min in 5 mL/min increments, all other parameters being kept constant (initial pH value: 6 for IgG and 5 for IgM; initial immunoglobulin concentration: 0.2 mg/mL; column height: 1000 mm; foaming time: 15 min). By experimentation, it was determined that a flow rate below 5 mL/min was not sufficient to generate adequate foam. On the other extreme, a flow rate of 15 mL/min or above resulted in foam that was too wet, with a high percentage of entrained solution and a low enrichment ratio.

Between these two extremes, a flow rate of 10 mL/min was found to be optimal, which can be seen in the plot for the transference of IgG (Figure 4.16). In

addition, the results for IgM also supported the conclusion that higher nitrogen flow rates caused a decrease in the enrichment ratio (Figure 4.17). As shown in both of the figures, all the plotted lines trend downward going to the right with progressively higher nitrogen flow rates. This observation applies to both the pretreated and non-treated immunoglobulin.

At low nitrogen flow rates, it takes longer for the foam to reach the top of the column, giving more time for drainage and resulting in less liquid being held up. As a result, the foam becomes less wet and more concentrated. At higher nitrogen flow rates, the liquid being held up is higher, thus the foamate is more dilute, leading to lower enrichment but higher mass recovery for a set time. Again, this matches results reported in the literature that, in general, a higher flow rate used in the foam fractionation process usually leads to a lower enrichment [LONDON, *et al.* 1954, VARLEY and BALL 1994]. Various authors have also found that, for different substances, high enrichment is obtained at low flow rates [GRIEVES and BHATTACHARYYA 1970, KISHIMOTO 1962, SCHNEPF and GADEN 1959].

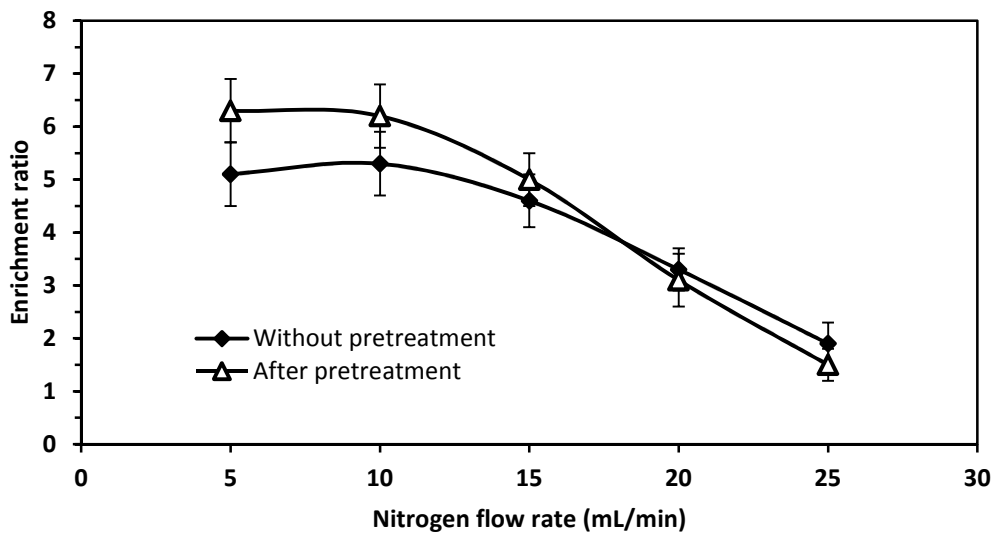


Figure 4.16 Enrichment ratio of rabbit IgG in response to the nitrogen flow rate (initial pH value: 6; initial immunoglobulin concentration: 0.2 mg/mL; column height: 1000 mm; foaming time: 15 min)

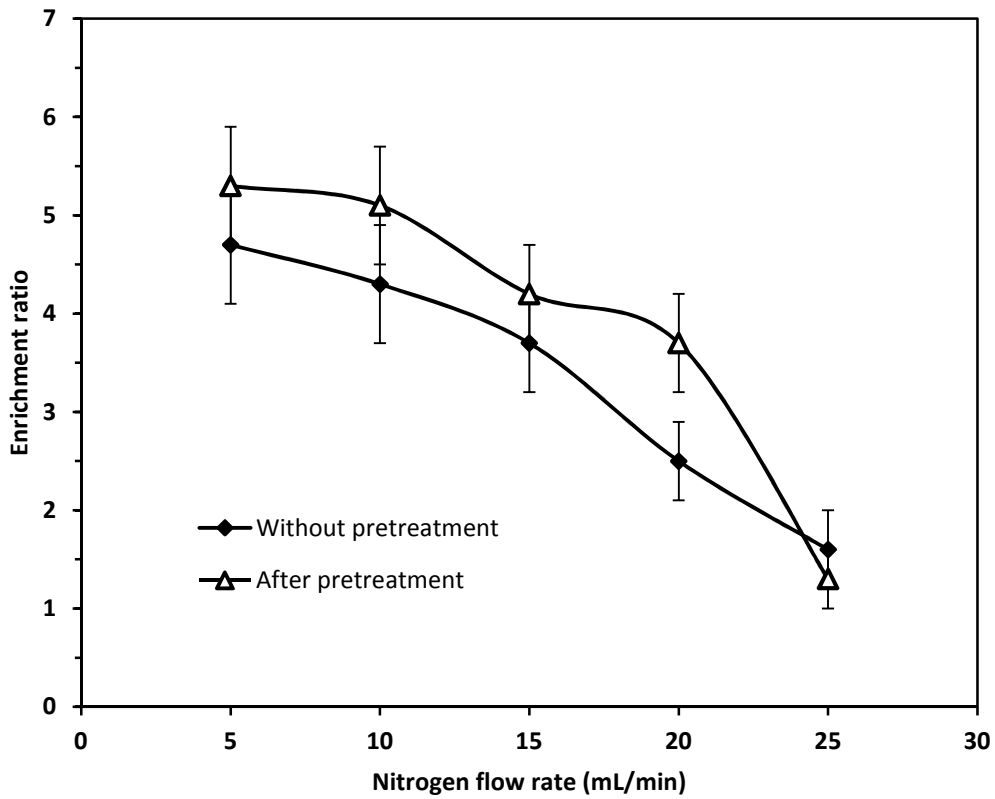


Figure 4.17 Enrichment ratio of human IgM in response to the nitrogen flow rate (initial pH value: 5; initial immunoglobulin concentration: 0.2 mg/mL; column height: 1000 mm; foaming time: 15 min)

4.2.5 Influence of Foaming Time

Another parameter that was found to have an effect with an optimal range after testing was the foaming time. To test the impact, the foaming time was adjusted from 5 minutes to 30 minutes in 5 minute increments, all other parameters being kept constant (initial pH value: 6 for IgG and 5 for IgM; initial immunoglobulin concentration: 0.2 mg/mL; nitrogen flow rate: 10 mL/min; column height: 1000 mm). The results showed that 15 minutes of foaming is near-optimal for IgG enrichment under the set conditions (Figure 4.18). Further foaming caused the total volume of the foamate to increase and thus decreased the enrichment ratio

due to dilution, so foaming times longer than 20 minutes were counter-productive. The same results were also seen in IgM enrichment, wherein 15 minutes of foaming was suitable to reasonably optimize IgM enrichment under the set conditions. Results for IgM are plotted in Figure 4.19.

As seen in both of the graphs, the enrichment ratios for both pretreated and non-treated milk initially increase somewhat sharply with an increase in the foaming time before peaking and then dropping off more slowly. Also, the enrichment ratios for both pretreated and non-treated milk were approximately the same at the extremes of the time range. At the five-minute mark, the enrichment ratios are approximately the same mostly because not enough foam was generated to allow for much of a difference. The dilution effect is mainly responsible for the negative slope of the lines after the peaks.

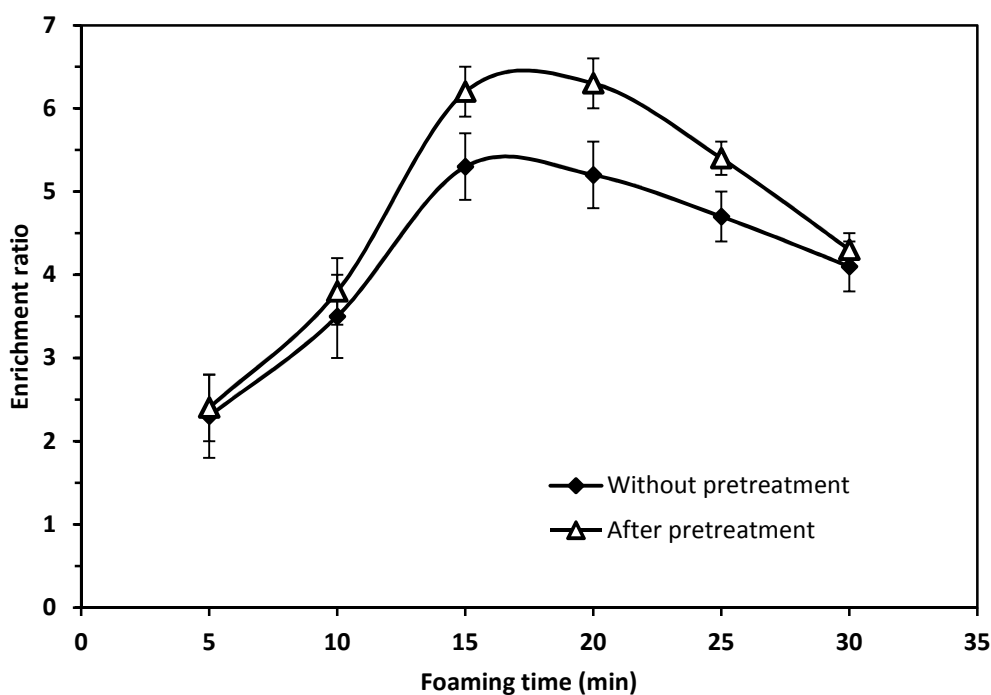


Figure 4.18 Enrichment ratio of rabbit IgG in response to the foaming time (initial pH value: 6; initial immunoglobulin concentration: 0.2 mg/mL; nitrogen flow rate: 10 mL/min; column height: 1000 mm)

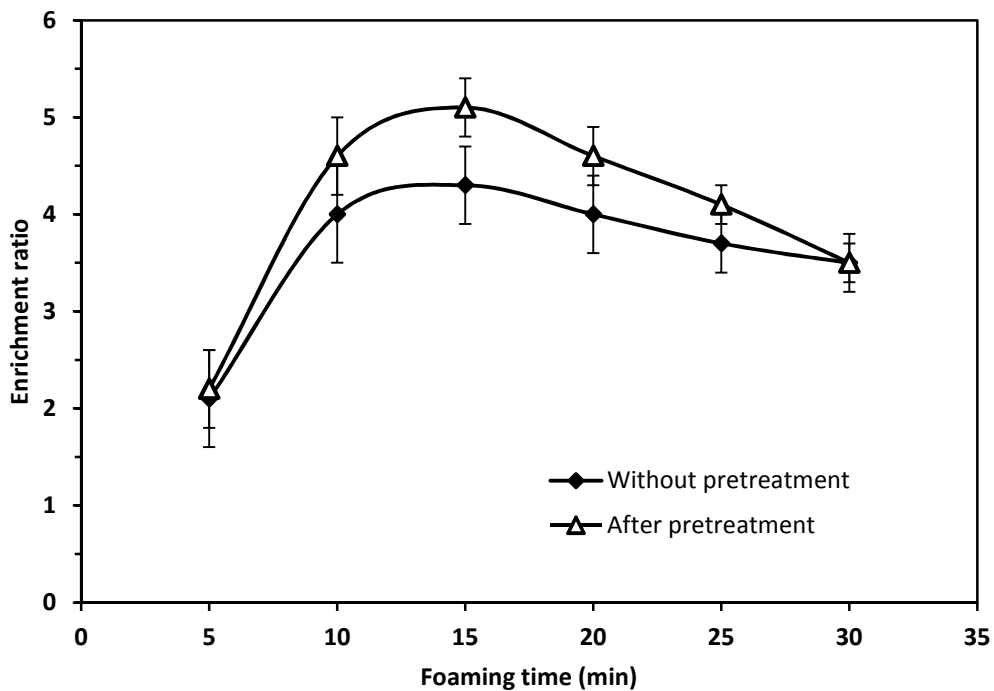


Figure 4.19 Enrichment ratio of human IgM in response to the foaming time (initial pH value: 5; initial immunoglobulin concentration: 0.2 mg/mL; nitrogen flow rate: 10 mL/min; column height: 1000 mm)

The enrichment ratio is one of the important response factors in purification, but a high enrichment ratio is not always accompanied by a high recovery. Based on these preliminary results, additional experiments were conducted to endeavor to find the optimum conditions for the enrichment of immunoglobulins in view of recovery. For all tests involving foaming time, a foaming time above 15 minutes led to IgG recoveries above 87.1%, which illustrates that it is possible to obtain IgG from milk with relatively high enrichment at pH 6 while still at a reasonably high recovery. Similar results with high recovery (85.1%) were also found in the IgM enrichment experiments. Figure 4.20 and Figure 4.21 show results for the recovery of IgG and IgM, respectively, over a range of time periods under conditions of an initial pH of 6 for IgG and 5 for IgM, an initial immunoglobulin concentration of 0.2 mg/mL, a nitrogen flow rate of 10 mL/min, and a column height of 1000 mm. As can be seen in the graphs, the recoveries for both pretreated and non-treated IgG and IgM initially rise rather sharply with an

increase in the foaming time before the rate of increase begins to fall off with longer foaming times.

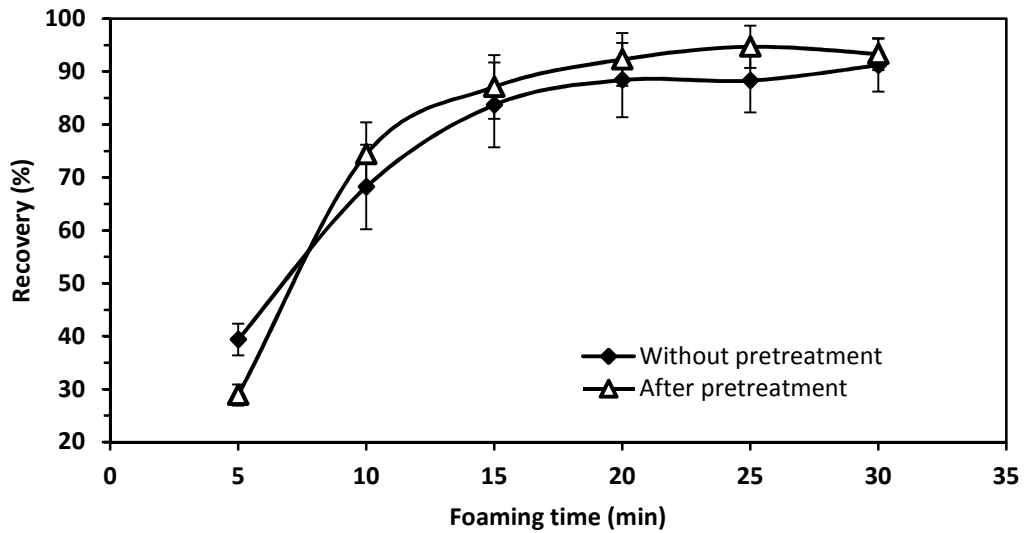


Figure 4.20 Recovery of rabbit IgG in response to the foaming time (initial pH value: 6; initial immunoglobulin concentration: 0.2 mg/mL; nitrogen flow rate: 10 mL/min; column height: 1000 mm)

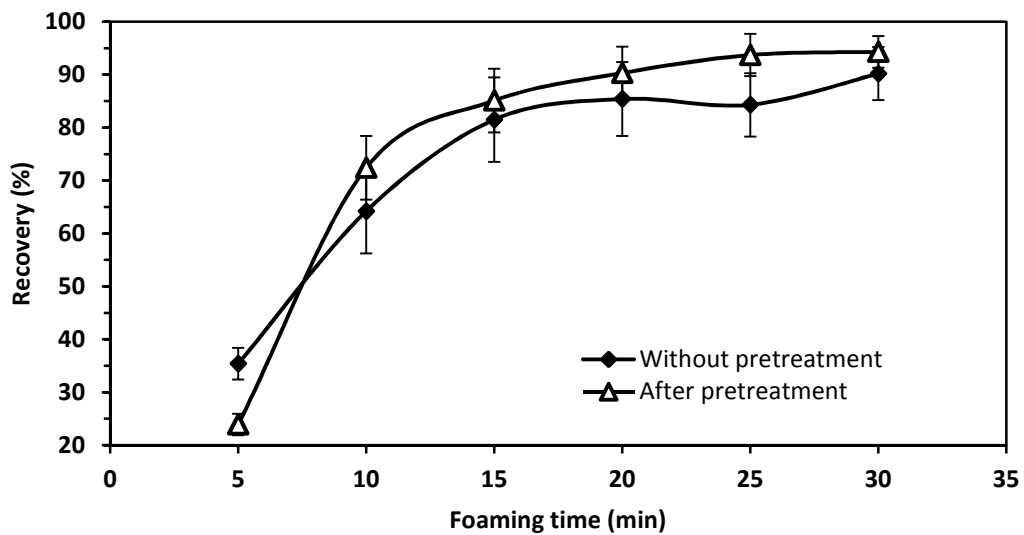


Figure 4.21 Recovery of human IgM in response to the foaming time (initial pH value: 5; initial immunoglobulin concentration: 0.2 mg/mL; nitrogen flow rate: 10 mL/min; column height: 1000 mm)

4.3 Using RSM in a Model System

4.3.1 Experimental Design of Variables and Results for IgG

After running the 20 experiments in triplicate (60 experiments in total) and taking measurements, the response variables (the enrichment ratio and recovery) were calculated and tabulated as shown in Table 4.1, wherein each line represents an experimental run.

Table 4.1 Experimental design of process variables and results for IgG in a model system showing values for the response variables calculated from measurements

Run	Type	Factor1: immunoglobulin concentration (mg/mL)	Factor 2: pH value	Factor 3: nitrogen flow rate (mL/min)	Response 1: enrichment ratio	Response 2: Recovery (%)
1	Center	0.60	6.5	15	4.9	74.1
2	Fact	1.00	11.0	5	1.2	0.2
3	Fact	0.20	2.0	25	1.5	48.5
4	Fact	0.20	2.0	5	2.7	91.2
5	Fact	1.00	2.0	25	1.0	37.8
6	Center	0.60	6.5	15	4.9	73.2
7	Fact	0.20	11.0	25	0.5	0.1
8	Fact	1.00	11.0	25	0.5	0.3
9	Fact	1.00	2.0	5	2.2	82.4
10	Fact	0.20	11.0	5	1.7	0.2
11	Center	0.60	6.5	15	4.9	74.0
12	Axial	0.60	6.5	5	5.1	96.0
13	Axial	0.60	11.0	15	0.9	0.3
14	Axial	1.27	6.5	15	4.1	59.0
15	Axial	0.60	2.0	15	1.9	65.7
16	Axial	0.20	6.5	15	5.5	81.4
17	Center	0.60	6.5	15	4.9	72.1
18	Center	0.60	6.5	15	5.1	71.0
19	Axial	0.60	6.5	30	3.3	42.5
20	Center	0.60	6.5	15	4.9	75.0

4.3.2 Enrichment Ratio of IgG Using Foam Fractionation

Design-Expert, the statistical analysis package used, provides several useful statistical tables that can be used to identify which response function model to choose for an in-depth study. The program calculates the effects for all model terms. It produces statistics, such as F-values, lack of fit and R-squared values, for comparison of the models. The software underlines and labels as “Suggested” the model that best meets the criteria specified by the user. The following three tables help to select the most appropriate model for a given response (the enrichment ratio in this case).

[Sequential Model Sum of Squares]

The Sequential Model Sum of Squares table shows the progressive improvement in the model fit as terms are added (Table 4.2).

Table 4.2 The sequential model sum of squares for the IgG enrichment ratio in a model system

Sequential Model Sum of Squares						
Source	Sum of Squares	DF	Mean Square	F Value	Prob > F	
Mean	190.34	1	190.34			
Linear	5.64	3	1.88	0.51	0.6795	
2FI	0.094	3	0.031	6.936E-003	0.9992	
<u>Quadratic</u>	<u>58.06</u>	<u>3</u>	<u>19.35</u>	<u>374.69</u>	<u>< 0.0001</u>	<u>Suggested</u>

Source

- ◆ Linear: the linear terms (A, B, and C)
- ◆ 2FI: the two-factor interaction terms (AB, AC, and BC)
- ◆ Quadratic: the quadratic terms (A^2 , B^2 and C^2)

Degrees of freedom (DF)

The column labeled “DF” provides the degrees of freedom contributed by each kind of term source. In the table, the value for the degrees of freedom equals

the number of model coefficients added by each term source.

F -value

The F-value shows the significance of adding each term source to the model, wherein higher values are more significant. In the table, the high F-value of 374.69 for the quadratic term indicates that it is much more significant for the model than the linear and two-factor interaction terms, which have small F-values.

p-value (Prob > F)

The column labeled “Prob > F” represents the probability of seeing the observed F value if the null hypothesis is true (there is no factor effect). Small probability values call for rejection of the null hypothesis. The probability equals the proportion of the area under the curve of the F-distribution that lies beyond the observed F value. A small p-value (Prob>F) indicates that adding the term has improved the model. The small p-value of less than 0.0001 for the quadratic term means that adding the term actually improved the model.

.....

[Lack of Fit Tests]

The next table (Table 4.3) displays lack of fit tests that diagnose how well each of the full models fit the data. Models with a significant lack of fit should not be used for predictions. Here, significance is largely a relative matter, as the model with the lowest lack of fit would typically be selected.

Table 4.3 The lack of fit tests for the IgG enrichment ratio in a model system

Lack of Fit Tests

Source	Sum of Squares	DF	Mean Square	F Value	Prob > F	
Linear	58.64	11	5.33	799.57	< 0.0001	
2FI	58.54	8	7.32	1097.65	< 0.0001	
<u>Quadratic</u>	<u>0.48</u>	<u>5</u>	<u>0.097</u>	<u>14.50</u>	<u>0.0054</u>	<u>Suggested</u>

Source

- ◆ Linear: the linear model
- ◆ 2FI: the two-factor interaction model
- ◆ Quadratic: the quadratic model

F -value

The low F-value of 14.50 for the quadratic model means that it doesn't have a significant lack of fit, which is desirable. But the linear and two-factor interaction models with much larger F-values (779.57 and 1097.65, respectively) do exhibit significant lack of fit, and thus would be disqualified as suitable candidate models.

.....

[Model Summary Statistics]

The "Model Summary Statistics" table lists other statistics used to compare models (Table 4.4). This table shows the standard deviation, R-squared, adjusted R-squared, predicted R-squared and the predicted residual error sum of squares (PRESS) statistic for each complete model. A low standard deviation, an R-Squared value near 1, and a relatively low PRESS value are best/desirable.

Table 4.4 The model summary statistics for the IgG enrichment ratio in a model system

Model Summary Statistics

Source	Std. Dev.	R-Squared	Adjusted R-Squared	Predicted R-Squared	PRESS	
Linear	1.91	0.0877	-0.0834	-0.4817	95.28	
2FI	2.12	0.0891	-0.3313	-3.6384	298.28	
<u>Quadratic</u>	<u>0.23</u>	<u>0.9920</u>	<u>0.9847</u>	<u>0.9031</u>	<u>6.23</u>	<u>Suggested</u>

Source

- ◆ Linear: the linear model
- ◆ 2FI: the two-factor interaction model
- ◆ Quadratic: the quadratic model

Standard Deviation (Std. Dev.)

The “Std. Dev.” column provides estimates of the standard deviation of the error in the design. A smaller value is better. As shown in the table, the quadratic model has a standard deviation of 0.23, which is markedly smaller than that of the linear and two-factor interaction models (1.91 and 2.12, respectively).

R-Squared

The R-Squared and related Adjusted R-Squared values should be close to one. A value of 1.0 represents the ideal case at which 100 percent of the variation in the observed values can be explained by the chosen model. The values of R-Squared for each model were about 0.09 for both the linear model and the two-factor interaction model (2FI) and 0.992 for the quadratic model. That is, the quadratic model desirably explains about 99% of the variability observed, whereas the values of R-Squared for the linear model and the two-factor interaction model (2FI) are relatively very small, suggesting that they are not suitable models.

Adjusted R-Squared

Because R-Squared always increases as terms are added to the model, some users prefer to use Adjusted R-Squared (instead of R-Squared). In general, Adjusted R-Squared will not always increase as variables are added to the model. In fact, if unnecessary terms are added, the value of Adjusted R-Squared will often decrease. For example, the Adjusted R-Squared value for the quadratic term is 0.9847, which is very close to the ordinary R-Squared value (0.9920). When the R-Squared and the Adjusted R-Squared values differ dramatically, there is a good chance that non-significant terms have been included in the model. The negative values for adjusted R-Squared of the linear model and the two-factor interaction model (2FI) indicate that there may be some unnecessary terms included in these two models.

Predicted R-Squared

The Predicted R-Squared value is an approximation of R-Squared for prediction. This statistic gives some indication of the predictive capability of the regression model. For example, the Predicted R-Squared value for the quadratic model is

0.9031. Therefore this model is expected to explain more than 90% of the variability in predicting new observations, as compared to the approximately 99.2% of the variability in the original data explained by the least squares fit. The overall predictive capability of the quadratic model based on this criterion seems very good.

PRESS

The predicted residual error sum of squares (PRESS), proposed by Allen, provides a useful residual scaling to indicate how well the model fits the data [ALLEN 1971, ALLEN 1974]. The PRESS for the chosen model should be small relative to the other models under consideration. The PRESS value of 6.23 for the quadratic model is much smaller than that of the linear model and the two-factor interaction model (95.28 and 298.28, respectively), thus recommending the use of the quadratic model for this RSM application.

.....

[Analysis of Variance (ANOVA)]

In statistics, analysis of variance (ANOVA) is a collection of statistical models and their associated procedures, in which the observed variance is portioned into components due to different explanatory variables. An ANOVA for the response surface quadratic model for the IgG enrichment ratio in a model system is given in Table 4.5.

Source

- ◆ Model: quadratic model
- ◆ A: coded form of the initial concentration of immunoglobulin
- ◆ B: coded form of the initial pH value
- ◆ C: coded form of the nitrogen gas flow rate
- ◆ A, B and C: linear terms
- ◆ A^2 , B^2 , and C^2 : quadratic terms
- ◆ AB, BC, and AC: two-factor interaction terms

Table 4.5 The analysis of variance table for the IgG enrichment ratio in a model system

Response: ER

ANOVA for Response Surface Quadratic Model

Analysis of variance table [Partial sum of squares]

Source	Sum of Squares	DF	Mean Square	F Value	Prob > F	
Model	63.79	9	7.09	137.22	< 0.0001	significant
A	0.86	1	0.86	16.64	0.0022	
B	2.02	1	2.02	39.21	< 0.0001	
C	3.25	1	3.25	62.96	< 0.0001	
A ²	1.282E-003	1	1.282E-003	0.025	0.8780	
B ²	41.28	1	41.28	799.14	< 0.0001	
C ²	0.43	1	0.43	8.35	0.0161	
AB	0.031	1	0.031	0.61	0.4547	
AC	0.031	1	0.031	0.61	0.4547	
BC	0.031	1	0.031	0.61	0.4547	

p-value (Prob > F)

The column labeled “Prob > F” represents the probability of seeing the observed F value if the null hypothesis is true (there is no factor effect). Again, small probability values call for rejection of the null hypothesis. The probability equals the proportion of the area under the curve of the F-distribution that lies beyond the observed F value. If the p-value (Prob>F) is very small (less than 0.05) for the model (shown in the first line), then the model is suitable for modeling the response behavior. The table shows that the quadratic model has a p-value less than 0.0001, thus this model is suitable for modeling the response behavior (here, the enrichment ratio). Again, if the p-value (Prob>F) is very small (less than 0.05) for the individual terms in the model, then these terms have a significant effect on the response. The table shows that the three linear terms (A, B, and C) and two of the three quadratic terms (B² and C²) have significant effects on the response, where as the other terms (A², AB, AC, and BC) do not.

Equation

After analyzing the variance from Table 4.5, the equation below was considered to suitably describe the enrichment ratio. Note that, for example, the coefficient for the quadratic A² term (0.013) is much smaller than those for the other two quadratic terms (B² and C²), since it is not so significant.

Final equation for the enrichment ratio (ER) in terms of coded factors:

$$\begin{aligned} \text{ER} = & 4.9 - 0.29*A - 0.45*B - 0.56*C - 0.013*A^2 - 3.27*B^2 - 0.27*C^2 \\ & + 0.062*AB + 0.062*AC + 0.062*BC \end{aligned} \tag{4.1}$$

(ER: the enrichment ratio of IgG in a model system, A: the initial concentration of immunoglobulin, B: the initial pH value and C: the nitrogen flow rate)

.....

[Perturbation Plot]

Next, the perturbation plot was analyzed, which provides silhouette views of the response surface. The main purpose of this plot is to aid in the selection of axes and constants for 2-D (contour) and 3-D (surface) response plots. For response surface designs, the perturbation plot shows how the response changes as each factor moves away from the chosen reference point (where all lines meet), with all other factors being held constant at the reference value. In this case, the center values of the three variables were chosen to establish the reference point (an initial concentration of immunoglobulin of 0.60 mg/mL, an initial pH value of the start solution of 6.50, and a nitrogen gas flow rate of 15 mL/min), though other values could have been chosen. The results (shown in Figure 4.22) show that the initial concentration of immunoglobulin and the nitrogen flow rate have relatively small effects as they move away from the reference point, but changes in the initial pH value cause a more significant effect on the enrichment ratio.

ER

Actual Factors

A: Conc = 0.60

B: pH = 6.50

C: Flow Rate = 15.00

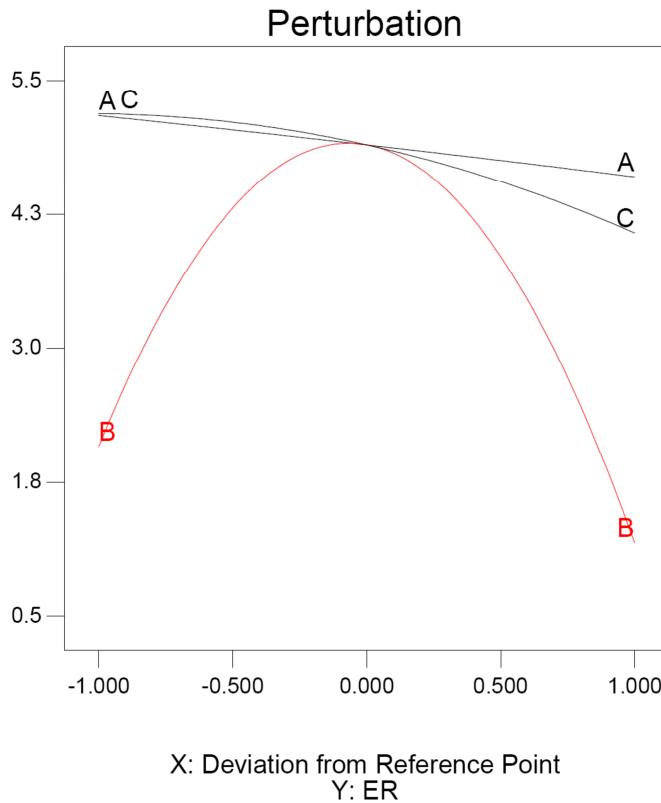


Figure 4.22 Perturbation plot for the enrichment ratio of IgG in a model system

In the figure, notice how movement along either line A (for the initial concentration) or line C (for the nitrogen flow rate) barely affects the response variable, the enrichment ratio in this case, but movement away from the reference point (where all three lines meet at a point) along the B line (for the initial pH value) dramatically affects the level of the enrichment ratio, since the enrichment ratio rapidly falls off going in either direction.

[2-D and 3-D Response Surface Plots]

It is the graphical perspective of the problem environment that has led to the term response surface methodology (RSM). It is also convenient to view the response surface in a two-dimensional plane. In the plane view, the plane is viewed from the top and response values having the same value are connected to form one line. This type of graphical representation is called a contour plot. For this contour plot, the initial pH value and the nitrogen flow rate were selected for the x- and

y-axes, respectively, due to their having the greatest impact on the response based on the perturbation plot (Figure 4.22). Note that in this contour plot, the boxed values label lines of constant response.

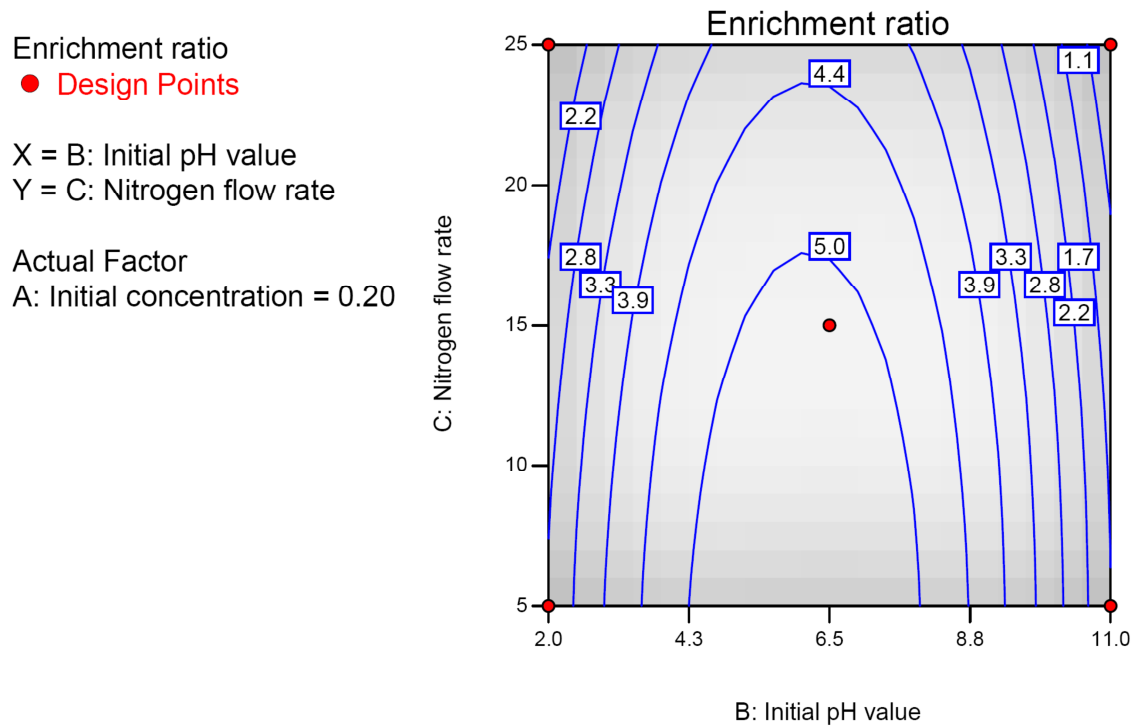


Figure 4.23 Two-dimensional isoresponse curve for the enrichment ratio of IgG in a model system

The effect of the initial pH value and nitrogen flow rate at a fixed initial concentration of immunoglobulin (0.2 mg/mL) was further revealed both from a contour plot (Figure 4.23) and a surface plot (Figure 4.24), the enrichment ratio being maximum near the center values for the pH level and smaller nitrogen flow rates. In the surface plot, the z-axis is the enrichment ratio.

Enrichment ratio
X = B: Initial pH value
Y = C: Nitrogen flow rate

Actual Factor
A: Initial concentration = 0.20

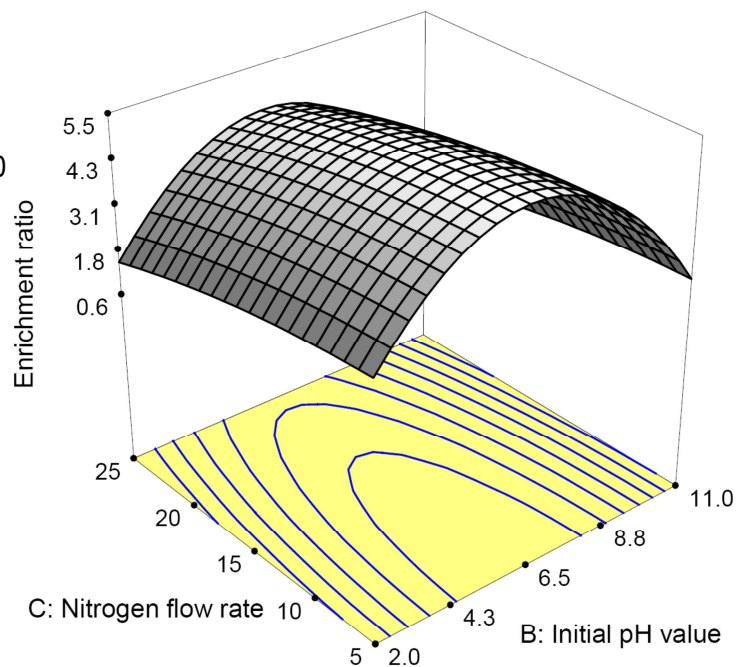


Figure 4.24 Three-dimensional surface for the enrichment ratio of IgG in a model system

4.3.3 Recovery of IgG Using Foam Fractionation

After analysis of the enrichment ratio, the other response, recovery, was then analyzed using Design-Expert, the statistical analysis package. Again, it provides several useful statistical tables that can be used to identify which response function model to choose for an in-depth study. The program calculates the effects for all model terms. It produces statistics, such as F-values, lack of fit and R-squared values, for comparison of the models. Again, the software underlines and labels as “Suggested” the model that most closely meets the criteria specified by the user. The following three tables help to select the most appropriate model for a given response (the recovery in this case).

[Sequential Model Sum of Squares]

The Sequential Model Sum of Squares table shows the progressive improvement in the model fit as terms are added (Table 4.6).

Table 4.6 The sequential model sum of squares for the IgG recovery in a model system

Sequential Model Sum of Squares					
Source	Sum of Squares	DF	Mean Square	F Value	Prob > F
Mean	54080.00	1	54080.00		
Linear	12474.64	3	4158.21	7.00	0.0032
2FI	1018.50	3	339.50	0.52	0.6757
<u>Quadratic</u>	<u>8183.69</u>	<u>3</u>	<u>2727.90</u>	<u>91.18</u>	<u>< 0.0001</u> <u>Suggested</u>

Source

- ◆ Linear: the linear terms (A, B, and C)
- ◆ 2FI: the two-factor interaction terms (AB, AC, and BC)
- ◆ Quadratic: the quadratic terms (A^2 , B^2 and C^2)

Degrees of freedom (DF)

The column labeled “DF” provides the degrees of freedom contributed by each kind of term source. In the table, the value for the degrees of freedom equals the number of model coefficients added by each term source.

F-value

The F-value shows the significance of adding each term source to the model, wherein higher values are more significant. In the table, the high F-value of 91.18 for the quadratic term means that it is much more significant for the model than the linear and two-factor interaction terms, which have small F-values (7.00 and 0.52, respectively).

p-value (Prob > F)

The “Prob >F” column represents the probability of seeing the observed F value if the null hypothesis is true (there is no factor effect). Small probability values

call for rejection of the null hypothesis. The probability equals the proportion of the area under the curve of the F-distribution that lies beyond the observed F value. A small p-value (Prob>F) indicates that adding the term has improved the model. The small p-value of less than 0.0001 for the quadratic term means that adding the term actually improves the model.

[Lack of Fit Tests]

The next table (Table 4.7) displays lack of fit tests that indicate how well each of the full models fit the data. Models with a significant lack of fit should not be used for predictions. Here, the model with the lowest lack of fit would typically be selected.

Table 4.7 The lack of fit tests for the IgG recovery in a model system

Lack of Fit Tests

Source	Sum of Squares	DF	Mean Square	F Value	Prob > F	
Linear	9490.52	11	862.77	398.20	< 0.0001	
2FI	8472.02	8	1059.00	488.77	< 0.0001	
<u>Quadratic</u>	<u>288.33</u>	<u>5</u>	<u>57.67</u>	<u>26.61</u>	<u>0.0013</u>	<u>Suggested</u>

Source

- ◆ Linear: the linear model
- ◆ 2FI: the two-factor interaction model
- ◆ Quadratic: the quadratic model

F-value

The low F-value of 26.61 for the quadratic model means that it doesn't have a significant lack of fit, which is desirable. But the linear and two-factor interaction models with much larger F-values (862.77 and 1059.00, respectively) do exhibit significant lack of fit, and thus these candidate models would be dismissed.

[Model Summary Statistics]

The “Model Summary Statistics” table lists other statistics used to compare models (Table 4.8). This table shows the standard deviation, R-squared, adjusted R-squared, predicted R-squared and the predicted residual error sum of squares (PRESS) statistic for each complete model. A low standard deviation, an R-Squared value near 1, and a relatively low PRESS value are best/desirable.

Table 4.8 The model summary statistics for the IgG recovery in a model system

Model Summary Statistics						
Source	Std. Dev.	R-Squared	Adjusted R-Squared	Predicted R-Squared	PRESS	
Linear	24.37	0.5676	0.4866	0.2717	16004.64	
2FI	25.54	0.6140	0.4358	-0.9695	43281.56	
<u>Quadratic</u>	<u>5.47</u>	<u>0.9864</u>	<u>0.9741</u>	<u>0.8629</u>	<u>3012.54</u>	<u>Suggested</u>

Source

- ◆ Linear: the linear model
- ◆ 2FI: the two-factor interaction model
- ◆ Quadratic: the quadratic model

Standard Deviation (Std. Dev.)

The “Std. Dev.” column provides estimates of the standard deviation of the error in the design. A smaller value is better. As shown in the table, the quadratic model has a standard deviation of 5.47, which is markedly smaller than that of the linear and two-factor interaction models (24.37 and 25.54, respectively).

R-Squared

The R-Squared and related Adjusted R-Squared values should be close to one. A value of 1.0 represents the ideal case at which 100 percent of the variation in the observed values can be explained by the chosen model. The values of R-Squared for each model were 0.57 and 0.61 for the linear model and the two-factor interaction model, respectively, and 0.986 for the quadratic model. That is, the quadratic model explains about 99% of the variability observed. The values of R-Squared for the linear model and the two-factor interaction model (2FI) are relatively small, suggesting that they are not suitable models.

Adjusted R-Squared

R-Squared always increases as terms are added to the model, so some users prefer to use Adjusted R-Squared. The adjusted R-Squared value will not always increase as variables are added to the model, as the addition of unnecessary terms can often cause the value of Adjusted R-Squared to decrease. For example, the Adjusted R-Squared value for the quadratic term is 0.9741, which is very close to the ordinary R-Squared value (0.9864). When R-Squared and Adjusted R-Squared differ dramatically, there is a good chance that non-significant terms have been included in the model. The small values for adjusted R-Squared of the linear model and the two-factor interaction model (0.49 and 0.44, respectively) indicate that there may be some unnecessary terms included in these two models.

Predicted R-Squared

The Predicted R-Squared is an approximate R-Squared for prediction. This statistic gives some indication of the predictive capability of the regression model. For example, the Predicted R-Squared value for the quadratic model is 0.8629. Therefore this model is expected to explain 86.29% of the variability in predicting new observations, as compared to the approximately 98.64% of the variability in the original data explained by the least squares fit. The overall predictive capability of the quadratic model based on this criterion seems very good.

PRESS

The predicted residual error sum of squares (PRESS) provides a useful residual scaling. The PRESS statistic indicates how well the model fits the data. The PRESS for the chosen model should be small relative to the other models under consideration. The PRESS value of 3,012 for the quadratic model is much smaller than that of the linear model and the two-factor interaction model (16,004 and 43,281, respectively), thus recommending the use of the quadratic model for this RSM application.

.....

[Analysis of Variance (ANOVA)]

In statistics, analysis of variance (ANOVA) is a collection of statistical models and their associated procedures, in which the observed variance is portioned into components due to different explanatory variables. An ANOVA for the response surface quadratic model for IgG recovery in a model system is given in Table 4.9.

Table 4.9 The analysis of variance table for the IgG recovery in a model system

Response: Recovery

ANOVA for Response Surface Quadratic Model

Analysis of variance table [Partial sum of squares]

Source	Sum of Squares	DF	Mean Square	F Value	Prob > F	
Model	21676.84	9	2408.54	80.51	< 0.0001	significant
A	156.65	1	156.65	5.24	0.0451	
B	10432.90	1	10432.90	348.74	< 0.0001	
C	1943.75	1	1943.75	64.97	< 0.0001	
A ²	22.83	1	22.83	0.76	0.4028	
B ²	5796.19	1	5796.19	193.75	< 0.0001	
C ²	23.93	1	23.93	0.80	0.3922	
AB	50.00	1	50.00	1.67	0.2251	
AC	0.50	1	0.50	0.017	0.8997	
BC	968.00	1	968.00	32.36	0.0002	

Source

- ◆ Model: quadratic model
- ◆ A: coded form of the initial concentration of immunoglobulin
- ◆ B: coded form of the initial pH value
- ◆ C: coded form of the nitrogen gas flow rate
- ◆ A, B and C: linear terms
- ◆ A², B², and C²: quadratic terms
- ◆ AB, BC, and AC: two-factor interaction terms

p-value (Prob > F)

The “Prob > F” column represents the probability of seeing the observed F value if the null hypothesis is true (there is no factor effect). Small probability values

call for rejection of the null hypothesis. The probability equals the proportion of the area under the curve of the F-distribution that lies beyond the observed F value. If the p-value (Prob>F) is very small (less than 0.05) for the model (shown in the first line), then the model is suitable for modeling the response behavior. The table shows that the quadratic model has a p-value less than 0.0001, thus this model is suitable for modeling the response behavior (the recovery in this case). Again, if the p-value (Prob>F) is very small (less than 0.05) for the individual terms in the model, then these terms have a significant effect on the response. Again, the table shows that the three linear terms (A, B, and C) and one of the three quadratic terms (B²) have significant effects on the response, which is not the case for the other terms (A², C², AB, AC, and BC).

Equation

After analyzing the variance from Table 4.9, the equation below was considered to suitably describe the recovery. Note that, for example, the coefficients for the quadratic term A² and C² (1.68 and 1.97, respectively) are much smaller than that for B² (38.71).

Final equation for the recovery (R) in terms of coded factors:

$$R = 73.93 - 3.88*A - 32.3*B - 13.62*C - 1.68*A^2 - 38.71*B^2 - 1.97*C^2 + 2.5*AB - 0.25*AC + 11*BC \tag{4.2}$$

(R: the recovery of IgG in a model system, A: the initial concentration of immunoglobulin, B: the initial pH value and C: the nitrogen flow rate)

.....

[Perturbation Plot]

Next, the perturbation plot was analyzed, which provides silhouette views of the response surface. The main purpose of this plot is to aid in the selection of axes and constants for 2-D (contour) and 3-D (surface) response plots. For response surface designs, the perturbation plot shows how the response changes as each factor moves from the chosen reference point (where all lines meet), with all

other factors being held constant at the reference value. In this case, the center values of the three variables were chosen to establish the reference point (an initial concentration of immunoglobulin of 0.60 mg/mL, an initial pH value for the start solution of 6.50, and a nitrogen gas flow rate of 15 mL/min). The results (shown in Figure 4.25) show that the initial concentration of immunoglobulin and the nitrogen flow rate have relatively small effects as they move away from the reference point, but changes in the initial pH value cause a more significant effect on the enrichment ratio.

Recovery

Actual Factors
 A: Conc = 0.60
 B: pH = 6.50
 C: Flow Rate = 15.00

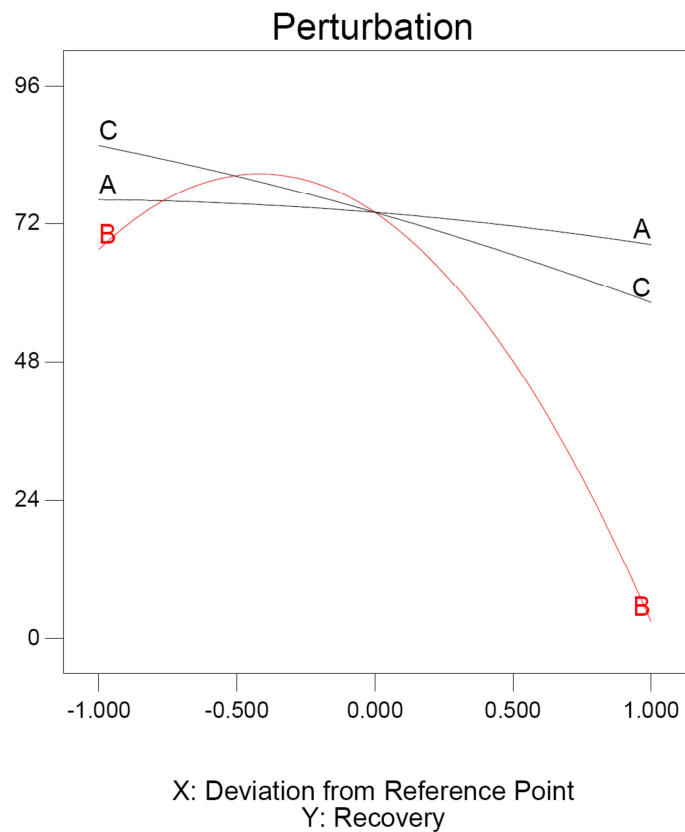


Figure 4.25 Perturbation plot for the recovery of IgG in a model system

In the figure, notice how movement along either line A (for the initial concentration) or line C (for the nitrogen flow rate) barely affects the response variable, the recovery in this case, but movement away from the reference point (again, where all three lines meet at a point) along the B line (for the initial pH value) dramatically affects the level of the recovery, since the level rapidly falls off going in either direction (especially in the case of a very high pH).

[2-D and 3-D Response Surface Plots]

Response surface methodology (RSM) provides graphical perspectives of the problem environment. It is convenient to view the response surface in a two-dimensional plane. In the plane view, the plane is viewed from the top and response values having the same value are connected to form one line. This type of graphical representation is called a contour plot. To produce a contour plot, the initial pH value and the nitrogen flow rate were selected for the x- and y-axes, respectively, due to their having the greatest impact on the response based on the perturbation plot (Figure 4.25). In this contour plot, the boxed values label lines of constant response.

The effect of the initial pH value and nitrogen flow rate at a fixed initial concentration of immunoglobulin (0.2 mg/mL) was further revealed not only from a contour plot (Figure 4.26) but also a surface plot (Figure 4.27), the recovery being maximum near a pH value of 4.3 and smaller nitrogen flow rates. In the surface plot, the z-axis is the recovery.

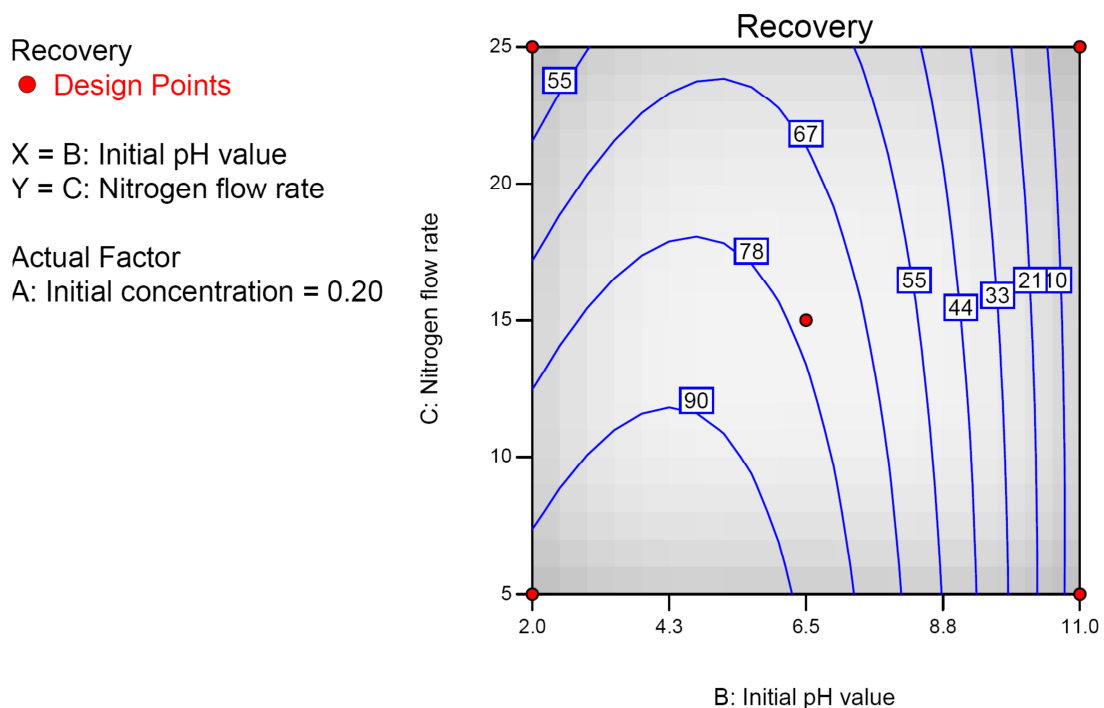


Figure 4.26 Two-dimensional isoresponse curve for the recovery of IgG in a model system

Recovery
 X = B: Initial pH value
 Y = C: Nitrogen flow rate
 Actual Factor
 A: Initial concentration = 0.20

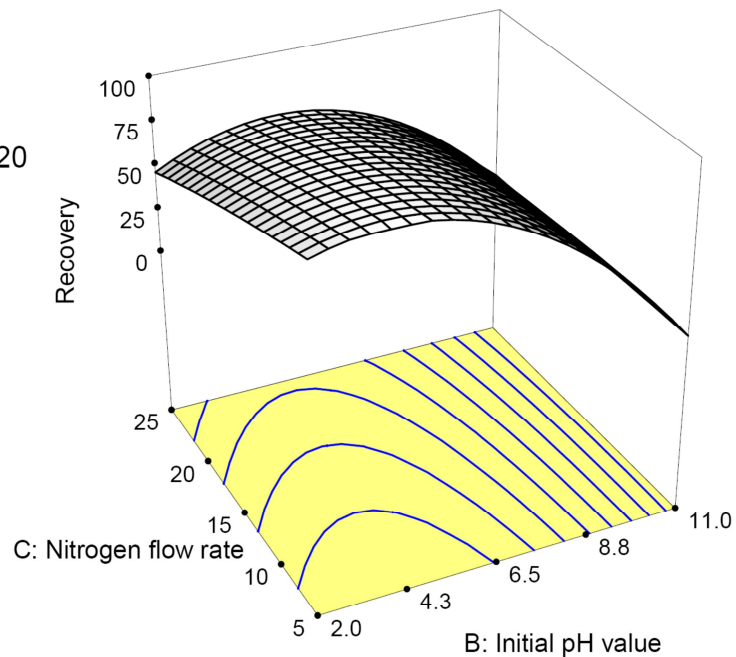


Figure 4.27 Three-dimensional surface for the recovery of IgG in a model system

4.3.4 Optimization of the Operating Variables for IgG Foam Fractionation

After selection of goals for the factors and responses by the researcher, the software package found the most suitable solution in terms of the goals. Based on software modeling and experimental evidence, the optimized values for the initial concentration of immunoglobulin in the start solution, the initial pH value and the nitrogen flow rate were 0.2 mg/mL, 5.47 and 5 mL/min, respectively (Table 4.10). In the table, the “Goal” column shows the settings selected by the researcher to constrain the factors and responses. Here, the response variables were set to be maximized and the input factors were in defined ranges.

Table 4.10 Predicted solutions for both the enrichment ratio and recovery of IgG from foam fractionation in a model system

Name	Goal	Lower	Upper	Lower	Upper	Importance
		Limit	Limit	Weight	Weight	
Conc	is in range	0.2	1	1	1	3
pH	is in range	2	11	1	1	3
Flow Rate	is in range	5	25	1	1	3
ER	maximize	0.5	5.5	1	1	5
Recovery	maximize	0	96	1	1	4

Solutions							
Number	Conc	pH	Flow Rate	ER	Recovery	Desirability	
1	<u>0.20</u>	<u>5.47</u>	<u>5.00</u>	<u>5.5</u>	<u>95.9992</u>	<u>0.999</u>	

1 Solutions found

Next, a foam fractionation experiment was conducted using the calculated input factors to check the accuracy of the predicted results from the software. The model predicted optimized values for the factors, the suggested values being: the initial concentration of immunoglobulin (0.2 mg/mL), the initial pH value (5.47), and the nitrogen flow rate (5 mL/min). The predicted responses were an enrichment ratio of 5.5 and a recovery of 96%, respectively. Further experiments were performed with the predicted values for the factors, and the experiments confirmed the model predictions with an enrichment ratio of 5.47 and recovery of 95.6%. For the obtained experimental results, there was very little deviation from the predicted values. The present work appeared to give quite good results at laboratory scale for foam fractionation of immunoglobulin in batch mode.

4.3.5 Optimization of the Operating Variables for IgM Foam Fractionation

Being presented first, the results for IgG in the above sections are provided in full detail. However, the results for IgM, here, are shortened to avoid replication and overlap. Here, only the equation for both enrichment ratio and recovery, as well as the optimization result, are presented. Despite the concise presentation, note

that, in order to get the optimization result, another 60 experiments were conducted, followed by analysis of their enrichment ratios and recoveries using “sequential model sum of squares”, “lack of fit tests”, “model summary statistics”, and “analysis of variance (ANOVA)”. A perturbation plot, 2-D and 3-D response surface plots were also needed. After all these processes, then an optimization of the operating variables for IgM foam fractionation can be achieved.

Equation for the Enrichment Ratio of IgM

After analyzing the variance, the equation below was considered to suitably describe the enrichment ratio. Note that, for example, the coefficients for A² and C² for the quadratic term (0.1 and 0.14, respectively) are smaller than that for B² (2.5), as they were less significant.

Final equation for the enrichment ratio (ER) in terms of coded factors:

$$ER = 3.89 - 0.23*A - 0.24*B - 0.48*C + 0.1*A^2 - 2.5*B^2 - 0.14*C^2 + 0.012*AB - 0.088*AC - 0.062*BC \tag{4.3}$$

(ER: enrichment ratio of IgM in a model system, A: initial concentration of immunoglobulin, B: initial pH value, C: nitrogen flow rate)

Equation for recovery of IgM

After analyzing the variance, the equation below was considered to suitably describe the recovery. Note that, for example, the coefficients for the quadratic term A² and C² (1.68 and 1.97, respectively) are much smaller than that for B².

Final equation for the recovery (R) in terms of coded factors:

$$R = 71.14 - 3.2*A - 31.5*B - 12.08*C - 1.28*A^2 - 37.56*B^2 - 1.34*C^2 + 2*AB + 0.75*AC + 9.75*BC \tag{4.4}$$

(R: recovery of IgM in a model system, A: initial concentration of immunoglobulin, B: initial pH value, C: nitrogen flow rate)

After selection of goals for the factors and responses by the researcher, the software package found two solutions and identified the most suitable one in terms of the goals. Based on software modeling and experimental evidence, the optimized values for the initial concentration of immunoglobulin in the start solution, the initial pH value and the nitrogen flow rate were 0.2 mg/mL, 5.53 and 5 mL/min, respectively (Table 4.11). In the table, the “Goal” column shows the settings selected by the researcher to constrain the factors and responses. Again, the response variables were set to be maximized and the input factors were in defined ranges.

Then, a foam fractionation experiment was conducted using the calculated input factors to check the accuracy of the predicted results by the software. The model predicted optimized values for the factors, the values being: the initial concentration of immunoglobulin (0.2 mg/mL), the initial pH value (5.53), and the nitrogen flow rate (5 mL/min). The predicted responses were an enrichment ratio of 4.4 and a recovery of 92%, respectively. Further experiments were performed with the predicted values for the factors, and the experiments confirmed the model predictions with an enrichment ratio of 4.43 and recovery of 91.6%. For the obtained experimental results, there was very little deviation from the predicted values. Once again, this work appeared to give quite good results at laboratory scale for foam fractionation of immunoglobulin in batch mode.

Table 4.11 Predicted solutions for both the enrichment ratio and recovery of IgM from foam fractionation in a model system

Name	Goal	Lower	Upper	Lower	Upper	Importance
		Limit	Limit	Weight	Weight	
Conc	is in range	0.2	1	1	1	3
pH	is in range	2	11	1	1	3
Flow Rate	is in range	5	25	1	1	3
ER	maximize	0.6	4.7	1	1	5
Recovery	maximize	0	93	1	1	4

Solutions							
Number	Conc	pH	Flow Rate	ER	Recovery	Desirability	
1	<u>0.20</u>	<u>5.53</u>	<u>5.00</u>	<u>4.4</u>	<u>92.1302</u>	<u>0.954</u>	
2	1.00	5.61	5.00	4.1	82.9751	0.873	

2 Solutions found

4.4 Using RSM in a Milk System

4.4.1 Experimental Design of Variables and Results for IgG

After running the 20 experiments in triplicate (60 experiments in total) and taking measurements, the response variables (the enrichment ratio and recovery) were calculated and tabulated as shown in Table 4.12, wherein each line represents an experimental run.

Table 4.12 Experimental design of process variables and results for IgG in a real system showing values for the response variables calculated from measurements

Run	Type	Factor1: immunoglobulin concentration (mg/mL)	Factor 2: pH value	Factor 3: nitrogen flow rate (mL/min)	Response 1: enrichment ratio	Response 2: Recovery (%)
1	Fact	1.00	11.0	25	0.2	0.1
2	Axial	0.60	11.0	15	0.4	0.3
3	Center	0.60	6.5	15	5.1	74.1
4	Axial	0.60	6.5	30	3.5	45.3
5	Fact	1.00	2.0	5	2.5	80.2
6	Center	0.60	6.5	15	5.0	74.7
7	Center	0.60	6.5	15	4.8	73.5
8	Center	0.60	6.5	15	4.7	72.2
9	Axial	1.27	6.5	15	4.2	64.5
10	Fact	0.20	11.0	25	0.2	0.1
11	Fact	0.20	2.0	25	1.7	49.0
12	Fact	0.20	11.0	5	0.9	0.2
13	Axial	0.60	6.5	5	5.4	92.1
14	Fact	0.20	2.0	5	2.8	89.3
15	Center	0.60	6.5	15	5.2	73.7
16	Axial	0.60	2.0	15	2.0	66.9
17	Fact	1.00	2.0	25	1.1	34.2
18	Axial	0.20	6.5	15	5.6	80.3
19	Center	0.60	6.5	15	5.0	71.2
20	Fact	1.00	11.0	5	0.5	0.2

4.4.2 Enrichment Ratio of IgG Using Foam Fractionation

Design-Expert, the statistical analysis package used, provides several useful statistical tables that can be used to identify which response function model to choose for an in-depth study. The program calculates the effects for all model terms. It produces statistics, such as F-values, lack of fit and R-squared values, for comparison of the models. The software underlines and labels as “Suggested” the model that best meets the criteria specified by the user. The following three tables help to select the most appropriate model for a given response (the enrichment ratio in this case).

[Sequential Model Sum of Squares]

The Sequential Model Sum of Squares table shows the progressive improvement in the model fit as terms are added (Table 4.13).

Table 4.13 The sequential model sum of squares for the IgG enrichment ratio in a real system

Sequential Model Sum of Squares						
Source	Sum of Squares	DF	Mean Square	F Value	Prob > F	
Mean	184.83	1	184.83			
Linear	8.93	3	2.98	0.70	0.5672	
2FI	0.31	3	0.10	0.020	0.9960	
<u>Quadratic</u>	<u>67.24</u>	<u>3</u>	<u>22.41</u>	<u>293.02</u>	<u>< 0.0001</u>	<u>Suggested</u>

Source

- ◆ Linear: the linear terms (A, B, and C)
- ◆ 2FI: the two-factor interaction terms (AB, AC, and BC)
- ◆ Quadratic: the quadratic terms (A^2 , B^2 and C^2)

Degrees of freedom (DF)

The column labeled “DF” provides the degrees of freedom contributed by each kind of term source. In the table, the value for the degrees of freedom equals the number of model coefficients added by each term source.

F -value

The F-value shows the significance of adding each term source to the model, wherein higher values are more significant. In the table, the high F-value of 293.02 for the quadratic term indicates that it is much more significant for the model than the linear and two-factor interaction terms, which have small F-values.

p-value (Prob > F)

The column labeled “Prob > F” represents the probability of seeing the observed F value if the null hypothesis is true (there is no factor effect). Small probability values call for rejection of the null hypothesis. The probability equals the proportion of the area under the curve of the F-distribution that lies beyond the observed F value. A small p-value (Prob>F) indicates that adding the term has improved the model. The small p-value of less than 0.0001 for the quadratic term means that adding the term actually improved the model.

.....

[Lack of Fit Tests]

The next table (Table 4.14) displays lack of fit tests that aid in determining how well each of the full models fit the data. Models with a significant lack of fit should not be used for predictions. Here, significance is largely a relative matter, as the model with the lowest lack of fit would typically be selected.

Table 4.14 The lack of fit tests for the IgG enrichment ratio in a real system

Lack of Fit Tests

Source	Sum of Squares	DF	Mean Square	F Value	Prob > F	
Linear	68.14	11	6.19	178.70	< 0.0001	
2FI	67.83	8	8.48	244.58	< 0.0001	
<u>Quadratic</u>	<u>0.59</u>	<u>5</u>	<u>0.12</u>	<u>3.41</u>	<u>0.1020</u>	<u>Suggested</u>

Source

- ◆ Linear: the linear model
- ◆ 2FI: the two-factor interaction model
- ◆ Quadratic: the quadratic model

F -value

The low F-value of 3.41 for the quadratic model means that it doesn't have a significant lack of fit, which is desirable. But the linear and two-factor interaction models with much larger F-values (178.70 and 244.58, respectively) do exhibit significant lack of fit, and thus would be disqualified as suitable candidate models.

.....

[Model Summary Statistics]

The "Model Summary Statistics" table lists other statistics used to compare models (Table 4.15). This table shows the standard deviation, R-squared, adjusted R-squared, predicted R-squared and the predicted residual error sum of squares (PRESS) statistic for each complete model. A low standard deviation, an R-Squared value near 1, and a relatively low PRESS value are best/desirable.

Table 4.15 The model summary statistics for the IgG enrichment ratio in a real system

Model Summary Statistics

Source	Std. Dev.	R-Squared	Adjusted R-Squared	Predicted R-Squared	PRESS	
Linear	2.07	0.1156	-0.0502	-0.4422	111.40	
2FI	2.29	0.1197	-0.2866	-3.4806	346.12	
<u>Quadratic</u>	<u>0.28</u>	<u>0.9901</u>	<u>0.9812</u>	<u>0.8941</u>	<u>8.18</u>	<u>Suggested</u>

Source

- ◆ Linear: the linear model
- ◆ 2FI: the two-factor interaction model
- ◆ Quadratic: the quadratic model

Standard Deviation (Std. Dev.)

The “Std. Dev.” column provides estimates of the standard deviation of the error in the design. A smaller value is better. As shown in the table, the quadratic model has a standard deviation of 0.28, which is markedly smaller than that of the linear and two-factor interaction models (2.07 and 2.29, respectively).

R-Squared

The R-Squared and related Adjusted R-Squared values should be close to one. A value of 1.0 represents the ideal case at which 100 percent of the variation in the observed values can be explained by the chosen model. The values of R-Squared for each model were about 0.12 for both the linear model and the two-factor interaction model (2FI) and 0.99 for the quadratic model. That is, the quadratic model desirably explains about 99% of the variability observed, whereas the values of R-Squared for the linear model and the two-factor interaction model (2FI) are relatively very small, suggesting that they are not suitable models.

Adjusted R-Squared

Because R-Squared always increases as terms are added to the model, some users prefer to use Adjusted R-Squared instead of R-Squared. In general, Adjusted R-Squared will not always increase as variables are added to the model. In fact, if unnecessary terms are added, the value of Adjusted R-Squared will often decrease. For example, the Adjusted R-Squared value for the quadratic term is 0.9812, which is very close to the ordinary R-Squared value (0.9901). When R-Squared and Adjusted R-Squared differ dramatically, there is a good chance that non-significant terms have been included in the model. The negative values for adjusted R-Squared of the linear model and the two-factor interaction model (2FI) indicate that there may be some unnecessary terms included in these two models.

Predicted R-Squared

The Predicted R-Squared value is an approximation of R-Squared for prediction. This statistic gives some indication of the predictive capability of the regression model. For example, the Predicted R-Squared value for the quadratic model is

0.8941. Therefore this model is expected to explain more than 89% of the variability in predicting new observations, as compared to the approximately 99% of the variability in the original data explained by the least squares fit. The overall predictive capability of the quadratic model based on this criterion seems very good.

PRESS

The predicted residual error sum of squares (PRESS) provides a useful residual scaling to indicate how well the model fits the data. The PRESS for the chosen model should be small relative to the other models under consideration. The PRESS value of 8.18 for the quadratic model is much smaller than that of the linear model and the two-factor interaction model (111.40 and 346.12, respectively), thus recommending the use of the quadratic model for this RSM application.

.....

[Analysis of Variance (ANOVA)]

In statistics, analysis of variance (ANOVA) is a collection of statistical models and their associated procedures, in which the observed variance is portioned into components due to different explanatory variables. An ANOVA for the response surface quadratic model for the IgG enrichment ratio in a real system is given in Table 4.16.

Source

- ◆ Model: quadratic model
- ◆ A: coded form of the initial concentration of immunoglobulin
- ◆ B: coded form of the initial pH value
- ◆ C: coded form of the nitrogen gas flow rate
- ◆ A, B and C: linear terms
- ◆ A^2 , B^2 , and C^2 : quadratic terms
- ◆ AB, BC, and AC: two-factor interaction terms

Table 4.16 The analysis of variance table for the IgG enrichment ratio in a real system

Response: ER

ANOVA for Response Surface Quadratic Model

Analysis of variance table [Partial sum of squares]

Source	Sum of Squares	DF	Mean Square	F Value	Prob > F	
Model	76.48	9	8.50	111.10	< 0.0001	significant
A	0.75	1	0.75	9.82	0.0106	
B	6.24	1	6.24	81.59	< 0.0001	
C	2.63	1	2.63	34.39	0.0002	
A ²	1.208E-003	1	1.208E-003	0.016	0.9025	
B ²	49.02	1	49.02	640.86	< 0.0001	
C ²	0.27	1	0.27	3.47	0.0921	
AB	0.031	1	0.031	0.41	0.5371	
AC	1.250E-003	1	1.250E-003	0.016	0.9008	
BC	0.28	1	0.28	3.68	0.0842	

p-value (Prob > F)

The column labeled “Prov > F” represents the probability of seeing the observed F value if the null hypothesis is true (there is no factor effect). Small probability values call for rejection of the null hypothesis. The probability equals the proportion of the area under the curve of the F-distribution that lies beyond the observed F value. If the p-value (Prob>F) is very small (less than 0.05) for the model (shown in the first line), then the model is suitable for modeling the response behavior. The table shows that the quadratic model has a p-value less than 0.0001, thus this model is suitable for modeling the response behavior (here, the enrichment ratio). Again, if the p-value (Prob>F) is very small (less than 0.05) for the individual terms in the model, then those terms have a significant effect on the response. The table shows that the three linear terms (A, B, and C) and one of the three quadratic terms (B²) have significant effects on the response, which is not the case for the other terms (A², C², AB, AC, and BC).

Equation

After analyzing the variance from Table 4.16, the equation below was considered to suitably describe the enrichment ratio. Note that, for example, the coefficients for the quadratic A^2 term (0.012) and for the C^2 term (0.21) are smaller than that of the other quadratic term (B^2), since they are not so significant.

Final equation for the enrichment ratio (ER) in terms of coded factors:

$$ER = 4.97 - 0.27*A - 0.79*B - 0.50*C - 0.012*A^2 - 3.56*B^2 - 0.21*C^2 + 0.062*AB + 0.013*AC + 0.19*BC \quad (4.5)$$

(ER: the enrichment ratio of IgG in milk, A: the initial concentration of immunoglobulin, B: the initial pH value and C: the nitrogen flow rate)

.....

[Perturbation Plot]

Next, the perturbation plot was analyzed, which provides silhouette views of the response surface. The main purpose of this plot is to aid in the selection of axes and constants for 2-D (contour) and 3-D (surface) response plots. For response surface designs, the perturbation plot shows how the response changes as each factor moves away from the chosen reference point (where all lines meet), with all other factors being held constant at the reference value. In this case, the center values of the three variables were chosen to establish the reference point (an initial concentration of immunoglobulin of 0.60 mg/mL, an initial pH value for the start solution of 6.50, and a nitrogen gas flow rate of 15 mL/min). The results (shown in Figure 4.28) show that the initial concentration of immunoglobulin and the nitrogen flow rate have relatively small effects as they move away from the reference point, but changes in the initial pH value cause a more significant effect on the enrichment ratio.

ER

Actual Factors

A: Conc = 0.60

B: pH = 6.50

C: Flow Rate = 15.00

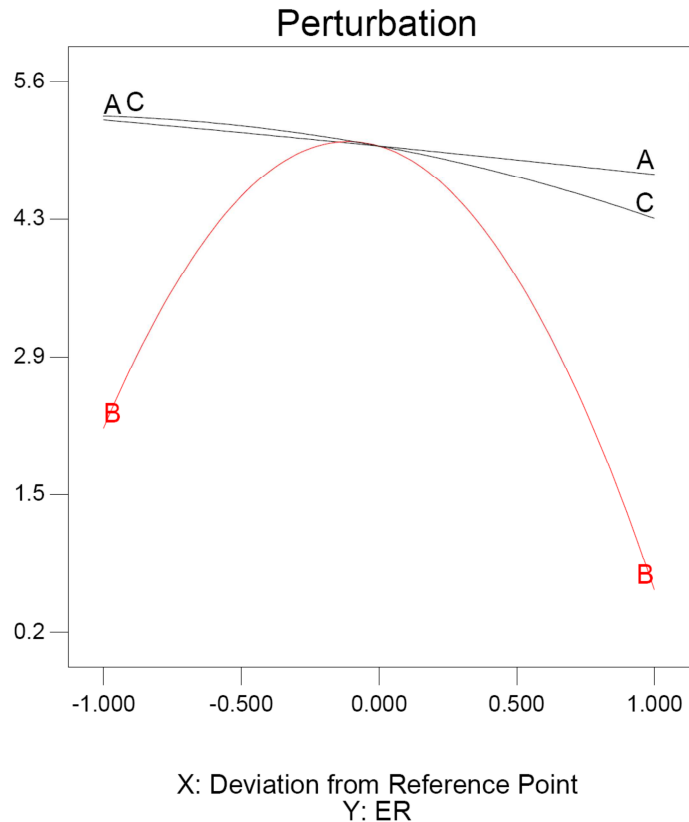


Figure 4.28 Perturbation plot for the enrichment ratio of IgG in a real system

In the figure, notice how movement along either line A (for the initial concentration) or line C (for the nitrogen flow rate) barely affects the response variable, the enrichment ratio in this case, but movement away from the reference point (where all three lines meet at a point) along the B line (for the initial pH value) dramatically affects the level of the enrichment ratio, since the enrichment ratio level rapidly falls off going in either direction.

[2-D and 3-D Response Surface Plots]

It is also convenient to view the response surface in a two-dimensional plane. In the plane view, the plane is viewed from the top, wherein response values having the same value are connected to form one line. This type of graphical representation is called a contour plot (Figure 4.29). For this contour plot, the initial pH value and the nitrogen flow rate were selected for the x- and y-axes, respectively, due to their having the greatest impact on the response based on the

perturbation plot. Note that in this contour plot, the boxed values label lines of constant response.

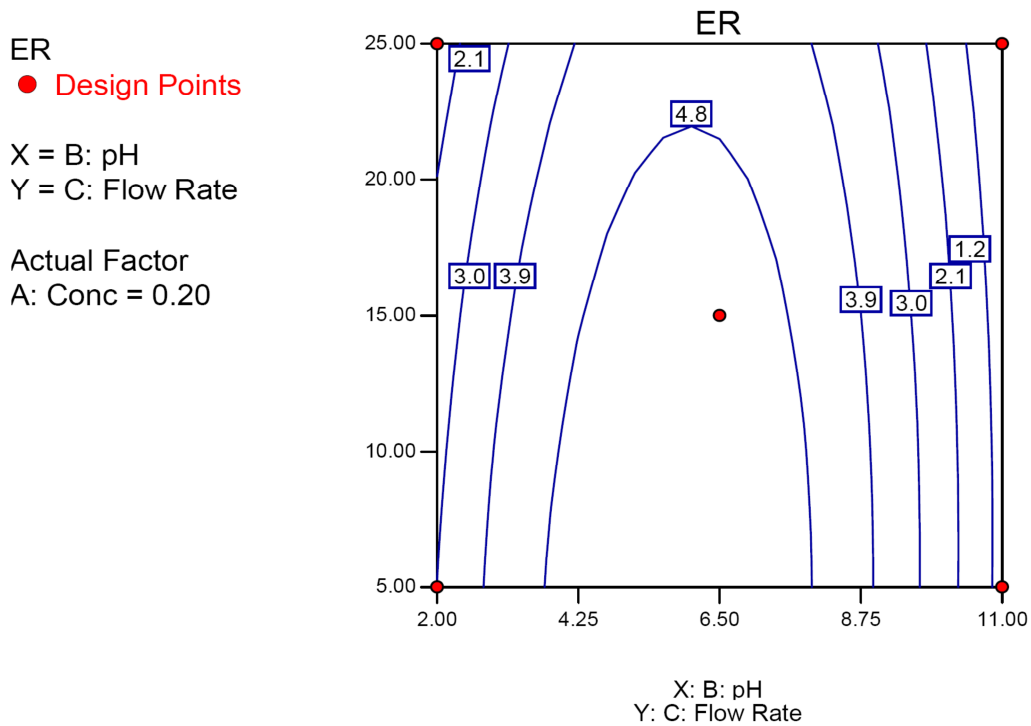


Figure 4.29 Two-dimensional isoresponse curve for the enrichment ratio of IgG in a real system

The effect of the initial pH value and nitrogen flow rate at a fixed initial concentration of immunoglobulin (0.2 mg/mL) was further revealed from surface plot (Figure 4.30), wherein the enrichment ratio is maximum near the center values for the pH level and smaller nitrogen flow rates. In the surface plot, the z-axis is the enrichment ratio.

ER
X = B: pH
Y = C: Flow Rate

Actual Factor
A: Conc = 0.20

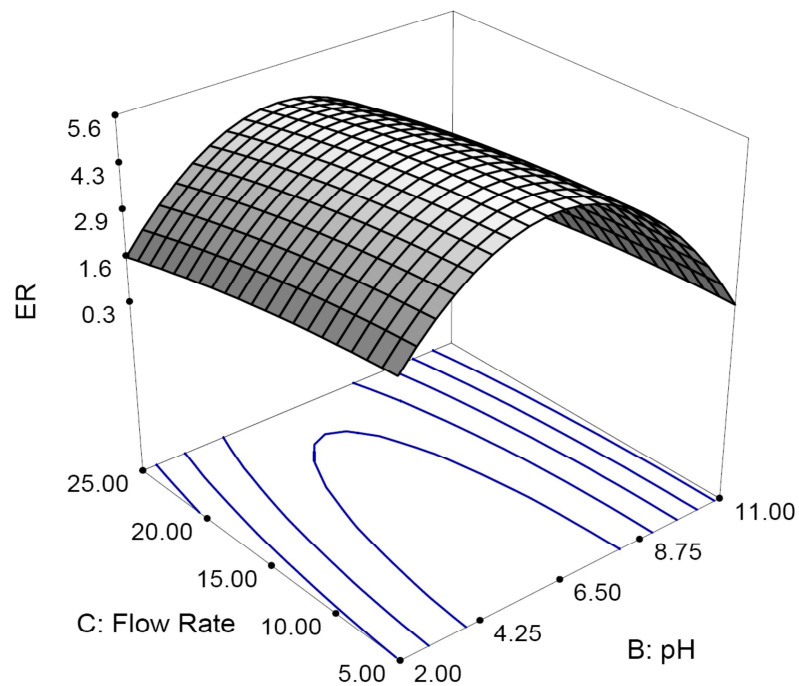


Figure 4.30 Three-dimensional surface for the enrichment ratio of IgG in a real system

4.4.3 Recovery of IgG Using Foam Fractionation

After analysis of enrichment ratio, the other response, recovery, was then analyzed using Design-Expert, the statistical analysis package. Again, it provides several useful statistical tables that can be used to identify which response function model to choose for an in-depth study. The program calculates the effects for all model terms, and it produces statistics, such as F-values, lack of fit and R-squared values, for comparison of the models. Again, the software underlines and labels as “Suggested” the model that most closely meets the criteria specified by the user. The following three tables help to select the most appropriate model for a given response (the recovery in this case).

[Sequential Model Sum of Squares]

The Sequential Model Sum of Squares table shows the progressive improvement in the model fit as terms are added (Table 4.17).

Table 4.17 The sequential model sum of squares for the IgG recovery in a real system

Sequential Model Sum of Squares

Source	Sum of Squares	DF	Mean Square	F Value	Prob > F	
Mean	54298.62	1	54298.62			
Linear	11903.75	3	3967.92	6.63	0.0041	
2FI	1002.11	3	334.04	0.51	0.6847	
<u>Quadratic</u>	<u>8431.49</u>	<u>3</u>	<u>2810.50</u>	<u>191.25</u>	<u>< 0.0001</u>	<u>Suggested</u>

Source

- ◆ Linear: the linear terms (A, B, and C)
- ◆ 2FI: the two-factor interaction terms (AB, AC, and BC)
- ◆ Quadratic: the quadratic terms (A^2 , B^2 and C^2)

Degrees of freedom (DF)

The column labeled “DF” provides the degrees of freedom contributed by each kind of term source. In the table, the value for the degrees of freedom equals the number of model coefficients added by each term source.

F-value

The F-value shows the significance of adding each term source to the model, wherein higher values are more significant. In the table, the high F-value of 191.25 for the quadratic term means that it is much more significant for the model than the linear and two-factor interaction terms, which have small F-values (6.63 and 0.51, respectively).

p-value (Prob > F)

The column labeled “Prob > F” represents the probability of seeing the observed F value if the null hypothesis is true (there is no factor effect). Small probability values call for rejection of the null hypothesis. The probability equals the proportion of the area under the curve of the F-distribution that lies beyond the observed F value. A small p-value (Prob>F) indicates that adding the term has

improved the model. The small p-value of less than 0.0001 for the quadratic term means that adding the term actually improves the model.

[Lack of Fit Tests]

The next table (Table 4.18) displays lack of fit tests that indicate how well each of the full models fit the data. Models with a significant lack of fit should not be used for predictions. Here, the model with the lowest lack of fit would typically be selected.

Table 4.18 The lack of fit tests for the IgG recovery in a real system

Lack of Fit Tests

Source	Sum of Squares	DF	Mean Square	F Value	Prob > F	
Linear	9572.16	11	870.20	518.39	< 0.0001	
2FI	8570.05	8	1071.26	638.16	< 0.0001	
<u>Quadratic</u>	<u>138.56</u>	<u>5</u>	<u>27.71</u>	<u>16.51</u>	<u>0.0040</u>	<u>Suggested</u>

Source

- ◆ Linear: the linear model
- ◆ 2FI: the two-factor interaction model
- ◆ Quadratic: the quadratic model

F-value

The low F-value of 16.51 for the quadratic model means that it doesn't have a significant lack of fit, which is desirable. But the linear and two-factor interaction models with much larger F-values (518.39 and 638.16, respectively) do exhibit significant lack of fit, and thus would be disqualified as suitable candidate models.

[Model Summary Statistics]

The “Model Summary Statistics” table lists other statistics used to compare models (Table 4.19). This table shows the standard deviation, R-squared, adjusted R-squared, predicted R-squared and the predicted residual error sum of squares (PRESS) statistic for each complete model. A low standard deviation, an R-Squared value near 1, and a relatively low PRESS value are best.

Table 4.19 The model summary statistics for IgG recovery in a real system

Model Summary Statistics						
Source	Std. Dev.	R-Squared	Adjusted R-Squared	Predicted R-Squared	PRESS	
Linear	24.47	0.5541	0.4705	0.2402	16323.86	
2FI	25.69	0.6007	0.4164	-1.1030	45182.51	
<u>Quadratic</u>	<u>3.83</u>	<u>0.9932</u>	<u>0.9870</u>	<u>0.9399</u>	<u>1291.82</u>	<u>Suggested</u>

Source

- ◆ Linear: the linear model
- ◆ 2FI: the two-factor interaction model
- ◆ Quadratic: the quadratic model

Standard Deviation (Std. Dev.)

The “Std. Dev.” column provides estimates of the standard deviation of the error in the design. A smaller value is better. As shown in the table, the quadratic model has a standard deviation of 3.83, which is markedly smaller than that of the linear and two-factor interaction models (24.47 and 25.69, respectively).

R-Squared

The R-Squared and related Adjusted R-Squared values should be close to one. A value of 1.0 represents the ideal case at which 100 percent of the variation in the observed values can be explained by the chosen model. The values of R-Squared for each model were 0.55 and 0.60 for the linear model and the two-factor interaction model, respectively, and 0.99 for the quadratic model. That is, the quadratic model explains about 99% of the variability observed. The values of R-Squared for the linear model and the two-factor interaction model (2FI) are relatively small, suggesting that they are not suitable models.

Adjusted R-Squared

R-Squared always increases as terms are added to the model, so some users prefer to use Adjusted R-Squared. The adjusted R-Squared value will not always increase as variables are added to the model. The addition of unnecessary terms can often cause the value of Adjusted R-Squared to decrease. For example, the Adjusted R-Squared value for the quadratic term is 0.987, which is very close to the ordinary R-Squared value (0.993). When R-Squared and Adjusted R-Squared differ dramatically, there is a good chance that non-significant terms have been included in the model. The small values for adjusted R-Squared of the linear model and the two-factor interaction model (0.47 and 0.42, respectively) indicate that there may be some unnecessary terms included in these two models.

Predicted R-Squared

The Predicted R-Squared is an approximate R-Squared for prediction. This statistic gives some indication of the predictive capability of the regression model. For example, the Predicted R-Squared value for the quadratic model is 0.94. Therefore this model is expected to explain 94% of the variability in predicting new observations, as compared to the approximately 99% of the variability in the original data explained by the least squares fit. The overall predictive capability of the quadratic model based on this criterion seems very good.

PRESS

The predicted residual error sum of squares (PRESS) provides a useful residual scaling. The PRESS statistic indicates how well the model fits the data. The PRESS for the chosen model should be small relative to the other models under consideration. The PRESS value of 1,292 for the quadratic model is much smaller than that of the linear model and the two-factor interaction model (16,323 and 45,182, respectively), thus recommending the use of the quadratic model for this RSM application.

.....

[Analysis of Variance (ANOVA)]

In statistics, analysis of variance (ANOVA) is a collection of statistical models and their associated procedures, in which the observed variance is portioned into components due to different explanatory variables. An ANOVA for the response surface quadratic model for the IgG recovery in a real system is given in Table 4.20.

Table 4.20 The analysis of variance table for IgG recovery in a real system

Response: Recovery

ANOVA for Response Surface Quadratic Model

Analysis of variance table [Partial sum of squares]

Source	Sum of Squares	DF	Mean Square	F Value	Prob > F	
Model	21337.36	9	2370.82	161.33	< 0.0001	significant
A	144.96	1	144.96	9.86	0.0105	
B	10156.97	1	10156.97	691.17	< 0.0001	
C	1663.77	1	1663.77	113.22	< 0.0001	
A ²	2.53	1	2.53	0.17	0.6867	
B ²	6062.90	1	6062.90	412.57	< 0.0001	
C ²	37.53	1	37.53	2.55	0.1411	
AB	71.40	1	71.40	4.86	0.0521	
AC	4.06	1	4.06	0.28	0.6106	
BC	926.65	1	926.65	63.06	< 0.0001	

Source

- ◆ Model: quadratic model
- ◆ A: coded form of the initial concentration of immunoglobulin
- ◆ B: coded form of the initial pH value
- ◆ C: coded form of the nitrogen gas flow rate
- ◆ A, B and C: linear terms
- ◆ A², B², and C²: quadratic terms
- ◆ AB, BC, and AC: two-factor interaction terms

p-value (Prob > F)

The “Prob > F” column represents the probability of seeing the observed F value if the null hypothesis is true (there is no factor effect). Small probability values call for rejection of the null hypothesis. The probability equals the proportion of the area under the curve of the F-distribution that lies beyond the observed F value. If the p-value (Prob>F) is very small (less than 0.05) for the model (shown in the first line), then the model is suitable for modeling the response behavior. The table shows that the quadratic model has a p-value less than 0.0001, thus this model is suitable for modeling the response behavior (the recovery in this case). Again, if the p-value (Prob>F) is very small (less than 0.05) for the individual terms in the model, then these terms have a significant effect on the response. Again, the table shows that the three linear terms (A, B, and C), one of the three quadratic terms (B²), and one of the two-factor interaction terms (BC) have significant effects on the response, which is not the case for the other terms (A², C², AB and AC).

Equation

After analyzing the variance from Table 4.20, the equation below was considered to suitably describe the recovery. Note that, for example, the coefficients for the quadratic term A² and C² (0.56 and 2.47, respectively) are much smaller than that for B² (39.59).

Final equation for the recovery (R) in terms of coded factors:

$$R = 74.06 - 3.73*A - 31.87*B - 12.61*C - 0.56*A^2 - 39.59*B^2 - 2.47*C^2 + 2.99*AB - 0.71*AC + 10.76*BC \tag{4.6}$$

(R: the recovery of IgG in milk, A: the initial concentration of immunoglobulin, B: the initial pH value and C: the nitrogen flow rate)

.....

[Perturbation Plot]

Next, the perturbation plot was analyzed, which provides silhouette views of the response surface. The main purpose of this plot is to aid in the selection of axes and constants for 2-D (contour) and 3-D (surface) response plots. For response surface designs, the perturbation plot shows how the response changes as each factor moves from the chosen reference point (where all lines meet), with all other factors being held constant at the reference value. In this case, the center values of the three variables were chosen to establish the reference point (an initial concentration of immunoglobulin of 0.60 mg/mL, an initial pH value of the start solution of 6.50 and a nitrogen gas flow rate of 15 mL/min). The results (shown in Figure 4.31) show that the initial concentration of immunoglobulin and the nitrogen flow rate have relatively small effects as they move away from the reference point, but changes in the initial pH value cause a more significant effect on the enrichment ratio.

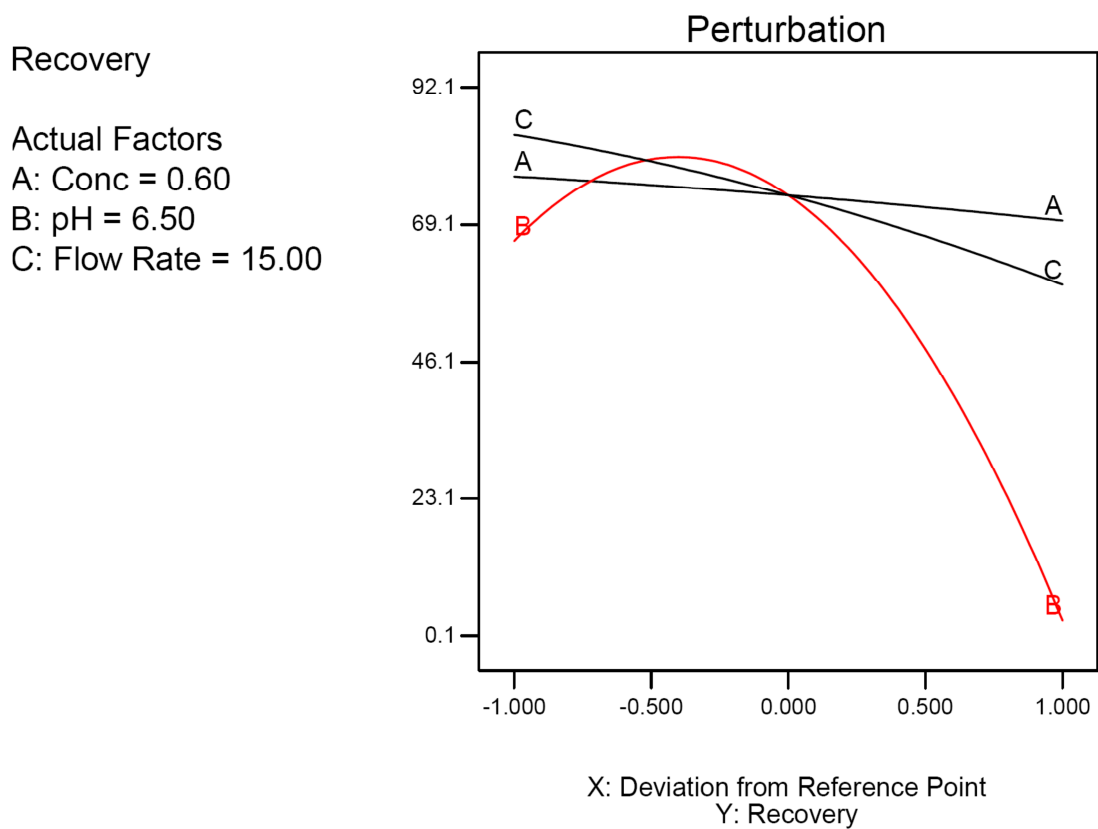


Figure 4.31 Perturbation plot for the recovery of IgG in a real system

As before, notice how movement along either line A (for the initial concentration) or line C (for the nitrogen flow rate) barely affects the response variable, the recovery in this case, but movement away from the reference point (again, where all three lines meet at a point) along the B line (for the initial pH value) dramatically affects the level of the recovery, since the level rapidly falls off going in either direction (especially in the case of a very basic pH).

[2-D and 3-D Response Surface Plots]

It is convenient to view the response surface in a two-dimensional plane. In the plane view, the plane is viewed from the top and response values having the same value are connected to form one line. This type of graphical representation is called a contour plot (Figure 4.32). For this contour plot, the initial pH value and the nitrogen flow rate were selected for the x- and y-axes, respectively, due to their having the greatest impact on the response based on the perturbation plot. In this contour plot, the boxed values label lines of constant response.

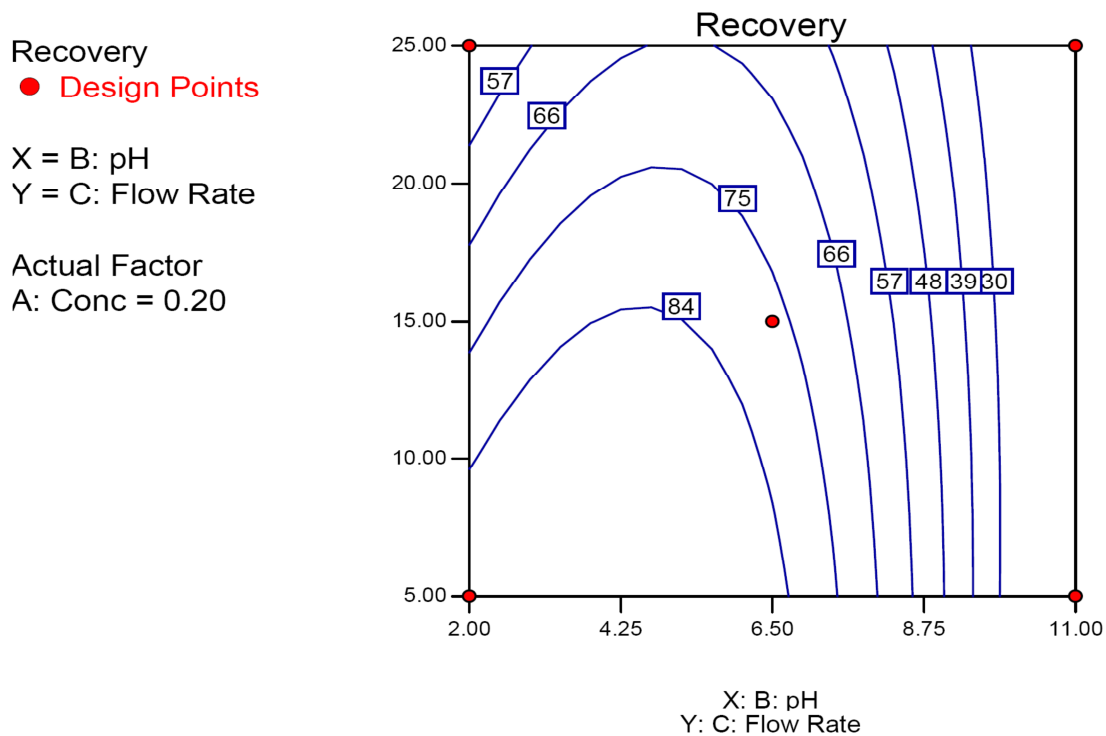


Figure 4.32 Two-dimensional isoresponse curve for the recovery of IgG in a real system

The effect of the initial pH value and nitrogen flow rate at a fixed initial concentration of immunoglobulin (0.2 mg/mL) was further revealed from a surface plot (Figure 4.33), wherein the recovery is maximum near a pH value of 4.3 and smaller nitrogen flow rates. In the surface plot, the z-axis is the recovery.

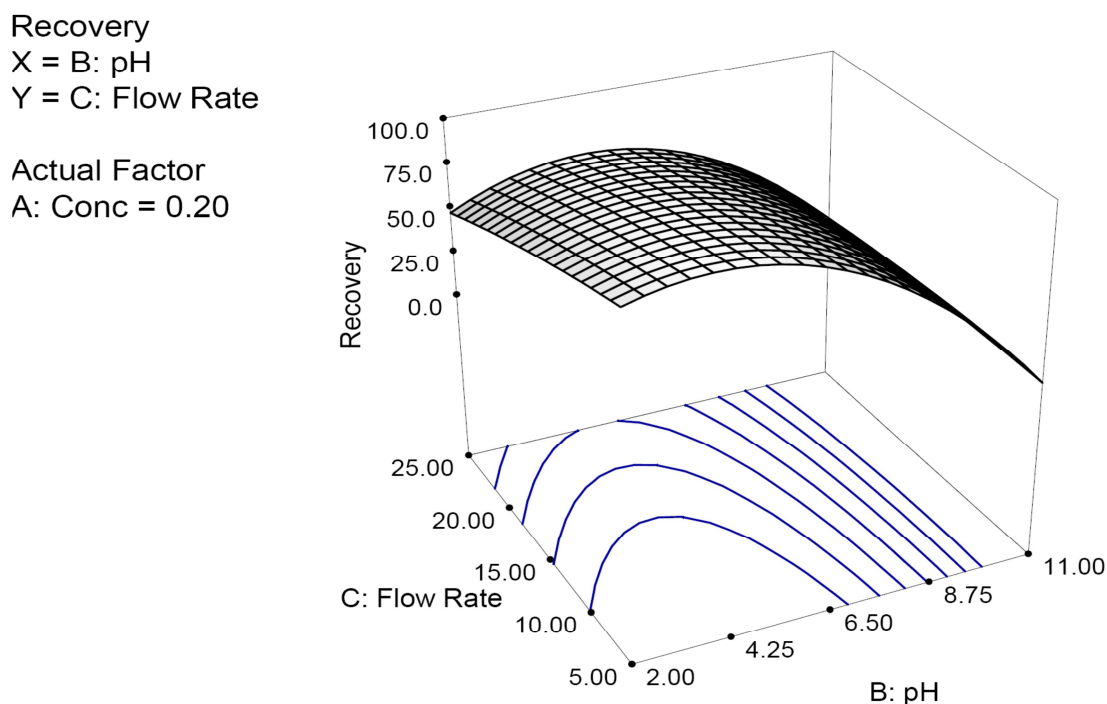


Figure 4.33 Three-dimensional surface for the recovery of IgG in a real system

4.4.4 Optimization of the Operating Variables for IgG Foam Fractionation

After selection of goals for the factors and responses by the researcher, the software package found the most suitable solution in terms of the goals. Based on software modeling and experimental evidence, the optimized values for the initial concentration of immunoglobulin in the start solution, the initial pH value and the nitrogen flow rate were 0.2 mg/mL, 5.76 and 5.06 mL/min, respectively (Table 4.21). In the table, the “Goal” column shows the settings selected by the researcher to constrain the factors and responses. Here, the response variables were set to be maximized and the input factors were in defined ranges.

Table 4.21 Predicted solutions for both the enrichment ratio and recovery of IgG from foam fractionation in a real system

Name	Goal	Lower Limit	Upper Limit	Lower Weight	Upper Weight	Importance
Conc	is in range	0.2	1	1	1	3
pH	is in range	2	11	1	1	3
Flow Rate	is in range	5	25	1	1	3
ER	maximize	0.2	5.6	1	1	5
Recovery	maximize	0.1	92.1	1	1	4

Solutions

Number	Conc	pH	Flow Rate	ER	Recovery	Desirability
1	0.20	5.83	5.15	5.6	92.4	1.000
2	<u>0.20</u>	<u>5.76</u>	<u>5.06</u>	<u>5.6</u>	<u>93.1</u>	<u>1.000</u>
3	0.82	5.46	5.00	5.1	89.7	0.940

3 Solutions found

Then, a foam fractionation experiment was conducted using the calculated input factors to check the accuracy of the predicted results from the software. The model predicted optimized values for the factors. The suggested values being: the initial concentration of immunoglobulin (0.2 mg/mL), the initial pH value (5.76), and the nitrogen flow rate (5 mL/min instead of 5.06 mL/min due to the limited settings of the flow meter). The predicted responses were an enrichment ratio of 5.6 and a recovery of 93.1%, respectively. Further experiments were performed with the predicted, values for the factors, and the experiments confirmed the model predictions with an enrichment ratio of 5.01 and recovery of 86.4%. For the obtained experimental results, there was larger deviation from the predicted values than in a model system. This might be due to the complex components of the milk system.

4.4.5 Optimization of the Operating Variables for IgM Foam Fractionation

Being presented first, the results for IgG in the above sections provide full details. However, the results for IgM, here, are shortened to avoid replication and overlap. Here, only the equation for both the enrichment ratio and recovery as well as the optimization result are presented. Despite the concise presentation, note that, in

order to get the optimization result, another 60 experiments were conducted, followed by analysis of their enrichment ratios and recoveries using “sequential model sum of squares”, “lack of fit tests”, “model summary statistics”, and “analysis of variance (ANOVA)”. A perturbation plot, 2-D and 3-D response surface plots were also needed. After all these processes, then an optimization of the operating variables for IgM foam fractionation can be achieved.

Equation for enrichment ratio of IgM

After analyzing the variance, the equation below was considered to suitably describe the enrichment ratio. Note that, the coefficient for A² is too small, thus is neglected by the software.

Final equation for the enrichment ratio (ER) in terms of coded factors:

$$ER = 4.78 - 0.19*A - 0.98*B - 0.54*C - 3.36*B^2 - 0.14*C^2 + 0.11*AB - 0.013*AC + 0.21*BC \quad (4.7)$$

(ER: enrichment ratio of IgM in milk, A: initial concentration of immunoglobulin, B: initial pH value, C: nitrogen flow rate)

Equation for recovery of IgM

After analyzing the variance, the equation below was considered to suitably describe the recovery. Note that, for example, the coefficients for the quadratic term A² and C² (1.35 and 3.60, respectively) are much smaller than that for B² (41.86).

Final equation for the recovery (R) in terms of coded factors:

$$R = 75.50 - 1.98*A - 31.56*B - 12.23*C + 1.35*A^2 - 41.86*B^2 - 3.60*C^2 + 1.91*AB - 0.64*AC + 11.14*BC \quad (4.8)$$

(R: recovery of IgM in a milk, A: initial concentration of immunoglobulin, B: initial pH value, C: nitrogen flow rate)

After selection of goals for the factors and responses by the researcher, the software package found two solutions and identified the most suitable one in terms of the goals. Based on software modeling and experimental evidence, the optimized values for the initial concentration of immunoglobulin in the start solution, the initial pH value and the nitrogen flow rate were 0.2 mg/mL, 5.63 and 5 mL/min, respectively (Table 4.22). In the table, the “Goal” column shows the settings selected by the researcher to constrain the factors and responses. Again, the response variables were set to be maximized and the input factors were in defined ranges.

Table 4.22 Predicted solutions for both the enrichment ratio and recovery of IgM from foam fractionation in a real system

Name	Goal	Lower	Upper	Lower	Upper	Importance
		Limit	Limit	Weight	Weight	
Conc	is in range	0.2	1	1	1	3
pH	is in range	2	11	1	1	3
Flow Rate	is in range	5	25	1	1	3
ER	maximize	0.1	5.6	1	1	5
Recovery	maximize	0.1	90	1	1	4

Solutions							
Number	Conc	pH	Flow Rate	ER	Recovery	Desirability	
1	<u>0.20</u>	<u>5.63</u>	<u>5.00</u>	<u>5.5</u>	<u>93.9</u>	<u>0.987</u>	
2	0.26	5.54	5.00	5.4	93.8	0.985	

Then, a foam fractionation experiment was conducted using the calculated input factors to check the accuracy of the predicted results from the software. The model predicted optimized values for the factors. The values being: the initial concentration of immunoglobulin (0.2 mg/mL), the initial pH value (5.63), and the nitrogen flow rate (5 mL/min). The predicted responses were an enrichment ratio of 5.4 and a recovery of 93.9 %, respectively. Further experiments were performed with the predicted values for the factors, and the experiments confirmed the model predictions, with an enrichment ratio of 5.27 and recovery of 90.5%. For the obtained experimental results, there was very little deviation from the predicted values. Once again, this work gave good results at laboratory scale for foam fractionation of immunoglobulin in batch mode.

5. Summary and Conclusions

The demand for purified biochemicals, such as proteins has markedly increased in the last few decades. As such, there is an interest in cost-effective methods that can isolate and enrich biochemicals. Immunoglobulins represent an important kind of protein in the biological sciences, with numerous pharmaceutical or biotechnological applications.

Traditional immunoglobulin enrichment methods, based mostly on chromatographic processes, generally involve costly purification and lead to expensive final products. As such, there is a definite need to develop techniques capable of increasing capacity and decreasing total costs. Foam fractionation, which uses no organic solvents, is a candidate for the enrichment of biochemicals, and, on a larger scale, could be a method to substitute for or complement the currently available separation techniques. Therefore, foam fractionation processes have much potential due to their simplicity and scalability. However, little, if any, literature exists documenting the utilization of foam fractionation in the enrichment of immunoglobulin.

The aim of this study was to develop an enrichment process for immunoglobulin using foam fractionation. To accomplish this, the statistical method known as response surface methodology (RSM) was applied to help analyze the complex enrichment processes. A model system was first utilized to help select the test ranges for different parameters. Milk was then utilized as an immunoglobulin production source to serve as an example of a real system.

Enrichment of immunoglobulin in a model system

To establish a model system, the foam fractionation of immunoglobulin was studied with the aid of albumin as a foaming agent. The investigation examined the effects of varying six different process parameters: the initial pH value, the initial concentration of immunoglobulin, the nitrogen flow rate, the initial concentration of albumin, the column height and the foaming time.

The main conclusions are as follows:

- ◆ Varying the initial pH value was found to influence the enrichment, and a maximum enrichment ratio was achieved at a pH corresponding to the pI of the target immunoglobulin (pH 7 for IgG and pH 6-7 for IgM).
- ◆ Both the enrichment ratios for IgG and IgM showed that lower initial immunoglobulin concentrations achieved higher enrichment ratios.
- ◆ The nitrogen flow rate must be sufficient to produce stable foam, but not too high (i.e., kept at or below 15 mL/min) or the enrichment of immunoglobulin will be adversely affected.
- ◆ A solution containing immunoglobulin alone hardly produces foam, but the addition of albumin to the system makes it possible to generate enough foam to rise in the column. However, initial albumin concentrations higher than 1 mg/mL had only a slight effect on the enrichment ratio.
- ◆ With higher column heights, it takes longer for the foam to reach the top of the column, giving more time for drainage and resulting in less liquid being held up. As a result, the foam becomes more concentrated, which is beneficial.
- ◆ The enrichment ratio was found to be optimal during a certain foaming time range. Longer foaming times caused the total volume of the foamate to increase and thus decreased the enrichment ratio due to dilution.
- ◆ Experimentation demonstrated that immunoglobulin may be effectively enriched by foam fractionation. The maximum enrichment ratios after optimization of different process parameters were 5.1 for IgG and 4.3 for IgM, along with more than a 94% recovery for both.
- ◆ The separation of IgG and IgM was investigated. Use of only foam fractionation cannot separate IgG and IgM from each other, and the enrichment of both IgG and IgM decreased.
- ◆ To determine suitable candidates for multi-component mixtures, serum and milk were both investigated. Under the set condition, in the milk system, an enrichment ratio over 5 was achieved, but, in the serum system, the enrichment ratio was only near 2.

Enrichment of immunoglobulin in a milk system

To consider the effectiveness of foam fractionation in enriching multi-component mixtures, the foam fractionation of immunoglobulin in milk was investigated. The investigation focused on the effects of varying five different process parameters: the initial pH value, the initial concentration of immunoglobulin, the column height, the nitrogen flow rate and the foaming time.

The main conclusions are as follows:

- ◆ The results showed that, under extreme conditions (i.e., too acidic or too basic), enrichment was poor, as the optimal pH value for enrichment of immunoglobulins by foam fractionation is their pI values.
- ◆ A solution containing immunoglobulin alone hardly produces foam, but a combination with milk protein makes it possible to generate sufficient foam to rise in the column (without the addition of a foaming agent, such as albumin).
- ◆ Both the enrichment ratios for IgG and IgM showed that lower initial immunoglobulin concentrations achieved higher enrichment ratios.
- ◆ Varying the column height influenced the enrichment, and better immunoglobulin enrichment ratios were achieved at higher column heights.
- ◆ The results for both IgG and IgM supported the conclusion that higher nitrogen flow rates caused a decrease in the enrichment ratio.
- ◆ An optimal range for the foaming time exists, with longer foaming times being counter-productive.
- ◆ The pretreatment process was found to have a positive effect on the enrichment ratio.
- ◆ Experimental results demonstrated that immunoglobulin could effectively be enriched from milk by foam fractionation. The maximum enrichment ratio with pretreatment (using pH 4.6 precipitation) was 6.30 along with a more than 92% recovery for IgG, and an enrichment ratio of 5.1 with 85% recovery for IgM.

Use of RSM on enrichment of immunoglobulin in a model system

Response surface design experiments examined the effect of various initial concentrations of immunoglobulin, pH values and nitrogen flow rates on the enrichment ratio and recovery in a model system by foam fractionation.

The main conclusions are as follows:

- ◆ The analysis of the variance (ANOVA) showed that the quadratic models have p-values less than 0.0001, thus the selected models are significant to the responses of enrichment ratio and immunoglobulin recovery (Table 4.5 and Table 4.9).
- ◆ The independent process variables exhibited different effects on each of the response variables. In these models, the initial immunoglobulin concentration, pH value and nitrogen flow rate (A, B and C) were highly significant ($p \leq 0.01$) for both the enrichment ratio and recovery.
- ◆ The ANOVA model for the enrichment ratio revealed that the three linear terms (A, B and C) and two of the three quadratic terms (B^2 and C^2) have significant effects on the response, whereas the other terms (A^2 , AB, AC and BC) do not.
- ◆ The ANOVA model for the immunoglobulin recovery revealed that the three linear terms (A, B and C) and one of the three quadratic terms (B^2) have significant effects on the response, which is not the case for the other terms (A^2 , C^2 , AB, AC and BC).
- ◆ The perturbation plots demonstrated that the initial concentration of immunoglobulin and the nitrogen flow rate have relatively small effects on the enrichment ratio as they deviate from the reference point, but the initial pH value has a more significant effect.
- ◆ Surface plots confirmed that pH values near the isoelectric point resulted in higher enrichment ratios for foam fractionation with lower initial immunoglobulin concentrations and smaller nitrogen flow rates.
- ◆ The empirical regression equations [Eq (4.1) and Eq (4.2) for IgG; Eq (4.3) and Eq (4.4) for IgM] as a function of the independent process variables were derived by the RSM model for the enrichment ratio and immunoglobulin recovery.

- ◆ The prediction equations for both the enrichment ratio and immunoglobulin recovery were verified through validation experiments. The predicted responses were an enrichment ratio of 5.5 and recovery of 96% for IgG, while the experimental values were 5.47 and 95.6%, respectively, which match quite well.
- ◆ Appropriate process conditions can be selected using the established response surface model to achieve a high enrichment ratio and immunoglobulin recovery, the suggested values being 0.2 mg/mL for A, 5.47 for B, and 5 mL/min for C.

Use of RSM on enrichment of immunoglobulin in a milk system

Response surface design experiments examined the effect of various initial concentrations of immunoglobulin, pH values and nitrogen flow rates on the enrichment ratio and the recovery in a real system by foam fractionation.

The main conclusions are as follows:

- ◆ The analysis of the variance (ANOVA) showed that the quadratic models have p-values less than 0.0001, thus the selected models are significant to the responses, the immunoglobulin enrichment ratio and recovery (Table 4.16 and Table 4.20).
- ◆ The independent process variables exhibited different effects on each of the response variables. In these models, the initial immunoglobulin concentration, pH value and nitrogen flow rate (A, B and C) were highly significant ($p \leq 0.01$) for both the enrichment ratio and recovery.
- ◆ The ANOVA model for the enrichment ratio revealed that the three linear terms (A, B and C) and one of the three quadratic terms (B^2) have significant effects on the response, which is not the case for the other terms (A^2 , C^2 , AB, AC and BC).
- ◆ The ANOVA model for the immunoglobulin recovery revealed that the three linear terms (A, B and C), one of the three quadratic terms (B^2), and one of the two-factor interaction terms (BC) have significant effects on the response, which is not the case for the other terms (A^2 , C^2 , AB and AC).

- ◆ The perturbation plots demonstrated that the initial concentration of immunoglobulin and the nitrogen flow rate have relatively small effects on the enrichment ratio as they move away from the reference point, but the initial pH value has a more significant effect.
- ◆ Surface plots confirmed that a pH near the isoelectric point (pI) resulted in higher enrichment ratios for foam fractionation with lower initial immunoglobulin concentrations and smaller nitrogen flow rates.
- ◆ The empirical regression equations [Eq (4.5) and Eq (4.6) for IgG; Eq (4.7) and Eq (4.8) for IgM] as a function of the independent process variables were derived by the RSM model for the enrichment ratio and immunoglobulin recovery.
- ◆ The prediction equations for both the immunoglobulin enrichment ratio and recovery were verified through validation experiments. The predicted responses were an enrichment ratio of 5.6 and recovery of 93.1% for IgG, while the experimental values were 5.01 and 86.4%, respectively.
- ◆ The prediction equations for both the immunoglobulin enrichment ratio and recovery were verified through validation experiments. The predicted responses were an enrichment ratio of 5.5 and recovery of 93.9% for IgM, while the experimental values were 5.27 and 90.5%, respectively.
- ◆ Appropriate process conditions can be selected using the established response surface model to achieve a high enrichment ratio and immunoglobulin recovery, the suggested values being 0.2 mg/mL for A, 5.76 for B, and 5 mL/min for C.

The response surface method and central composite design were used to determine conditions leading to a high enrichment ratio and immunoglobulin recovery in both model and real systems. Thus, simpler and less time-consuming experimental designs appear to generally suffice for the optimization of the immunoglobulin enrichment processes by foam fractionation, which could speed up adoption of foam fractionation processing of immunoglobulins.

Experimental results demonstrated that immunoglobulin could effectively be enriched from milk by foam fractionation. The maximum enrichment ratio with pretreatment was 6.3 along with a more than 92% recovery for IgG and 5.3 with 91% recovery for IgM. As such, foam fractionation of immunoglobulin appears to have great potential to work together with commonly applied methods, with the advantages that relatively simple processes and relative low costs can be expected. Foam fractionation is also suitable to processes with higher volumes that may be used in downstream processing, which further recommends its use in enrichment.

Previous experimental results demonstrated that immunoglobulin could effectively be enriched by foam fractionation. However, further studies are still needed before its direct application to the industry. The recommendations for future work are as follows:

- ◆ Foam fractionation methods should be developed for the enrichment of immunoglobulin in a continuous mode of operation.
- ◆ Industrial scale-up should be developed with the help of response surface methodology.
- ◆ Better design and operation of multi-stage foaming system might lead to higher enrichment and immunoglobulin separation.
- ◆ New foaming agents or additives might be designed and synthesized to improve the enrichment and recovery of immunoglobulin.

6. Literature

- [ADACHI, *et al.* 2000] Adachi M., M. Harada, and S. Katoh, *Bioaffinity separation of chymotrypsinogen using antigen-antibody reaction in reverse micellar system composed of a nonionic surfactant*. Biochemical Engineering Journal, 2000, **4**: p. 149-151.
- [ADAMSON 1960] Adamson A.W., *Physical chemistry of surfaces*. Interscience, New York, 1960.
- [AGOSTONI, *et al.* 2000] Agostoni C., Carratu B., Boniglia C., Riva E. and Sanzini E., *Free amino acid content in standard infant formulas: Comparison with human milk*. Journal of the American College of Nutrition, 2000, **19**(4): p. 434-438.
- [AHMAD 1975] Ahmad S.I., *Laws of foam fractionation I. The effect of different operating parameters on the foam fractionation of albumin from a solution containing organic and inorganic materials*. Separation Science, 1975, **10** (6): p. 673–688.
- [ALLEN 1971] Allen D.M., *Mean square error of prediction as a criterion for selecting variables*. Technometrics, 1971, **13**: p. 469-475.
- [ALLEN 1974] Allen D.M., *The relationship between variable selection and data augmentation and a method for prediction*. Technometrics, 1974, **16**: p. 125-127.
- [ANAND and DAMODARAN 1995] Anand K. and Damodaran S., *Kinetics of adsorption of lysozyme and bovine serum albumin at the air-water interface from a binary mixture*. Journal of Colloid Interface Science, 1995, **176**: p. 63–73.
- [AZEVEDO, *et al.* 2007a] Azevedo A.M., A.G. Gomes, P.A.J. Rosa, I.F. Ferreira, A.M.M.O. Pisco, and M.R. Aires-Barros, *Partitioning of human antibodies in polyethylene glycol – sodium citrate aqueous two-phase systems*. Separation and Purification Technology, 2007.
- [AZEVEDO, *et al.* 2007b] Azevedo A.M., Rosa P.A.J., Ferreira I.F., and Aires-Barros M.R., *Optimisation of aqueous two-phase extraction of human antibodies*. Journal of Biotechnology, 2007, **132**: p. 209-217.

- [BHAKTA and RUCKENSTEIN 1995] Bhakta A. and Ruckenstein E., *Foams and concentrated emulsions: dynamics and ‘phase’ behavior*. Langmuir, 1995, **11**: p. 4642-4652.
- [BIRCH and RACHER 2006] Birch J.R., and Racher A.J., *Antibody production*. Advanced Drug Delivery Reviews, 2006, **58**: p. 671-685.
- [BOSCHETTI and GUERRIER 2001] Boschetti E., and L. Guerrier, *Purification of antibodies by HCIC and impact of ligand structure*. International Journal of Bio-Chromatography, 2001, **6**: p. 269-283.
- [BOSZE, *et al.* 2008] Bosze Z., Baranyi M. and Whitelaw C.B.A., *Producing recombinant human milk proteins in the milk of livestock species*. Advances in Experimental Medicine and Biology, 2008, p. 357-393.
- [BOX and WILSON 1951] Box G.E.P. and Wilson K.B., *On the experimental attainment of optimum conditions*. Journal of the Royal Statistical Society, Series B, 1951, **13**: p. 1-45.
- [BOX, *et al.* 1978] Box G.E.P., Hunter W.G. and Hunter J. S., *Statistics for experiments*. John Wiley and Sons, New York, 1978, p. 291-334.
- [BOX and DRAPER 1975] Box G.E.P. and Draper N.R., *Robust designs*. Biometrika, 1975, **62**: p. 347-352.
- [BOX and DRAPER 1987] Box G.E.P. and Draper N.R., *Empirical model-building and response surfaces*. John Wiley&Sons, New York, 1987.
- [BRUSSOW, *et al.* 1978] Brussow H., Hilpert H. and Walther I., *Bovine milk immunoglobulins for passive immunity to infantile rotavirus gastroenteritis*. Journal of Clinical Microbiology, 1978, **25**(6): p. 982-986.
- [BUTLER 1969] Butler J.E., *Bovine immunoglobulins: A review*. Journal of Dairy Science, 1969, **52**(12): p. 1895-1909.
- [BUTLER 1983] Butler J. E., 1983. *Bovine immunoglobulins: An augmented review*. Veterinary Immunology and Immunopathology, 1983, **4**: p. 43-152.
- [CABRAL and AIRES-BARROS 1993] Cabral J. M. S. and M. R. Aires-Barros, *Recovery processes for biological materials*. John Wiley and Sons Ltd, 1993, **9**: p. 247-271.
- [CALMETTES, *et al.* 1991] Calmettes P., L. Cser, and E. Rajnavolgyi, *Temperature and pH Dependence of Immunoglobulin G Conformation*. Archives of Biochemistry and Biophysics, 1991. **291**: p. 277-283.

- [CHARM 1972] Charm S.E., *Foam separation of enzymes and other proteins*. In: Adsorptive Bubble Separation Techniques. Ed: Lemlich, R. Academic Press, New York, 1972, p. 157-174.
- [CILLIERS] Cilliers J. “www.tcd.ie/Physics/Schools/what/materials/foam/”
- [CLARK, *et al.* 1988] Clark, D.C., Smith, L.J. and Wilson, D.R., *A spectroscopic study of the conformational properties of foamed bovine serumalbumin*. Journal of Colloid Interface Science, 1988, **121**: p. 136–147.
- [DAVIES and RIEDEL 1963] Davies J.T. and Riedel E.K., *Interfacial phenomena*. Academic Press, New York, 1963.
- [DONOVAN and ODLE 1994] Donovan S.M. and Odle J., *Growth factors in milk as mediators of infant development*. Annual Review of Nutrition, 1994, **14**: p. 147-167.
- [EASTOE and DALTON 2000] Eastoe J. and Dalton J.S., *Advance Colloid Interface Science*, 2000, **85**: p. 103.
- [ECHELARD, *et al.* 2006] Echelard Y., Ziomek C.A. and Meade H.M., *Production of recombinant therapeutic proteins in the milk of transgenic animals*. BioPharm International, 2006, **19**(8): p. 36-46.
- [ECHELARD, *et al.* 2008] Echelard Y., Williams J.L., Destrempe M.M., Koster J.A., Overton S.A., Pollock D.P., Rapiejko K.T., Behboodi E., Masiello N.C., Gavin W.G. and others, *Production of recombinant albumin by a herd of cloned transgenic cattle*. Transgenic Research, 2008, p. 1-16.
- [EIGEL, *et al.* 1984] Eigel W.N., Butler J.E., Ernstrom C.A., Farrell H.M.J., Harwalkar V.R., Jenness R. and Whitney R.M., *Nomenclature of proteins of cow's milk*. Journal of Dairy Science, 1984, **67**(8): p. 1599-1631.
- [EL-LOLY 2007] El-Loly M.M., *Bovine milk immunoglobulins in relation to human health*. International Journal of Dairy Science, 2007, **2**(3): p. 183-195.
- [FARRELL, *et al.* 2004] Farrell H.M. Jr., Jimenez-Flores R., Bleck G.T., Brown E.M., Butler J.E., Creamer L.K., Hicks C.L., Hollar C.M., Ng-Kwai-Hang K.F. and Swaisgood H.E., *Nomenclature of the proteins of cows' milk*. Journal of Dairy Science, 2004, **87**(6): p. 1641-1674.
- [FASSINA, *et al.* 2001] Fassina G., M. Ruvo, G. Palombo, A. Verdoliva, and M. Marino, *Novel ligands for the affinitychromatographic purification of*

- antibodies*. Journal of Biochemical and Biophysical Methods, 2001, **49**: p. 481-490.
- [GALFRE and SECHER 1990] Galfre G.L. and Secher D.S., *Monoclonal Antibodies*. Ullmann's encyclopedia of industrial chemistry, 1990. **16**: p 699-710.
- [GERHARDT and DUNGAN 2002] Gerhardt N.I., and Dungan S.R., *Time-dependent solubilization of IgG in AOT-brine-isooctane microemulsions: Role of cluster formation*. Biotechnology and Bioengineering, 2002, **78**: p. 60-72.
- [GIBBS 1928] Gibbs J.W., Collected Works. Longmans Green, New York, 1928.
- [GRAY 1993] Gray C.J., *Stability and preservation of activity of proteins during extraction, separation and purification*. J.F. Kennedy, J.M.S .Cabral (Eds), Recovery Processes for Biological Materials, John Wiley and Sons Ltd, 1993. p 11-45.
- [GRIEVES 1975] Grieves R.B., *Foam separations: A review*. The Chemical Engineering Journal, 1975, **9**(2): p. 93-106.
- [GRIEVES and BHATTACHARYYA 1970] Grieves R.B. and Bhattacharyya D., *Foam fractionation rates*. Separation Science, 1970, **5**: p. 583-601.
- [HALLER, *et al.* 2010] Haller D., Ekici P., Friess A., Parlar H., *High enrichment of MMP-9 and carboxypeptidase A by tweezing adsorptive bubble separation (TABS)*. Applied Biochemistry and Biotechnology, 2010. DOI 10.1007/s1210-010-8936-x
- [HEREMANS 1974a] Heremans J.F., *The IgA system in connection with local and systemic immunity*. Advances in Experimental Medicine and Biology, 1974, **45**(0): p. 3-11.
- [HEREMANS 1974b] Heremans J.F., *Structure and function of immunoglobulin IgA*. Behring Institute Mitteilungen, 1974, **54**: p. 1-8.
- [HILL and HUNTER 1996] Hill W.J. and Hunter W.G., *A review of response surface methodology: a literature review*. Technometrics, 1996, **8**: p. 571-590.
- [HILPERT, *et al.* 1987] Hilpert H., Brussow H. and Mietens C., *Use of bovine milk concentrate containing antibody to rotavirus to treat rotavirus gastroenteritis in infants*. Journal of Infectious Diseases, 1987, **156**(1): p. 158-166.

- [HOLSCHUH and SCHWAMMLE 2005] Holschuh K., and Schwammle A., *Preparative purification of antibodies with protein A-an alternative to conventional chromatography*. Journal of Magnetism and Magnetic Materials, 2005, **293**: p. 345-348.
- [HONG, *et al.* 2000] Hong D.P., Lee S.S., and Kuboi R., *Conformational transition and mass transfer in extraction of proteins by AOT-alcohol-isooctane reverse micellar systems*. Journal of Chromatography B, 2000, **743**: p. 203-213.
- [HOUDEBINE 2002a] Houdebine L.M., *Antibody manufacture in transgenic animals and comparisons with other systems*. Current Opinion in Biotechnology, 2002, **13**(6): p. 625-629.
- [HOUDEBINE 2002b] Houdebine L.M., *The methods to generate transgenic animals and to control transgene expression*. Journal of Biotechnology, 2002, **98**(2-3): p. 145-160.
- [HUANG, *et al.* 2002] Huang J., Wu L., Yalda D., Adkins Y., Kelleher S.L., Crane M., Lonnerdal B., Rodriguez R.L. and Huang N., *Expression of functional recombinant human lysozyme in transgenic rice cell culture*. Transgenic Research, 2002, **11**: p. 229-239.
- [HUSU, *et al.* 1993] Husu J., Syvaaja E.L., Ahola-Luttilla H., Kalsta H., Sivela S. and Kosunen T.U., *Production of hyperimmune bovine colostrum against Campylobacter jejuni*. Journal of Applied Bacteriology, 1993, **74**(5): p. 564-569.
- [JOHNSON 1986] Johnson R.D., *The processing of biomacromolecules - A challenge for the eighties*. Fluid Phase Equilibria, 1986, **29**: p. 109-123.
- [KARGER, *et al.* 1967] Karger B.L.; Grieves R.B.; Lemlich R., Rubin A.J. and Sebba F., *Nomenclature recommendations for adsorptive bubble separation methods*. Separation Science, 1967, **2**(3): p. 401-404.
- [KARGER and DEVIVO 1968] Karger B.L. and DeVivo D.G., *General survey of the adsorptive bubble separation process*. Separation Sciences, 1968, **3**: p. 393.
- [KELLER, *et al.* 1997] Keller R.C., Orsel R. and Hamer R.J., *Competitive adsorption behavior of wheat flour components and emulsifiers at the air-water interface*. Journal of Cereal Science, 1997, **25**: p. 175-183.

- [KELLY 2003] Kelly G.S., *Bovine colostrums: A review of clinical uses*. *Alternative Medicine Review*, 2003, **8**(4): p. 378-394.
- [KHURI and CORNELL 1996] Khuri A.I. and Cornell J.A., *Response surfaces*. 2nd edition, Marcel Dekker, New York, 1996.
- [KISHIMOTO 1962] Kishimoto H., Foam separation of surface-active substances. *Kolloid-Zeitschrift und Zeitschrift für Polymere*, 1962, **192**(1-2): p. 66-101.
- [KITCHENER and COOPER 1959] Kitchener J.A. and Cooper C.F., *Current concepts in the theory of foaming*. *Quarterly Reviews of the Chemical Society*, 1959, **13**: p. 71-97.
- [KORHONEN 1998] Korhonen H., *Colostrum immunoglobulins and the complement system-potential ingredients of functional foods*. *Bulletin: International Dairy Federation*, 1998, **336**: p. 36-40.
- [KORHONEN, *et al.* 2000] Korhonen H., Marnila P., and Gill H.S. *Bovine milk antibodies for health*. *British Journal of Nutrition*, 2000, **84**: p. 135-146.
- [KUROIWA, *et al.* 2009] Kuroiwa Y., Kasinathan P., Sathiyaseelan T., Jiao J.A., Matsushita H., Sathiyaseelan J., Wu H., Mellquist J., Hammitt M. and Koster J., *Antigen-specific human polyclonal antibodies from hyperimmunized cattle*. *Nature Biotechnology*, 2009, **27**(2): p. 173-181.
- [LEMLICH 1968] Lemlich R., *Principles of foam fractionation*. In: *Progress in Separation and Purification*. Ed: Perry E.S., New York, p. 1-56.
- [LEMLICH 1972a] Lemlich R., *Adsubble Methods*. In *Recent Advancements in Separation Science*, 1972, **1**: p. 113-127.
- [LEMLICH 1972b] Lemlich R., *Introduction. Principles of foam separation and drainage*. In: *Adsorptive Bubble Separation Techniques*. Ed: Lemlich R.. Academic Press, New York, 1972, p. 1-4.
- [LEMLICH 1972c] Lemlich R., *Foam fractionation and bubble fractionation*. *Journal of Geophysical Research*, 1972, **77**(27): p. 5204-5210.
- [LILIUS and MARNILA 2001] Lilius E.M. and Marnila P., *The role of colostrum antibodies in prevention of microbial infections*. *Current Opinion in Infectious Diseases*, 2001, **14**(3): p. 295-300.

- [LINKE, *et al.* 2007] Linke D., Zorn H., Gerken B., Parlar H. and Berger R.G., *Laccase isolation by foam fractionation - New prospects of an old process*. Enzyme and Microbial Technology, 2007. **40**(2): p. 273-277.
- [LIU, *et al.* 2003] Liu Y., Zhao R., Shangguan D.H., Zhang H.W., and Liu G.Q., *Novel sulfamethazine ligand used for one-step purification of immunoglobulin G from human plasma*. Journal of Chromatography B-Analytical Technologies in the Biomedical and Life Sciences, 2003, **792**: p. 177-185.
- [LOCKWOOD, *et al.* 2000] Lockwood C.E., Jay M., and Bummer P.M., *Foam fractionation of binary mixtures of lysozyme and albumin*. Journal of Pharmaceutical Sciences, 2000, **89**(6): p. 693–704.
- [LONDON, *et al.* 1954] London M., Cohen M. and Hudson P.B., *Some general characteristics of enzyme foam fractionation*. Biochimica et Biophysica Acta, 1954, **13**: p. 111-120.
- [LONNERDAL and STKINSON 1995] Lonnerdal B. and Atkinson S., *Nitrogenous components of milk A. Human milk proteins*. Jensen R.G., editor. San Diego, CA: Academic Press, 1995, p. 351-368.
- [LOW, *et al.* 2007] Low D., O’Leary R., and Pujar N.S., *Future of antibody purification*. Journal of Chromatography B, 2007, **848**: p. 48-63.
- [MAAS 1974] Maas K., *Adsorptive bubble separation techniques*. Methodicum Chemicum. Vol.1. Ed: Korte, F., Academic Press, New York, 1974, p. 165-171.
- [MAHNE 1971] Mahne E.J., *Foam separation processes*. Chemistry in Canada, 1971, **3**: p.32-33.
- [MALYSA and WARSZYNSKI 1995] Malysa K. and Warszynski P., *Dynamic effects in the stability of dispersed systems*. Advance Colloid Interface Science, 1995, **56**: p. 105–139
- [MRC 2005] Medical Research Council (MRC), *What are monoclonal antibodies?* “www.mrc.ac.uk”, June, 2005.
- [MCVEY and LOAN 1989] McVey D.S. and Loan R.W., *Total and antigen-specific serum immunoglobulin isotype concentrations in hyperimmunized cattle that have undergone plasmapheresis*. American Journal of Veterinary Research, 1989, **50**(5): p. 758-761.

- [MEAD and PIKE 1975] Mead R. and Pike D.J., *A review of response surface methodology from a biometric viewpoint*. Biometrics, 1975, **31**: p. 803-851.
- [MEHRA, *et al.* 2006] Mehra R., Marnila P. and Korhonen H., *Milk immunoglobulins for health promotion*. International Dairy Journal, 2006, **16**(11): p. 1262-1271.
- [MEISEL 1997] Meisel H., *Biochemical properties of bioactive peptides derived from milk proteins: Potential nutraceuticals for food and pharmaceutical applications*. Livestock Production Science, 1997, **50**(1-2): p. 125-138.
- [MYERS 1976] Myers R.H., *Response surface methodology*. Blacksburg, VA., 1976.
- [MYERS, *et al.* 1989] Myers R.H., Khuri A.I. and Carter W.H., *Response surface methodology: 1966-1988*. Technometrics, 1989, **3**: p. 137-317.
- [MYERS and MONTGOMERY 1995] Myers R.H. and Montgomery D.C., *Response surface methodology: Process and product optimization using designed experiments*. Toronto: John Wiley and Sons, Inc., 1995, p. 700.
- [MYERS 1999] Myers R.H., *Response surface methodology: current status and future directions*. Journal of Quality Technology, 1999, **31**: p. 30-44.
- [NICOLAI, *et al.* 2008] Nicolai A., Friess A., and Parlar H., *Efficient enrichment of alpha, beta-unsaturated bovine insulins-(C12)(n) using tweezing adsorptive bubble separation (TABS) with bovine serum albumin*. Journal of Separation Science, 2008. **31**(12): p. 2310-2317.
- [NISHIKI, *et al.* 1998] Nishiki T., Sato I., Muto A., and Kataoka T., *Mass transfer characterization in forward and back extractions of lysozyme by AOT-isooctane reverse micelles across a flat liquid-liquid interface*. Biochemical Engineering Journal, 1998, **1**: p. 91-97.
- [NOBLE, *et al.* 1998] Noble M., Brown A., Jauregi P., Kaul A. and Varley J., *Protein recovery using gas-liquid dispersions*. Journal of Chromatography B, 1998, **711**: p. 31-43.
- [NORD 2000] Nord L., *Structural analysis from Quillaja Saponaria Molina and methods for structure-property relationship studies*. PhD Thesis. Swedish University for Agricultural Sciences, 2000.
- [ORMROD and MILLER 1993] Ormrod D.J. and Miller T.E., *Milk from hyperimmunized dairy cows as a source of a novel biological response modifier*. Agents and Actions, 1993, **38**(1): p. 146-149.

- [PAKKANEN and AALTO 1997] Pakkanen R. and Aalto J., *Growth factors and antimicrobial factors of bovine colostrum*. International Dairy Journal, 1997, **7**(5): p. 285-297.
- [PARTHASARATHY, *et al.* 1988] Parthasarathy S., Das T.R. and Kumar R., *Foam separation of microbial cells*. Biotechnology and Bioengineering, 1988, **32**: p. 174-183.
- [PLAYNE, *et al.* 2003] Playne M.J., Bennett L.E. and Smithers G.W., *Functional dairy foods and ingredients*. Australian Journal of Dairy Technology, 2003, **58**(3): p. 242-264.
- [POLLOCK, *et al.* 1999] Pollock D.P., Kutzko J.P., Birck-Wilson E., Williams J.L., Echelard Y. and Meade H.M., *Transgenic milk as a method for the production of recombinant antibodies*. Journal of Immunological Methods, 1999, **231**(1-2): p. 147-157.
- [REITER and ORAM 1967] Reiter B. and Oram J.D., *Bacterial inhibitors in milk and other biological fluids*. Nature, 1967, **216**(5113): p. 328-330.
- [ROBERTSON and VERMEULEN 1969] Robertson G.H. and Vermeulen T., *Foam fractionation of rare health elements*. Lawrence Radiation Laboratory Report, 1969, UCRL-19525.
- [ROSA, *et al.* 2007] Rosa P.A.J., Azevedo A.M., Ferreira I.F., de Vries J., Korporaal R., Verhoef H. J., Visser T.J., and Aires-Barros M.R., *Affinity partitioning of human antibodies in aqueous two-phase systems*. Journal of Chromatography A, 2007, **1162**: p. 103-113.
- [ROSE, *et al.* 1970] Rose D., Brunner J.R., Kalan E.B., Larson B.L., Melnychyn P., Swaisgood H.E. and Waugh D.F., *Nomenclature of the proteins of cow's milk*. Journal of Dairy Science, 1970, **53**(1): p. 1-17.
- [SCHNEPF and GADEN 1959] Schnepf R.W. and Gaden E.L., *Foam fractionation of proteins—concentration of aqueous solutions of bovine serum albumin*. Biotechnology Bioengineering, 1959, **1**(1): p. 1–11.
- [SHAH 2000] Shah N.P., *Effects of milk-derived bioactives: An overview*. British Journal of Nutrition, 2000, **84**(1): p. 3-10.
- [SOMASUNDARAN 1972] Somasundaran P., *Foam separation methods*. Separation and Purification Methods, 1972, **1**(1): p. 117-198.

- [STEIJNS 2001] Steijns J.M., *Milk ingredients as nutraceuticals*. International Journal of Dairy Technology, 2001, **54**(3): p. 81-88.
- [STEPHAN, *et al.* 1990] Stephan W., Dichtelmuller H. and Lissner R., *Antibodies from colostrum in oral immunotherapy*. Journal of Clinical Chemistry and Clinical Biochemistry, 1990, **28**(1): p. 19-23.
- [STEVENSON 2000] Stevenson D., *Immuno-affinity solid-phase extraction*. Journal of Chromatography B: Biomedical Sciences and Applications, 2000, **745**: p. 39-48.
- [STEVENSON and JAMESON 2007] Stevenson P. and Jameson G.J., *Modelling continuous foam fractionation with reflux*. Chemical Engineering and Processing, 2007. **46**: p. 1286-1291.
- [SUBRAMANIAN 2002] Subramanian A., *Immunoaffinity chromatography*. Molecular Biotechnology, 2002, **20**: p. 41-47.
- [TOMASI and BIENENSTOCK 1968] Tomasi T.B. and Bienenstock J., *Secretory immunoglobulins*. Advances in Immunology, 1968, **9**: p. 1-96.
- [TOWNSEND and NAKAI 1983] Townsend A. and Nakai S., *Relationship between hydrophobicity and foaming characteristics of food proteins*. Journal of Food Science, 1983, **48**: p. 588-594.
- [URAZEE and NARSIMHAN 1990a] Uraizee F. and Narsimhan G., *Foam fractionation of proteins and enzymes: I. Applications*. Enzyme Microbial Technology, 1990, **3**: p. 232-233.
- [URAZEE and NARSIMHAN 1990b] Uraizee F. and Narsimhan G., *Foam fractionation of proteins and enzymes: II. Performance and modelling*. Enzyme Microbial Technology, 1990, **4**: p. 315-316.
- [URAZEE and NARSIMHAN 1996] Uraizee F. and Narsimhan G., *Effects of kinetics of adsorption and coalescence on continuous foam concentration of proteins: Comparison of experimental results with model predictions*. Biotechnology and Bioengineering, 1996, **51**(4): p. 384-398.
- [VANCAN, *et al.* 2002] Vancan S., Miranda E.A., and Bueno S.M.A., *IMAC of human IgG: studies with IDA-immobilized copper, nickel, zinc, and cobalt ions and different buffer systems*. Process Biochemistry, 2002. **37**: p. 573-579.

- [VARLEY and BALL 1994] Varley J. and Ball S.K., *Foam separation for enzyme recovery: Maintenance of activity*. Separations for Biotechnology 3, ed. D. L. Pyle, Cambridge: University of Reading, 1994, p. 525-531.
- [VASUDEVAN, *et al.* 1995] Vasudevan M., Tahan K., and Wiencek J.M., *Surfactant structure effects in protein separations using nonionic microemulsion*. Biotechnology And Bioengineering, 1995, **46**: p. 99-108.
- [WARD and TORDAI 1946] Ward A.F.H. and Tordai L., *Time-dependence of boundary tension of solutions I. the role of diffusion in time-effects*. Journal of Chemical Physics, 1946. **14**: p. 453.
- [WEINER, *et al.* 1999] Weiner C., Pan Q., Hurtig M., Borén T., Bostwick E. and Hammarström L., *Passive immunity against human pathogens using bovine antibodies*. Clinical and Experimental Immunology, 1999, **116**(2): p. 193-205.
- [WOLL, *et al.* 1989] Woll J.M., Hatton T.A., and Yarmush M.L., *Bioaffinity separations using reversed micellar extraction*. Biotechnology Progress, 1989, **5**: p. 57-62.
- [WONG, *et al.* 1996] Wong D.W.S., Camirand W.M. and Pavlath A.E., *Structures and functionalities of milk proteins*. Critical Reviews in Food Science and Nutrition, 1996, **36**(8): p. 807-844.
- [ZEITLIN, *et al.* 2000] Zeitlin L., Cone R.A., Moench T.R. and Whaley K.J., *Preventing infectious disease with passive immunization*. Microbes and Infection, 2000, **2**(6): p. 701-708.

LEBENS LAUF

PERSÖNLICHE DATEN

Name: Yen-Chih Chen
Geburtsdatum: 21.12.1982
Geburtsort: München, Deutschland
Staatsangehörigkeit: Taiwan (R.O.C.)

AUSBILDUNG

Promotion 10/2007 -	Technische Universität München Lehrstuhl für Chemisch-Technische Analyse und Chemische Lebensmitteltechnologie
Thema:	Enrichment Behavior of Immunoglobulin from Foam Fractionation Using Response Surface Methodology
Master-Abschluss 2005 - 2007	National Taiwan University Department of Agricultural Chemistry
Thema:	Utilization of recovered shoyu mash residue and studies on the hydrolysis of soy sauce koji and soy protein
Bachelor-Abschluss 2001 - 2005	National Taiwan University Department of Horticulture